UNIVERSITY OF SALERNO

DEPARTMENT OF CHEMISTRY AND BIOLOGY

and

UNIVERSITY OF BASILICATA

DEPARTMENT OF SCIENCE

Ph.D. in Chemistry - XXXI Cycle

BIO/10 - Biochemistry

Doctoral Thesis in

"The protein related to Pseudoxanthoma Elasticum regulates the purinergic system. New insight on the ABCC6 transporter"

Ph.D. Coordinator:
Prof. Gaetano Guerra

Ph.D. Student:
Dr. Fabio Martinelli

Tutor:
Prof. Faustino Bisaccia

Co-Tutor:
Prof. Magnus Monné

Academic Year 2017-2018

To my parents,

to my brother,

to my grandfather,

in particular to my nieces Alessia and Sofia

“The scientist is not the man

who provides the true answers;

that’s what asks the real questions.”

Claude Lévi-Strauss

Abbreviations:

$2^{(-\Delta\Delta Ct)}$	Fold Change
5'UTR	5' Untranslated region
1609dupA	Duplication of adenine in position 1609
A	Alanine (Ala)
A_1, A_{2a}, A_{2b}, A_3	Adenosine receptor A_1, A_{2a}, A_{2b}, A_3
ABC	ATP-binding cassette
ABCB	ATP-binding cassette, sub-family B
ABCC	ATP-binding cassette, sub-family C
ABCC6	ATP-binding cassette, sub-family C, member 6
ABCC6-Flag-pcDNA	Flag-pcDNA containing the sequence coding for *ABCC6*
ABCC6-Ψ	Pseudogene of *ABCC6*
ABCC6 Δ19Δ24	*ABCC6* mRNA without exons 19 and 24
ACDC	Arterial Calcification due to deficiency

	of CD73
ADP	Adenosine diphosphate
AMP	Adenosine monophosphate
AOPCP	α,β-methyleneadenosine-5'-diphosphate
APS	Persulfate ammonium
ATCC	American Type Culture Collection
ATP	Adenosine triphosphate
BCRP	Breast cancer resistance protein
BLAST	Basic Local Alignment Search Tool
BMP-2	Bone morphogenetic protein-2
bp	Base pairs
BSA	Bovine serum albumin
C	Cysteine (Cys)
Calcein-AM	Calcein-acetoxymethyl ester
CALJA	Calcification of joints and arteries
cAMP	Cyclic adenosine monophosphate
CD73	Cluster of differentiation 73

CD73L	Long CD73 isoform
CD73S	Short CD73 isoform
CDKs	Cyclin-dependent kinases
cDNA	Complementary DNA
CFTR	Cystic fibrosis transmembrane conductance regulator
cGMP	Cyclic guanosine monophosphate
Co^{2+}	Cobalt ion
CSCs	Cancer stem cells
Ct	Threshold cycle
D	Aspartic acid (Asp)
DCF	Dichlorofluorescein
DCFH	Dichlorodihydrofluorescein
DCFH-DA	2',7'-dichlorofluorescein diacetate
DMEM	Dulbecco's Modified Eagle's Medium
DMSO	Dimethyl sulfoxide
(g)DNA	(genomic) Deoxyribonucleic acid

dNTP	Deoxynucleotide
E	Glutamic acid (Glu)
ECM	Extracellular matrix
EDTA	Ethylenediaminetetraacetic acid
em.	Emission wavelength
ENPP1	Ecto-nucleotide pyrophosphate/ phosphodiesterase type I
ex.	Excitation wavelength
EX23_29del	Alu-mediated deletion from exon 23 to exon 29
FBS	Fetal bovine serum
Fetuin A	Alpha 2-Heremans-Schmid glycoprotein
Flag	DYKDDDDK tag
Flag-pcDNA	pcDNA vector that codifies for Flag tag
G	Glycine (Gly)
G418	Geneticin
GACI	Generalized arterial calcification of infancy

GBM	Glioblastoma multiform
$G_{i/o}$	G protein with α inhibitory subunit
GPI	Glycosylphosphatidylinositol
G_s	G protein with α stimulating subunit
HCC	Hepatocellular carcinoma
HEK293	Human embryonic kidney cells 293
HepG2	Human hepatocellular carcinoma cells
HNF4	Hepatocyte nuclear factor 4
HSCs	Hemapoietic stem cells
HuH-7	Human hepatocellular carcinoma well differentiated cells
K	Lysine (Lys)
kb	Kilobases
kDa	Kilodalton
K_i	Inhibition constant
L	Leucine (Leu)
L0	Connecting loop

MDA-MB-231	Triple-negative human breast cancer poorly differentiated cells
MDR	Multidrug resistance
Mg^{2+}	Magnesium ion
MGP	Matrix gla protein
mRNA	Messenger RNA
MRP	Multidrug-resistance associated protein
MRP6	Multidrug-resistance associated protein, member 6
MTT	3-(4,5-dimethylthiazol-2-yl)-2,5-diphenyltetrazolim bromide
NBD	Nucleotide-binding domain
NCBI	National Center for Biotechnology Information
NK-cells	Natural killer-cells
NT5E	Ecto-5'-nucleotidase

NT5E-1	Long transcript of ecto-5'-nucleotidase
NT5E-2	Short transcript of ecto-5'-nucleotidase
OC	Osteocalcin
OMIM	Online Mendelian Inheritance in Man
OPN	Osteopontin
p/q	Short/long arm of a chromosome
p	*p*-value
PBS	Phosphate buffered saline
PBS-T	PBS with 0.05% of Tween-20
PCR	Polymerase chain reaction
PGE2	Prostaglandin E2
P-gp	P-glycoprotein
P_i	Phosphate
PP_i	Pyrophosphate
Primer for	Primer forward
Primer rev	Primer reverse
PVDF	Polyvinylidene difluoride

PXE	Pseudoxhantoma Elasticum
Q	Glutamine (Gln)
R	Arginine (Arg)
RNA	Ribonucleic acid
ROS	Reactive oxygen species
rpm	Revolutions for minute
S	Serine (Ser)
SD	Standard deviation
SDS	Sodium dodecyl sulfate
SDS-PAGE	Sodium dodecyl sulfate - polyacrylamide gel electrophoresis
siRNA	Small interfering RNA
SO_4^{-}.	Sulfate radical
SUR	Sulfonylurea receptor
T	Threonine (Thr)
TBS	Tris buffered saline
TEMED	N,N,N',N'-tetramethylethane-1,2-diamine

TGF-β	Transforming growth factor-β
Tm	Melting temperature
TM	Transmembrane
TMD	Transmembrane domain
TNAP	Tissue non-specific alkaline phosphatase
TNF-α	Tumor necrosis factor-α
U	Units
URG7	Up-regulated gene 7
Y	Tyrosine (Tyr)
Zn^{2+}	Zinc ion
ΔCt	Difference between Ct of target gene and Ct of housekeeping gene
ΔΔCt	Difference between ΔCt of a target gene in a sample and ΔCt of the same gene in the calibrator sample

Index:

Abstract:

ABC (ATP-binding cassette) transporters are the largest superfamily of membrane proteins present in all organisms and they are particularly involved in transport of nutrients and drugs. Among these transporters we find ABCC6, belonging to sub-family C, which is an ATP-dependent transporter mainly present in the basolateral plasma membrane of hepatic and kidney cells. Mutations in the *ABCC6* gene are associated to the Pseudoxanthoma Elasticum (PXE), an autosomal recessive disease characterized by progressive ectopic mineralization processes at level of the skin, the retina and the vascular wall. It has been reported that PXE is caused in peripheral tissues by decreased levels of PP_i, a strong inhibitor of mineralization processes. In fact, the administration of PP_i reducing the effects of PXE is considered an efficient drug. It is known that the over-expression of ABCC6 in HEK293 cells results in the outflow of ATP and that is converted into AMP and PP_i by ENPP1 protein. Then, AMP is transformed into adenosine and P_i by CD73 protein; so ABCC6 protein could be involved both in providing extracellular adenosine and in the regulation of the purinergic system. Previous studies show that in *ABCC6*-silenced HepG2 cells there is a dysregulation of some genes involved in the mineralization processes. We performed experiments in order to evaluate the mechanism by which ABCC6 is able to promote this genic dysregulation. For this purpose, the ABCC6 transport activity was inhibited with an aspecific inhibitor of ABC transporters. The main

results obtained in HepG2 cells are partially similar to those ones obtained in *ABCC6*-silenced HepG2 cells. The greatest effects were obtained on *NT5E* and on *ABCC6*. As an inhibitor, probenecid was used to reduce the transport activity of ABCC6 into HEK293 cells. In order to confirm that the observed effect is closely related to the inhibition of ATP transport, and not to the presence of probenecid, the HepG2 cells were also treated with adenosine and ATP. The results show that in the presence of 10 and 100 μM of adenosine or 50 and 500 μM of ATP, the effects of probenecid are reversed. In order to confirm the effects of probenecid on the transport activity in these cells was tested the quercetin, another ABC inhibitor; the data confirm those ones previously obtained with probenecid on the expression of *ABCC6* and *NT5E*. In HepG2 cells treated with doxorubicin, whose presence increases the expression of *ABCC6*, we observed a proportional increase of *NT5E*. Experiments with probenecid, adenosine and ATP were also performed in cells expressing *ABCC6* at different levels. The results show that in the presence of probenecid in MDA-MB-231 cells there is no effect while in the HEK293 and HuH-7 cells there are poor effects. The effect of probenecid is obtained only in cells that over-express *ABCC6*; in all these cells, the addition of adenosine and ATP improves the expression of CD73. It was also analysed the cellular phenotype after the treatment with probenecid. Considering the role of CD73 in cellular migration processes, motility assays confirmed that HepG2 cells migrate more slowly, after this treatment.

Introduction

1.1 ABC transporters

Membrane transporters constitute a significant fraction of all proteins encoded in the genome of simple and complex organisms. They are divided into channels and carriers, two very large classes of proteins, within which there are superfamilies defined by both particular sequences of amino acids and specific secondary structures. The transporters bind their substrates with high stereo-specificity; among them there are passive transporters (which transport substrates according to a concentration gradient) and active transporters (which transport substrates through the membranes against concentration gradient). Some of these active transporters exploit the supplied energy by a chemical reaction, other of them by coupling the gradient versus transport with the gradient transport of another substrates. Among these active transporters, which perform their function using the energy deriving from the hydrolysis of ATP, one of the most important families is ABC (ATP-binding cassette) transporters. ABC transporters are the largest superfamily of membrane proteins **[1]** present in all living beings, from microbes to plants and animals **[2-4]**; they are able to couple the transport of a substrate across the membranes to the hydrolysis of the phosphate bond between the γ- and the β-phosphate of ATP **[5-7]**; they are codified by ABC genes that are highly conserved among species **[8]**. ABC transporters can work as either importers or exporters **[9]**, and are involved in nutrient uptake, in transport of drugs, peptides and saccharides **[10]**, hormonal and xenobiotic secretion,

ion and lipid homeostasis, antibiotic and multidrug resistance; for these reasons they are the main candidates for cellular regulation and pharmacological intervention **[11-14]**. The proteins of this group are mainly classified according to the sequence and organization of their cytoplasmic nucleotide-binding domains (NBDs) **[15]**. All ABC transporters show a common basic organization; their functional core consists of two NBDs and two transmembrane domains (TMDs) (**Fig. 1.1**).

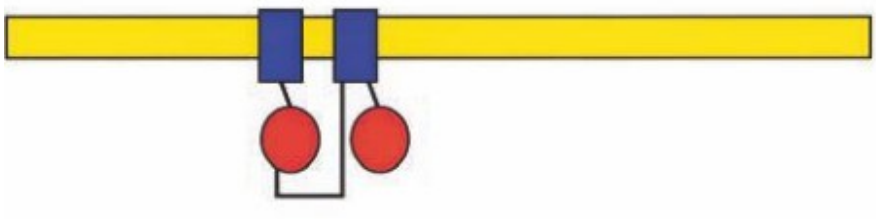

Fig. 1.1: Basic organization of ABC transporter with two NBDs (red) and two TMDs (blue) **[8]**.

The TMDs domains are constituted by 6-11 transmembrane α-helicals that form a cavity within the membrane through which the substrate can be transported. The low sequence similarity among these transmembrane domains of the various ABC proteins reflects the wide variety of substrates carried **[16-18]**. The NBDs domains, cytoplasmic domains, that bind and hydrolyze ATP, need magnesium (Mg^{2+}) for their activity; they are formed by 200-300 amino acids and contain the following motifs: A-loop involved in ATP positioning; Walker A, GXXGXGK(S/T) (where X is any amino acid), involved in phosphate

binding; Walker B, ϕϕϕϕD (where ϕ is an hydrophobic amino acid residue), involved in coordination of Mg^{2+}; D-loop, H-loop, Q-loop the main sites of interaction with TMDs, and the signature C motif (LSGGQ) located upstream of the Walker B and implicated in binding and hydrolysis of Mg^{2+}-ATP **[6] [15-16] [19]** (**Fig. 1.2**).

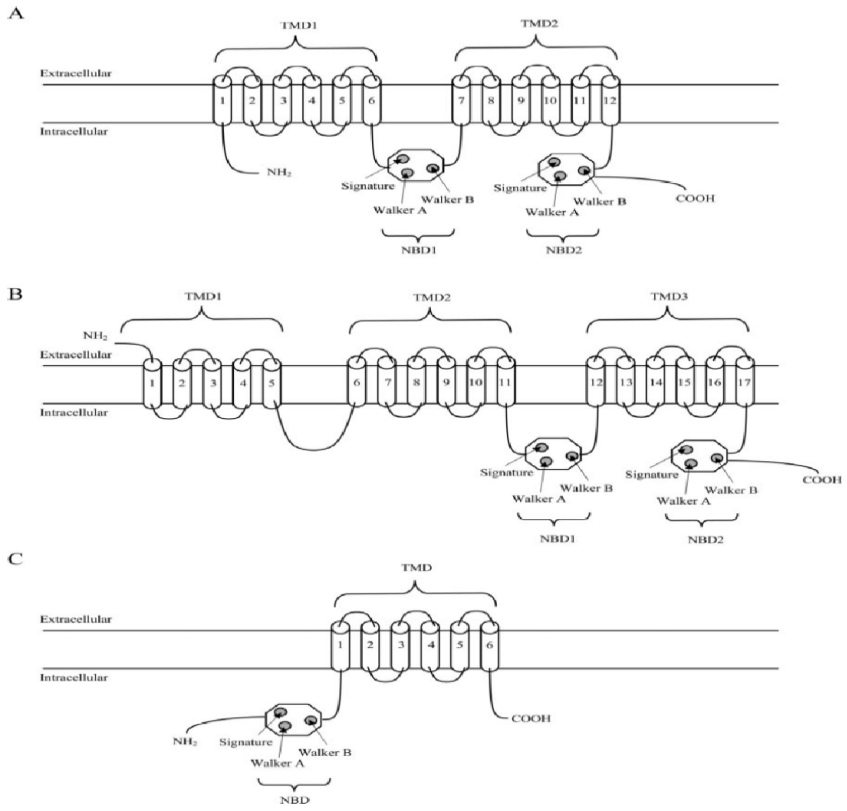

Fig. 1.2: General representation of the functional organization of the ABC proteins: **A**) ABC "full transporters" with 12 TM regions, divided into 2 TMDs, each with an NBD domain; **B**) ABC transporters with 5 extra TM regions, which form the TMD0 at the N-terminal; **C**) ABC "half-transporters" with 6 TM regions (one TMD) and one NBD **[20]**.

Prokaryotic transporters are located in plasma membrane and hydrolyze ATP in the cytoplasm, whereas eukaryotic ABC transporters are present both in plasma membrane and in organelle membranes and hydrolyze ATP in the cytoplasm (except for mitochondria and chloroplasts transporters). Eukaryotic ABC transporters can either be encoded as a single protein ("full transporters") or can be considered as a result of homo- or hetero-dimerization ("half-transporters") with only one TMD and one NBD **[8]** (see **Fig. 1.2**). Moreover, some ABC transporters contain an extension to the N-terminal consisting of five α-helicals that form the TMD0 domain **[18] [21]** (see **Fig. 1.2**). The transport mechanism of these proteins is based on the conformational change of the TMD domains, induced by the binding of the ATP to the NBD sites, which determines the opening to the outside and the release of the substrates. After the hydrolysis of the ATP the dimer NBD is deactivated and the conformation of the transporter returns to its original, facing inward, which represents the orientation with high affinity for the substrate **[6]** (**Fig. 1.3**).

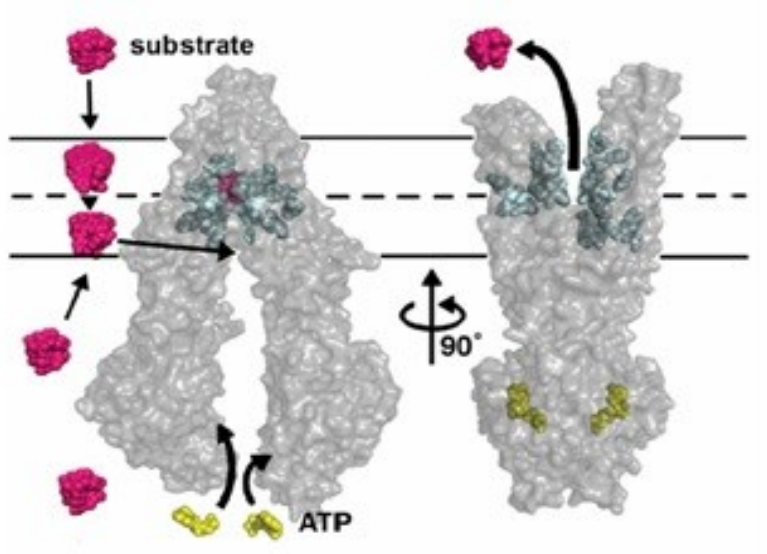

Fig. 1.3: Transport mechanism of ABC proteins **[21]**.

In literature there are structural studies of bacterial ABC transporters; for eukaryotic ABC transporters there are no high resolution structures **[17]**, but some medium resolution structures, such as P-glycoprotein (P-gp) **[17] [22]**.

1.2 Human ABC transporters

Human ABC proteins are encoded by 48 genes **[23-24]**, and have been classified into seven subfamilies from ABC-A to ABC-G based on the similarity in the gene structure, order of the domains, and sequence homology in the NBDs and TMDs **[23-26]**. These transporters are

expressed ubiquitously in non-tumor cells or in a tissue-specific manner and play a role in metabolic and/or detoxification processes **[1]**. In tissues there is a different distribution of ABC proteins and the sub-cellular localization of these proteins can be a discriminating feature **[26]**; moreover, the ABC transporters are highly expressed in many tumor cells, for example in leukemic and in breast cancer cells **[26]**. In **Table 1.1** we can find a list of all human *ABC* genes known with their chromosomal location, their subfamily, their expression pattern and their function (if it is known) **[8]**.

Gene	Alias	Location	Subfamily	Expression	Function
ABCA1	*ABC1*	9q31.1	ABC1	Ubiquitous	Cholesterol efflux onto HDL
ABCA2	*ABC2*	9q34	ABC1	Brain	Drug resistance
ABCA3	*ABC3, ABCC*	16p13.3	ABC1	Lung	
ABCA4	*ABCR*	1p22.1-p21	ABC1	Photoreceptors	N-retinylidene-PE efflux
ABCA5		17q24	ABC1	Muscle, heart, testes	
ABCA6		17q24	ABC1	Liver	
ABCA7		19p13.3	ABC1	Spleen, thymus	
ABCA8		17q24	ABC1	Ovary	
ABCA9		17q24	ABC1	Heart	
ABCA10		17q24	ABC1	Muscle, heart	
ABCA12		2q34	ABC1	Stomach	
ABCA13		7p11-q11	ABC1	Low in all tissues	
ABCB1	*PGY1, MDR*	7p21	MDR	Adrenal, kidney, brain	Multidrug resistance
ABCB2	*TAP1*	6p21	MDR	All cells	Peptide transport
ABCB3	*TAP2*	6p21	MDR	All cells	Peptide transport
ABCB4	*PGY3*	7q21.1	MDR	Liver	PC transport
ABCB5		7p14	MDR	Ubiquitous	
ABCB6	*MTABC3*	2q36	MDR	Mitochondria	Iron transport
ABCB7	*ABC7*	Xq12-q13	MDR	Mitochondria	Fe/S cluster transport
ABCB8	*MABC1*	7q36	MDR	Mitochondria	
ABCB9		12q24	MDR	Heart, brain	
ABCB10	*MTABC2*	1q42	MDR	Mitochondria	
ABCB11	*SPGP*	2q24	MDR	Liver	Bile salt transport
ABCC1	*MRP1*	16p13.1	CF/MRP	Lung, testes, PBMC	Drug resistance
ABCC2	*MRP2*	10q24	CF/MRP	Liver	Organic anion efflux
ABCC3	*MRP3*	17q21.3	CF/MRP	Lung, intestine, liver	Drug resistance
ABCC4	*MRP4*	13q32	CF/MRP	Prostate	Nucleoside transport
ABCC5	*MRP5*	3q27	CF/MRP	Ubiquitous	Nucleoside transport
ABCC6	*MRP6*	16p13.1	CF/MRP	Kidney, liver	
CFTR	*ABCC7*	7q31.2	CF/MRP	Exocrine tissue	Chloride ion channel
ABCC8	*SUR*	11p15.1	CF/MRP	Pancreas	Sulfonylurea receptor
ABCC9	*SUR2*	12p12.1	CF/MRP	Heart, muscle	
ABCC10	*MRP7*	6p21	CF/MRP	Low in all tissues	
ABCC11	*MRP8*	16q11-q12	CF/MRP	Low in all tissues	
ABCC12	*MRP9*	16q11-q12	CF/MRP	Low in all tissues	
ABCD1	*ALD*	Xq28	ALD	Peroxisomes	VLCFA transport regulation
ABCD2	*ALDL1, ALDR*	12q11-q12	ALD	Peroxisomes	
ABCD3	*PXMP1, PMP70*	1p22-p21	ALD	Peroxisomes	
ABCD4	*PMP69, P70R*	14q24.3	ALD	Peroxisomes	
ABCE1	*OABP, RNS41*	4q31	OABP	Ovary, testes, spleen	Oligoadenylate binding protein
ABCF1	*ABCS0*	6p21.33	GCN20	Ubiquitous	
ABCF2		7q36	GCN20	Ubiquitous	
ABCF3		3q25	GCN20	Ubiquitous	
ABCG1	*ABC8, White*	21q22.3	White	Ubiquitous	Cholesterol transport?
ABCG2	*ABCP, MXR, BCRP*	4q22	White	Placenta, intestine	Toxin efflux, drug resistance
ABCG4	*White2*	11q23	White	Liver	
ABCG5	*White3*	2p21	White	Liver, intestine	Sterol transport
ABCG8		2p21	White	Liver, intestine	Sterol transport

Table 1.1: Human ABC transporters: location, expression and function **[8]**.

Mutations of *ABC* genes are involved in several and various human inherited disorders (**Table 1.2**) including cystic fibrosis, Pseudoxanthoma Elasticum (PXE), tangier disease, alteration in metabolism and drug response **[6] [25] [27]**.

Gene (symbol)	Phenotype, disease/function
ABCA subfamily	
ABCA1	HDL deficiency/Cholesterol and phospholipid efflux
ABCA3	Pulmonary surfactant deficiency in newborn
ABCA4 (ABCR)	Stargardt disease 1
ABCA12	Harlequin ichthyosis
ABCA13	Schizophrenia, Bipolar Disorder, Depression
ABCB subfamily	
ABCB1 (MDR1)	Multidrug resistance in cancer/Export of xenobiotics
ABCB2 (TAP1)	Behçet's disease/Antigen peptide transport into ER lumen
ABCB3 (TAP2)	Behçet's disease/Antigen peptide transport into ER lumen
ABCB4 (MDR3)	Intrahepatic cholestasis/Secretion of phosphatidylcholine into bile
ABCB7	Sideroblastic anemia/Transport of iron-sulfate complexes in mitochondria
ABCB11 (BSEP, SPGP)	Intrahepatic cholestasis/Export of bile acid
ABCC subfamily	
ABCC1 (MRP1)	Multidrug resistance in cancer/Export of xenobiotics
ABCC2 (MRP2/cMOAT)	Dubin-Johnson syndrome/Export of bilirubin
ABCC6 (MRP6)	Pseudoxanthoma elasticum
ABCC7 (CFTR)	Cystic fibrosis/Cl^- channel
ABCC8 (SUR1)	PHHI/ATP sensitive K^+ channel regulator in pancreatic β-cells
ABCD subfamily	
ABCD1 (ALDP)	Adrenoleukodystrophy/Peroxysomal transport of very long fatty acid
ABCD2 (ALDR)	Adrenoleukodystrophy/Peroxysomal transport of very long fatty acid
ABCG subfamily	
ABCG2 (BCRP)	Gout/Export of Uric acid
ABCG5	Sitosterolemia/Export of phytosterols
ABCG8	Sitosterolemia/Export of phytosterols

Table 1.2: Diseases associated with mutations in ABC transporters **[25]**.

Moreover, the high expression of some ABC proteins in hematopoietic stem cells (HSCs) and in cancer stem cells (CSCs), compared to their more differentiated counterpart, could suggest the hypothesis that these proteins play a role in cellular differentiation **[28]**. Some ABC transporters are involved in the transport of xenobiotics and drugs (**Table 1.3**), and in particular the two subfamilies mainly involved in the development of the drug resistance are the subfamily B (known as MDR, Multi-Drug Resistance) and the subfamily C (known as MRP, Multi-drug Resistance-associated Proteins) **[20]**. The most important and pharmacologically investigated protein is ABCB1 (known as P-gp or MDR1), for its implications in drug resistance; the tumor cells that over-express this protein show MDR phenotype, and are resistant to the transport of many antineoplastic drugs (such as doxorubicin and vinblastine) **[29-30]**.

Properties of ABC transporters involved in transport of drugs

ABC Transporter	No. of Transmembrane Domains	Main Tissue Expression	Apical or Basolateral Membrane Localization	Substrates[a]	References
ABCB1 (MDR1 or P-gp)	2	Liver, kidney, intestine, brain, testis, adrenal gland, uterus, ovary	Apical	Quinidine, verapamil, celiprolol, talinolol, digoxin, daunorubicin, doxorubicin, vinblastine, etoposide, methotrexate, mitoxantrone, paclitaxel, topotecan, indinavir, nelfinavir, ritonavir, saquinavir	Kartner et al. (1983), Ueda et al. (1987), Pastan et al. (1988), de Lannoy and Silverman (1992), Hendricks et al. (1992), Peters and Roelofs (1992), Karlsson et al. (1993), de Graaf et al. (1996), Sparreboom et al. (1997), Kim et al. (1998), Gramatte and Oertel (1999), Verschraagen et al. (1999), Jones et al. (2001)
ABCB4 (MDR3)	2	Liver	Apical	Vinblastine, paclitaxel, digoxin	Smith et al. (2000)
ABCB11 (BSEP or SPGP)	2	Liver, intestine	Apical	Vinblastine, cyclosporin, rifampicin	Törok et al. (1999), Lecureur et al. (2000), Stieger et al. (2000)
ABCC1 (MRP1)	3	Intestine, brain, kidney, lung, testis	Basolateral	Doxorubicin, daunorubicin, vinblastine, vincristine, etoposide, methotrexate, paclitaxel, grepafloxacin	Cole et al. (1992, 1994), Flens et al. (1996), Sharp et al. (1998), Hooijberg et al. (1999), Evers et al. (2000), Tamai et al. (2000), Cherrington et al. (2002)
ABCC2 (MRP2 or cMOAT)	3	Liver, intestine, kidney	Apical	Cisplatin, doxorubicin, etoposide, vincristine, methotrexate, indinavir, ritonavir, saquinavir, adefovir, cidofovir	Schaub et al. (1997), Cui et al. (1999), Hooijberg et al. (1999), Kawabe et al. (1999), Fromm et al. (2000), Miller (2001), Huisman et al. (2002)
ABCC3 (MRP3)	3	Intestine, kidney, liver, pancreas, placenta, colon	Basolateral	Daunorubicin, doxorubicin, vincristine, etoposide, teniposide, methotrexate	Kool et al. (1997), Belinsky et al. (1998), Kool et al. (1999), Zeng et al. (1999), St-Pierre et al. (2000), Zelcer et al. (2001)
ABCC4 (MRP4)	2	Prostate, lung, adrenal gland, ovary, testis	Basolateral and apical (depending on cell type)	Methotrexate, adefovir	Lee et al. (1998), Schuetz et al. (1999), Lee et al. (2000), Chen et al. (2002
ABCC5 (MRP5)	2	Skeletal muscle, heart, brain	Basolateral	Adefovir	Kool et al. (1997), Belinsky et al. (1998), Wijnholds et al. (2000), Haimeur et al. (2004)
ABCC6 (MRP6)	3	Kidney, liver	Basolateral	Cisplatin, doxorubicin, etoposide, daunorubicin,	Belinsky and Kruh (1999), Bergen et al. (2000), Belinsky et al. (2002)
ABCC10 (MRP7)	3	Heart, skeletal, muscle, spleen, liver	Not determined	Doxorubicin, vinblastine, vincristine, paclitaxel, docetaxel	Kao et al. (2002), Orr et al. (2003), Hopper-Borge et al. (2004)
ABCC11 (MRP8)	2	Breast, testis	Not determined	Purine and pyrimidine nucleotide analogs	Bera et al. (2001)
ABCC12 (MRP9)	2	Breast, testis, brain, ovary, skeletal muscle	Not determined	Not determined	Bera et al. (2002)
ABCG2 (BCRP)	1	Placenta, brain	Apical	Daunorubicin, doxorubicin, etoposide, teniposide, methotrexate, mitoxantrone, topotecan	Doyle et al. (1998), Maliepaard et al. (1999, 2001), Volk et al. (2002), Allen et al. (2003), Volk and Schneider (2003), Wang et al. (2003), Aronica et al. (2005)
ABCA8	Not determined	Heart, skeletal muscle, liver	Not determined	Doxorubicin, digoxin	Tsuruoka et al. (2002)

cMOAT, canalicular multispecific organic anion transporter; BSEP, bile salt export pump; TAP, transporter associated with antigen processing; CFTR, cystic fibrosis transmembrane conductance regulator.
[a] Not an exhaustive list.

Table 1.3: ABC transporters involved in the transport of drugs **[20]**.

1.3 ABCC subfamily

The "C" subfamily of these transporters is one of the largest ABC subfamilies **[15]**. Its proteins are full transporters with various functions, such as ion transport, toxin secretion **[8],** and in particular drugs resistance (multidrug resistance-associated proteins (MRPs)) **[31-32]**. In this subfamily there are 12 members divided into three classes: the first one involved in regulation of potassium channels (ABCC8 and ABCC9, called SURs, sulfonylurea receptors), the second one involved in chloride ion channel (cystic fibrosis transmembrane conductance regulator (CFTR)), and the third one, with the other nine members, involved in drugs resistance (MRPs) **[8] [32-35]**. ABCC13, the thirteenth member of this family is a truncated protein that encodes a non-functional protein **[19] [36]**. Proteins codified by *ABCC* genes are divided into two groups: "long" transporters including MRP1, MRP2, MRP3, MRP6, MRP7, SUR1 and SUR2, and "short" transporters including MRP4, MRP5, MRP8, CFTR and probably MRP9; the difference between the two groups is the presence in "long" transporters of an extra NH_2-terminal TMD named as TMD0 and connected to the rest of the protein through a cytoplasmic loop indicated as L0 or as code CL3 (cytoplasmic loop 3) **[37-41]**, with five TMs and an extracellular N-terminus **[15]**. In "short" transporters there is only L0 linker without TMD0 domain **[42]** (**Fig. 1.4**).

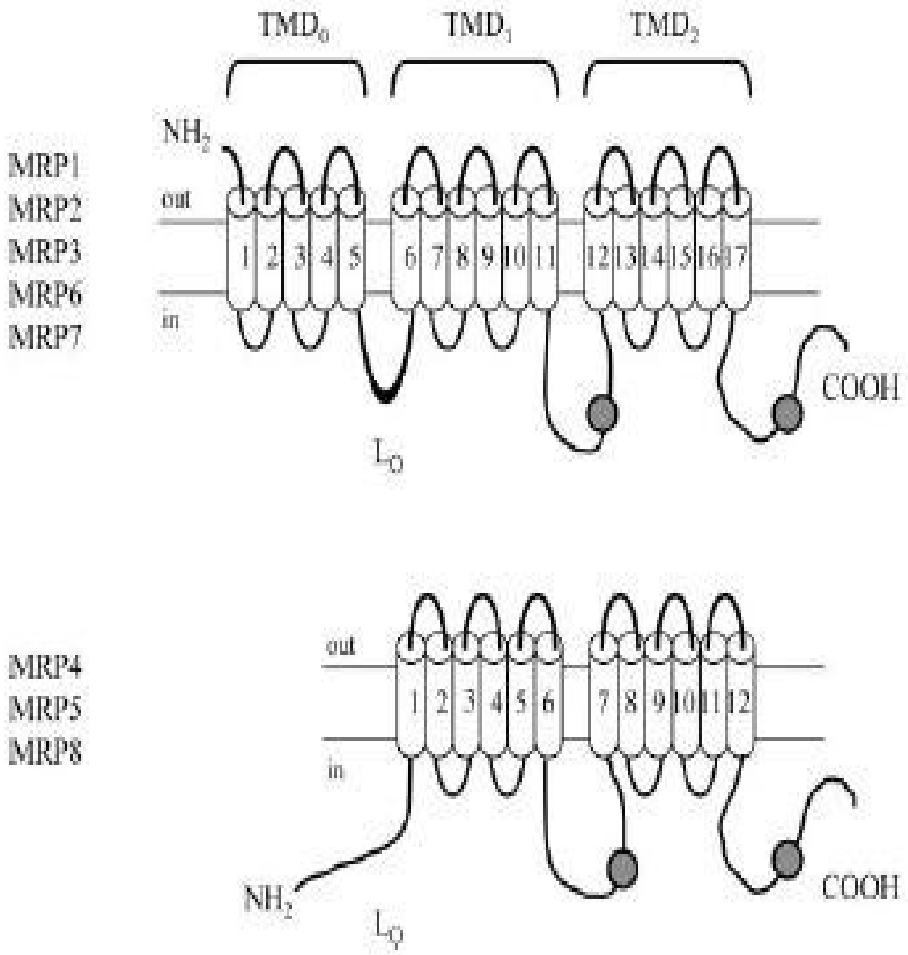

Fig. 1.4: Membrane topology of MRP proteins **[43]**.

TMD0 sequence is poorly conserved compared to the other two homologous TMDs, but the N-terminal region of L0 is relatively conserved both in ABCC "long" proteins and in ABCC "short" proteins **[10] [44]**. L0 is predicted to contain two amphipathic α-helicals in all ABCC proteins, including members without TMD0 **[45]**. The presence

of a TMD0 domain in the "long" ABCC transporters is unique and its eventual general function has to be clearly established **[39]**. For example, TMD0 of MRP1 does not play a crucial role either in transport activity of the protein, or in its proper routing into the basolateral membrane compartment, while the presence of L0 and of other domains is necessary for MRP1 transport activity and for the proper intracellular routing of this protein **[39] [46]**. Moreover, in this transporter the L0 region forms a distinct structural and functional domain, which interacts with the membrane and with the core region of the transporter **[39]**. TMD0 domain is important for trafficking and stabilization of MRP2 in the apical membrane **[47]**, and for the activity of SURs **[38] [48-49]**; L0 is essential for the localization of MPR2 **[45]** and for the regulation of trafficking of SURs **[49]**.

1.4 *ABCC6* gene and MRP6 protein

The human *ABCC6* gene belongs to the large ABCC subfamily and is mapped on chromosome 16 in position p13.1 **[50]**, between its two almost identical pseudogenes **[51]**. *ABCC6* gene is immediately near to *ABCC1* (that codifies MRP1 protein), but these gene are in opposite orientation, and the 3' ends are only 9 kb apart **[19] [35]** (**Fig. 1.5**). *ABCC6* gene spans about 73 kb of genomic DNA **[52]**, its mRNA about 5 kb with a coding sequence of 4.5 kb and it is made of 31 exons

(equal to the number of exons of *ABCC1*) **[35] [53]** that codify for the MRP6 protein (or ABCC6 protein) **[52]**.

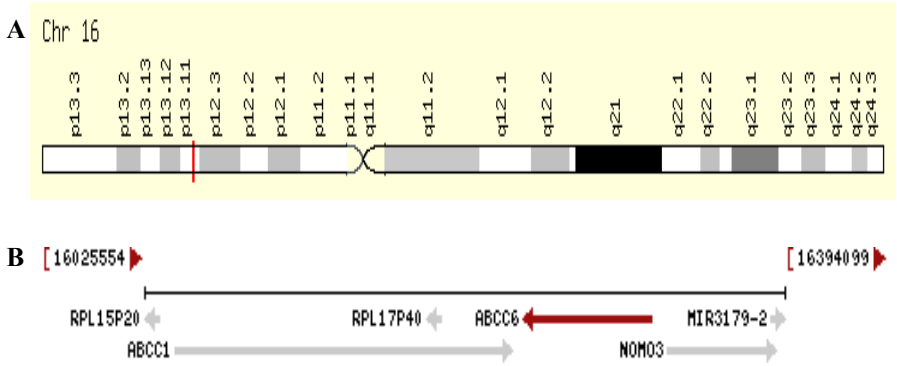

Fig. 1.5: Position of *ABCC6* gene on chromosome 16 (**A**). The region of chromosome 16 containing the *ABCC1* and *ABCC6* genes (**B**) **[43]**.

There is a splicing variant of *ABCC6* mRNA without exons 19 and 24 (*ABCC6 Δ19Δ24*), and, the product of the translation is a truncated protein that is suggested to be a half transporter **[54]**. *ABCC6* gene has about 45% of homology with the *ABCC1* gene **[35] [55]**. From mutational analysis, they have been found sequence variants of *ABCC6* gene deriving from duplication of the p13.1 region of the chromosome 16; these variants are *ABCC6* pseudogenes **[56]**. Two pseudogenes were found in the chromosome 16, *ABCC6-Ψ1* and *ABCC6-Ψ2*, at the terminal 5' of the *ABCC6* gene **[56]**. In particular, a polypeptide with 99 amino acids indicated as up-regulated gene 7 (URG7) **[57]** shows a high homology with the protein codified by *ABCC6-Ψ2* **[58]**. This protein, URG7, has the first 74 amino acids in common with MRP6 protein and their expression patterns are highly

similar because there is high degree of homology between *ABCC6* promoter and 5'UTR of *ABCC6-Ψ2* **[58]**. Expression tissue-specific of *ABCC6* gene is finely regulated by the presence on its promoter of sequences that bind specific transcription factors such as hepatocyte nuclear factor 4 (HNF4) **[59]** and tumor necrosis factor-α (TNF-α) which up-regulate and down-regulate, respectively, the promoter **[60]**. The protein MRP6 is codified by the *ABCC6* gene, as reported before, and has 1503 amino acids and a molecular weight of about 165 kDa **[35] [60-61]**. MRP6 is a "long" MRP transporter and it is formed by 17 TMs (grouped in three TMDs) and two cytoplasmic NBDs [TMD0(TMD-NBD)$_2$] **[62-63]** (**Fig. 1.4**), with conserved Walker A, Walker B and motif C **[52]**. It is mainly expressed in liver and kidney, in particular on the basolateral surface of hepatocytes **[41] [64-67]** and poorly expressed in salivary glands, in colon, in lungs and in the thyroid **[35]**. It is also expressed in acute myeloid leukemia **[68]**. Two possible functional models for transport of molecules through ABC transporters in general were proposed: the first one suggests that each NBD hydrolyzes an ATP molecule and that this reaction promotes the transport of a molecule of substrate **[19]**; the second one suggests that hydrolysis of an ATP molecule promote the substrate transport through the shift from a high- to low-affinity substrate binding state and hydrolysis of the other ATP molecule restores the high affinity substrate binding state **[15] [19]** (**Fig. 1.6**).

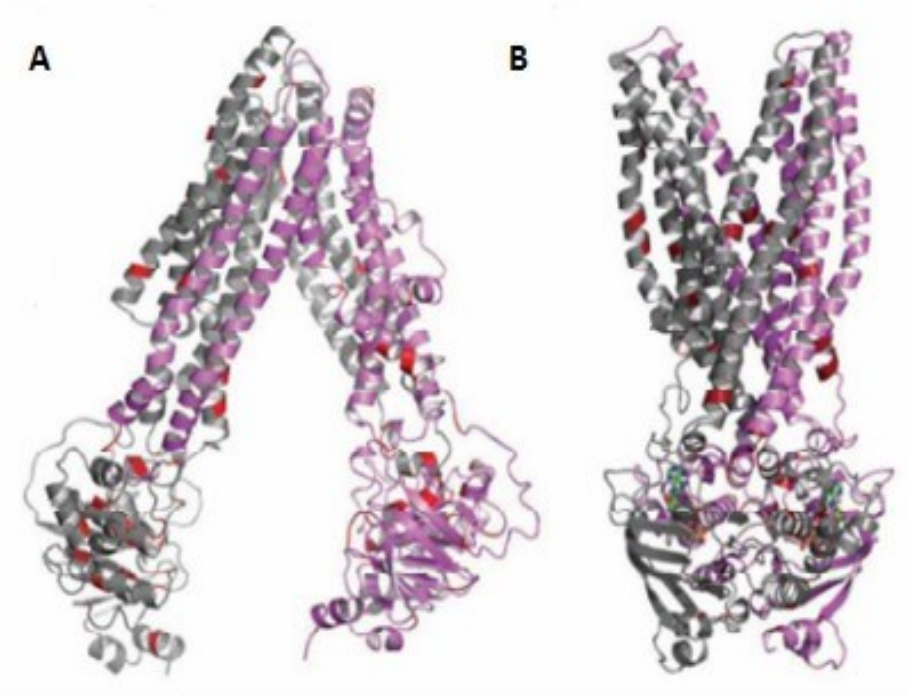

Figure 1.6: Three-dimensional model of MRP6: (**A**) nucleotide saturated conformational state and (**B**) nucleotide-free conformation. Missense mutations are indicated in red (modified from **[59]**).

In vitro experiments on chemically synthesized peptide E748-A785 (that correspond to a part of NBD1) **[69]**, on NBD1 **[70]** and NBD2 [**71**] produced in *Escherichia coli* by recombinant DNA technologies show the ability of these fragments in ATP binding. In particular, studies on NBD1 (D627-L851) show that the A- loop of this domain is important for affinity to ATP, while, NBD2 of MRP6 (T1252-V1503) is structured in order to bind and hydrolyze ATP with a lower efficiency [**71**]. *In vitro* transport assays on membrane vesicles enriched with

MRP6 show that this transporter is associated with ATP-dependent transport of glutathione S-conjugates; the transport of conjugates is a feature of MRPs that have the third TMD. MRP6 is also associated to low level of resistance to agents such as doxorubicin and teniposide **[15] [19] [23] [72-73]**: its natural substrate is not defined [**74**], and MRP6 transport is inhibited by organic anions such as probenecid [**75**]. Finally, the MRP6 is associated to the metabolism of vitamin K [**59**], and, recent studies in HepG2 cells show that low levels of expression of MRP6 induce a dysregulation of expression of some genes and a senescent-like phenotype (cellular cycle alteration) **[76-77]**.

1.5 *NT5E* gene and CD73 protein

The human *NT5E* gene is situated on chromosome 6 in position q14-q21 [**78**]; this gene spans 46 kb of genomic DNA, and it has a coding sequence of 1725 bp and is made of 9 exons that codify for CD73 protein **[78-79]**. Two transcripts of this gene have been identified as *NT5E-1* (3548 bp) and *NT5E-2* (3384 bp), and obtained by alternative splicing. The *NT5E-2* is a new splicing variant of *NT5E* gene expressed less than *NT5E-1* in normal tissues of human body but up-regulated in some pathological contexts such as in cirrhosis and in hepatocellular carcinoma (HCC) **[79]**. The difference between the two transcripts is exon 7 that is present in the longer transcript (*NT5E-1*) and absent in the

shorter transcript (*NT5E-2*); the two transcripts have the same N- and C- terminal [**79**] (**Fig. 1.7**).

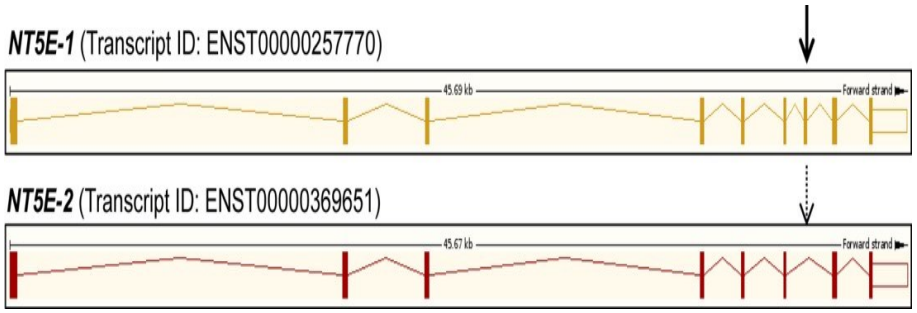

Fig. 1.7: Transcripts of *NT5E* gene: *NT5E-1* and *NT5E-2*. The black arrow indicates the position of exon 7 **[79]**.

In literature is reported that the expression of this gene is under the control of hypoxic conditions **[80-81]** and of several pro-inflammatory mediators such as transforming growth factor-β (TGF-β) or prostaglandin E2 (PGE2) **[82-83]**. It has also been reported that the increase of *NT5E* transcript, and of its correspondent CD73 protein in neoplastic tissues can play a key role in the onset and progression of neoplasia **[82]**. There is also a similar positive correlation between triple-negative breast cancer and *NT5E* levels associated to a poor prognosis **[84]**. The protein CD73, cluster of differentiation 73, is codified by the *NT5E* gene, as reported before, and has 574 amino acids and a molecular weight of about 70 kDa. *NT5E-1* encodes for CD73 long isoform (CD73L, 574 amino acids), the enzymatically active isoform, while, *NT5E-2* encodes for CD73 short isoform (CD73S, 524 amino acids), the enzymatically non-active isoform.

The mature CD73 form is a glycosylated dimeric enzyme located on the outer portion of the plasma membrane **[85-87]**, and it is present in different organs (such as colon, kidney, liver, heart **[88-89])** and cells (such as lymphocytes, macrophages and epithelial cells **[88])**. This protein is anchored to the external face of plasma membrane through glycosylphosphatidylinositol (GPI) situated on C-terminal **[86] [90-91]**, and, consists of two protein subunits united through non-covalent links. N-terminal domain coordinates the link of two divalent metal ions (Zn^{2+} and Co^{2+}) and is characterized by α/β-β-α-β secondary structure. C-terminal domain provides the linking pocket for AMP **[91]**, and has a sequence of non-charged and hydrophobic amino acids substituted with the GPI anchor linked to serine-523 **[92]**. The active site of the enzyme is located at the interface between the N- and C-terminal domains and shape among the residuals of both domains. Have been described different crystalline structures for CD73: if the conformation of CD73 is open it is characterized by a rather compact structure, if the conformation is closed it is characterized by a dimeric structure (**Fig. 1.8**).

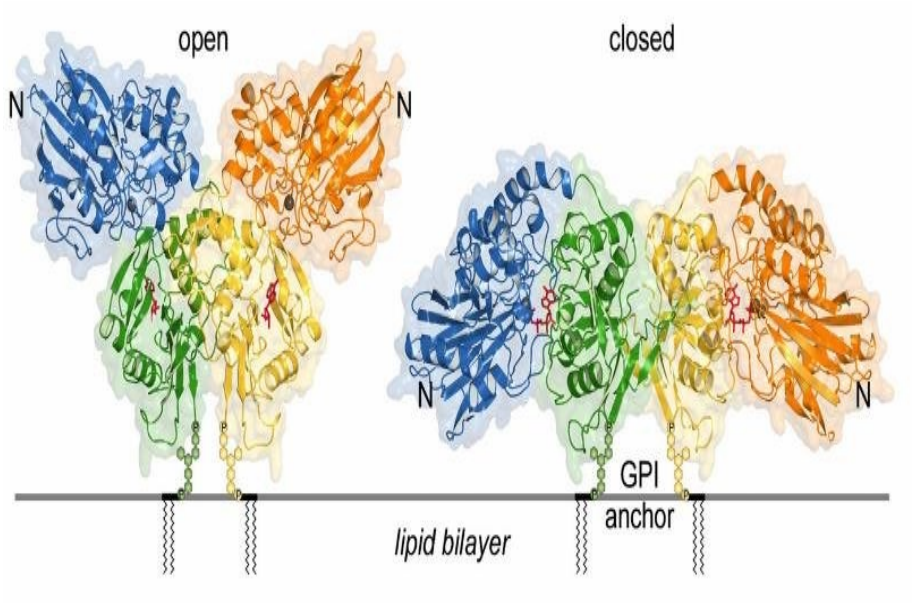

Fig. 1.8: Crystalline structure of CD73 in open and closed conformations **[90]**.

The two isoforms show different functions: CD73L is the isoform enzymatically active, an ecto-5'-nucleotidase, able to catalyze the conversion of extracellular AMP, produced by ENPP1 protein, to adenosine and P_i **[85]**; CD73S is the isoform catalytically inactive, unable to dimerize, but able to link both with the calnexin and with CD73L promoting proteasome-dependent CD73L degradation **[79]**. For its role in the production of extracellular adenosine CD73 can be considered a fundamental actor in the regulation of immunity response and in other pathways (for example: inflammation, ischemia, tissue fibrosis **[93]**). CD73-adenosine pathway is an important immunosuppressive pathway and this property is linked to its ability of tumor-promoting (via A_{2a} and A_{2b} adenosine receptors **[94]**).

The adenosine is a strong immune-suppressor, in particular, of antitumor T-cells response **[95]**. Increasing evidence shows that CD73 participates in tumor immune-escape by inhibiting the activation, clonal expansion, and homing of tumor-specific T cells **[96]**; the adenosine decreases the ability of natural killer cells (NK-cells) to produce TNF-α, to promote lytic activity **[97]**, and to decrease the activity of macrophages **[98]** and dendritic cells **[99-100]** (**Fig. 1.9**).

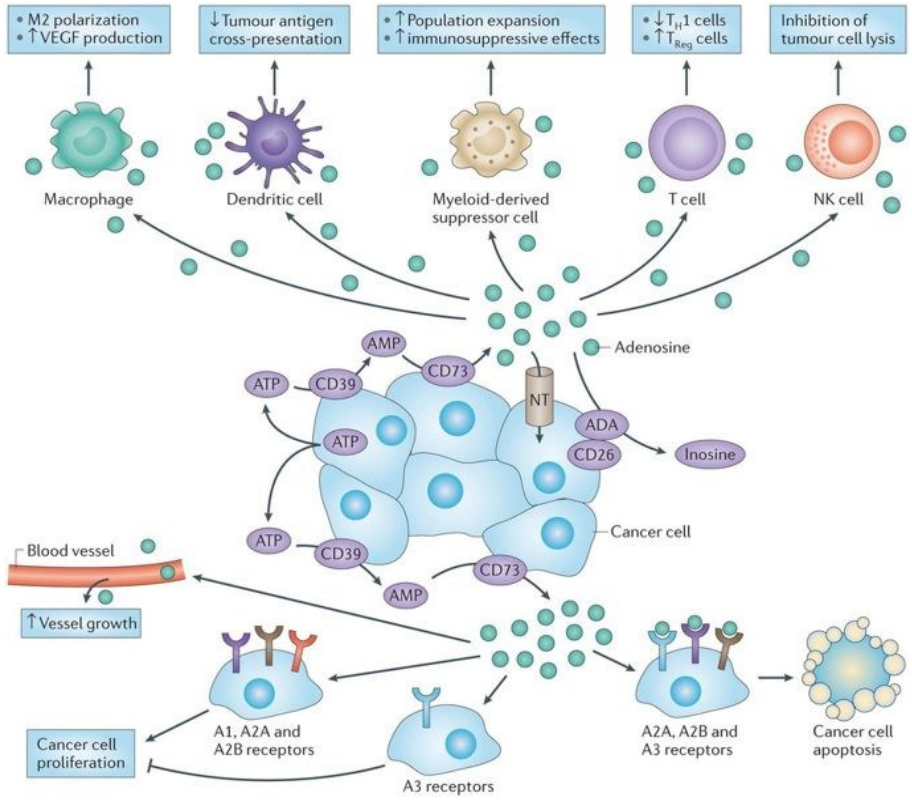

Fig. 1.9: The effects of adenosine (produced in cancer cells by CD73) on immunity response and on its receptors **[101]**.

Furthermore, CD73 is involved in drug resistance **[102]**, in tumor growth **[103]**, tumor metastasis (through binding to glycoproteins of the extracellular matrix (ECM), such as fibronectin and laminin) **[104-106]** and tumor angiogenesis **[107]**. In particular, recent studies show that in some types of cancer CD73 could promote the migration and invasion of cancer cells through regulation of EGFR expression, in others type of cancer, it could be an important regulator of epithelial-mesenchymal transition **[99]**. Different strategies are studied to control this protein using inhibitors, such as AOPCP, α,β-methyleneadenosine-5'-diphosphate, or using antibodies. CD73 is related to the metabolism of nucleotides and nucleosides (cellular messengers), and it can control different cellular processes in purinergic system. The purinergic system is a system deputed to cellular proliferation and transformation, cellular cycle progression, metabolic changes, cell-to-cell interactions, cytokine and chemokine secretion, inhibition of lipolysis, promotion of fatty liver insulin resistance, intracellular pathogen removal and generation of reactive oxygen species (ROS) **[108]**. Extracellular adenosine regulates a variety of physiological processes (previously mentioned) using a family of four receptors related to G-protein (A_1, A_{2a}, A_{2b}, A_3) each of which is characterized by a single pharmacological profile and tissue distribution. A_1, A_{2a} and A_{2b} protein sequences are highly conserved across mammalian species, while, A_3 is more variable. In human, A_1, A_{2a} and A_3 are considered as high affinity receptors for adenosine (K_i about 100-300 nM), while A_{2b} receptor has a lower affinity for adenosine (K_i about 15 μM) **[109-110]**. All these receptors

show a structure with seven transmembrane α-helicals, with an extracellular N-terminus and an intracellular C-terminus. Finally, these receptors perform their specific functions in different tissues because they regulate the cAMP levels differently (in particular, A_1 and A_3 receptors are coupled to inhibitory $G_{i/o}$ proteins, while, A_{2a} and A_{2b} receptors are coupled with to stimulating G_s proteins **[111])**.

1.6 Ectopic mineralization

The physiological process that provides for the formation of bone matrix and the functionality of skeletal tissue is known as mineralization (or calcification). This phenomenon, which is tightly controlled and restricted to specific body regions **[51]**, can also occur in soft tissues and it is known as ectopic mineralization. This type of pathological calcification occurs when calcium and phosphate complexes form hydroxyapatite crystals and they settle in the soft tissues causing serious consequences at the clinical level. Moreover, this complex multifactorial metabolic process is associated with different clinical conditions such as aging and diabetes **[112]**. There have been many advances in the study of ectopic mineralization processes both in terms of molecular mechanisms and of single gene disorders characterized by phenotypic traits typical of calcification processes; the following table shows the main diseases belonging to

ectopic mineralization (**Table 1.4**). In particular, Pseudoxantoma Elasticum (PXE) and Arterial calcification due to CD73 deficiency (ACDC) are related to *ABCC6* and *NT5E* gene mutations **[112]**.

Human Disease	Phenotypic Features	Arterial and cartilage calcification
Pseudoxanthoma elasticum (PXE)	Mineralization in the skin, eyes and cardiovascular system	*ABCC6*, ATP-binding cassette C subfamily, member 6
Generalized arterial calcification of infancy (GACI)	Arterial calcification, joint and spine ossification	*ENPP1*, Nucleotide pyrophosphatase/ phosphodiesterase 1
Arterial calcification due to CD73 deficiency (ACDC)	Vascular and joint calcification	*NT5E*, CD73
Normophosphatemic familial tumoral calcinosis (NFTC)	Ulcerative mineralization lesions in skin	*SAMD9*, Sterile alpha motif domain containing 9
Hyperphosphatemic familial tumoral calcinosis (HFTC)	Mineralization masses in skin	*KL*, Klotho, *GALNT3*, ppGaNTase-T3, *FGF23*, Fibroblast growth factor 23
Multiple vitamin K-dependent coagulation factor deficiency	Vitamin K-dependent coagulation factor deficiency, PXE-like skin changes	*GGCX*, Vitamin K-dependent gamma-carboxylase
Keutel syndrome	Arterial and cartilage calcification	*MGP*, Matrix gla protein

Table 1.4: Diseases characterized by ectopic mineralization **[112]**.

Calcium and phosphate precipitation is highly regulated by calcification inducers and inhibitors **[113-114]**. In particular, inorganic pyrophosphate (PP_i) **[115]** acts as a powerful inhibitor of mineralization; phosphate (P_i) is a pro-mineralization factor, and an appropriate PP_i/P_i ratio is essential for preventing the ectopic

mineralization under homeostatic conditions **[112] [116]**. Alterations of the metabolic pathway of extracellular ATP can be considered among the main causes of the manifestation of these pathological forms of mineralization. ATP, a precursor of PP_i and P_i, is released by the liver cells **[115] [117]**: its passage in the extracellular environment is facilitated by membrane transporters such as ABCC6 (other mechanisms are vesicular exocytosis, hemichannel connexion and pannexin channel **[118]**), and, recently, it has been suggested that, in pathological conditions, the loss of the ABCC6-dependent outflow of ATP would cause an alteration of the extracellular PP_i/P_i ratio **[119-120]**. Then, ATP is converted, in the vascular system of the liver, into PP_i and AMP, by ENPP1 protein, an ecto-nucleotide pyrophosphatase/phosphodiesterase 1, encoded by *ENPP1* gene **[121]**. AMP is converted into adenosine (an activator of the purinergic pathway) and P_i by CD73 **[85] [121]**. ABCC6 protein is thus involved in the production of extracellular adenosine and therefore could be involved in the activation of the purinergic pathway; however, the mechanism through which ABCC6 dysfunction causes diminished ATP release remains an enigma **[122]**. Finally, PP_i is converted in two molecules of P_i by TNAP protein, a tissue non-specific alkaline phosphatase, encoded by *TNAP* gene. For its ability to produce P_i, TNAP can be considered another important factor that controls the mineralization processes **[85]**, while, adenosine is considered an inhibitor of TNAP **[86]**. The reactions above mentioned are well schematized in the **Fig. 1.10**. Moreover, in recent years some studies

have hypothesized that adenosine could control the phenomenon of ectopic calcification not only by acting on TNAP expression, but also by activating the A_{2a} receptor and consequently the membrane translocation of the protein ENPP1, whose expression is crucial in the regulation of the processes of mineralization of soft tissues **[123]**.

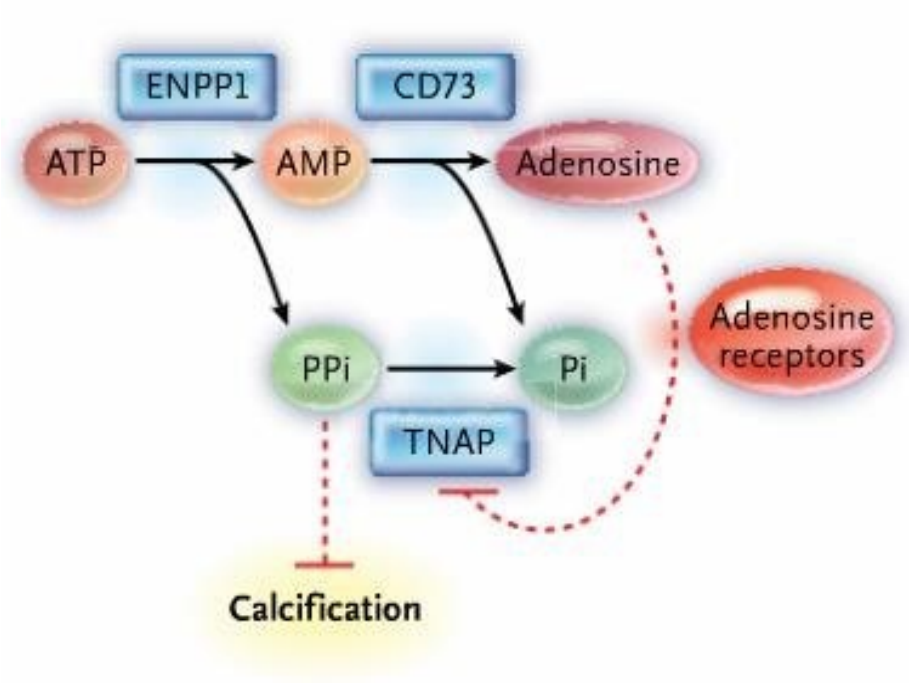

Fig. 1.10: Pathway of extracellular ATP **[85].**

At the moment, it is not known the mechanism through which ABCC6 promotes the release of ATP in extracellular space. It is not defined whether ABCC6 directly or indirectly transports ATP **[119]**. Moreover, it is not clear whether ABCC6 may favor the activation of the

purinergic system, and therefore regulate some fundamental physiological processes such as proteic, glucidic, and lipidic metabolisms, immunity and mineralization processes **[124-126]**. Other important actors of mineralization processes in soft tissues are: matrix gla protein (MGP), osteocalcin (OC), osteopontin (OPN), bone morphogenetic protein-2 (BMP-2) and alpha 2-Heremans-Schmid glycoprotein (Fetuin-A) **[113]**. In particular, MGP acts through the repression of BMP-2 and consequently is an inhibitor of formation of calcium crystals **[113]**. Fetuin-A is an important serum carrier of calcium and phosphate and is an inhibitory factor of calcification of soft tissues **[113]**. OPN, an acidic secreted phosphoprotein, is involved in blocking hydroxyapatite deposition and promoting crystal resorption **[127]**.

1.7 Pseudoxanthoma Elasticum (PXE)

Alterations in relationships of factors involved in mineralization of soft tissues promote an ectopic mineralization that causes different diseases such as Pseudoxanthoma Elasticum (PXE). PXE (OMIM, online Mendelian inheritance in man, 264800) is a disease caused by mutations of *ABCC6* gene. There have been found more than of 300 mutations in *ABCC6* NBD domains such as deletions, insertions or substitutions **[52] [128-130]**, as reported in **Fig. 1.11**. R1141X (where X

is a stop codon), is the most frequent mutation (about 30%); EX23_29del deletion is also recurrent (about 10%) in European patients suffering from PXE **[52] [130-131]**. Furthermore, some mutations cause truncated forms of the protein and/or ABCC6 incorrect localization.

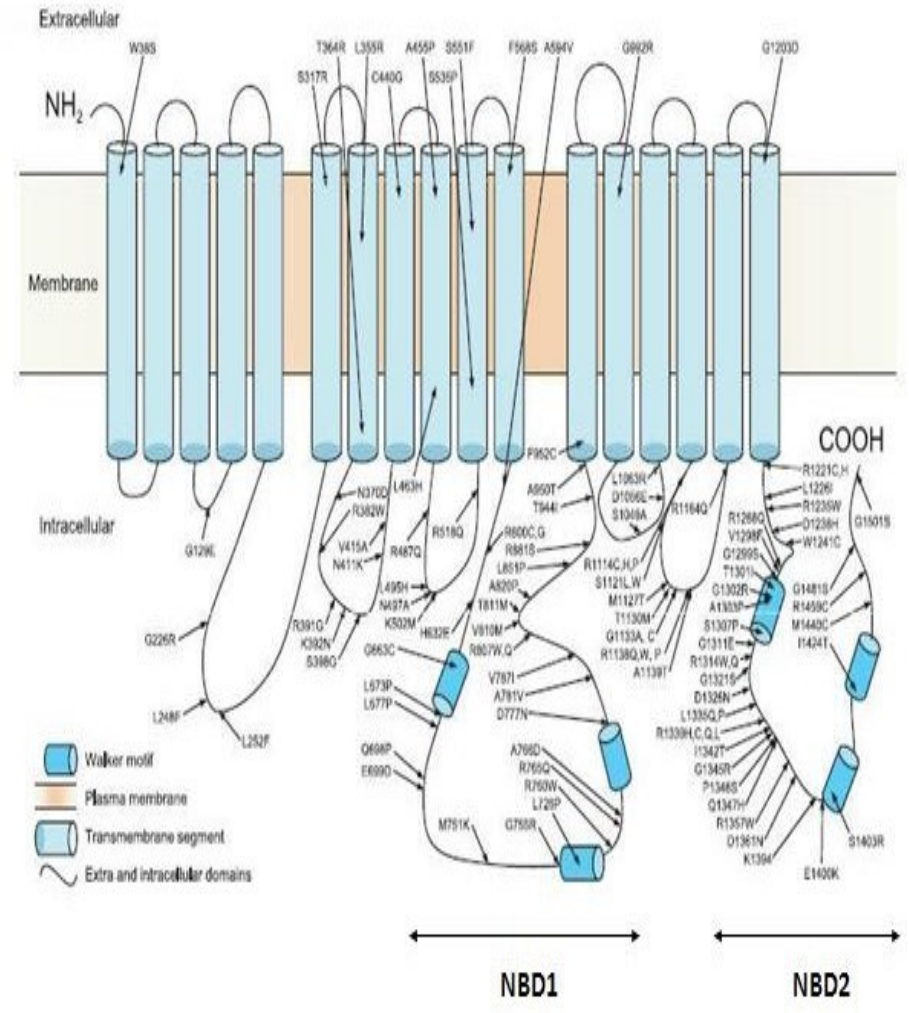

Fig. 1.11: Schematic representation of ABCC6 protein with the positions related to mutations identified in patients with PXE **[61]**.

This disease is an autosomal recessive disorder characterized by calcified and fragmented elastic fibers at level of the skin (plaques), the retina (peau d'orange, retinal angioid streaks, break of Bruch's membrane **[129]**) and the vascular wall (atherosclerosis, angina pectoris) **[122] [132-133]**, as reported in **Fig. 1.12**.

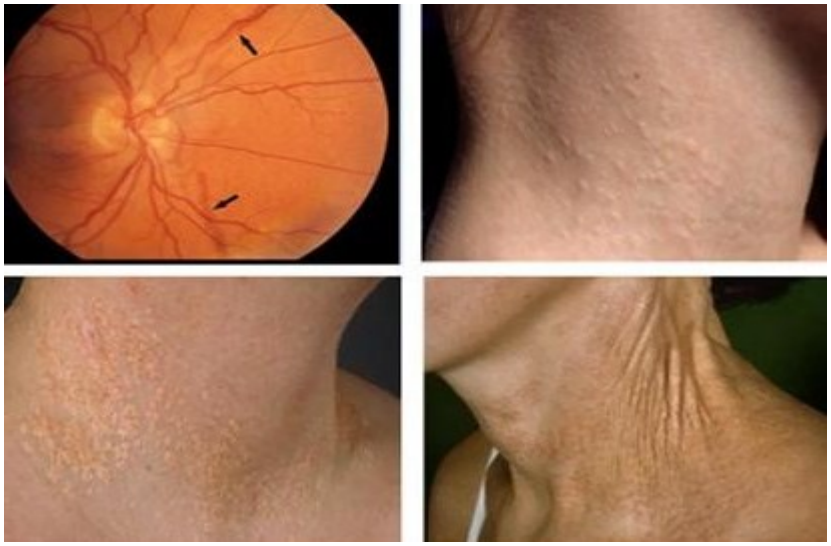

Fig. 1.12: Typical manifestations of PXE **[134]**.

The prevalence of PXE is unknown. It is estimated its presence in about 1:50,000-1:100,000 people **[132] [135]**, with a slight female predominance **[136]**. This pathology is sometimes underdiagnosed for its rarity and for its highly variable phenotype **[132]**. Heterogeneity phenotype of PXE suggests the influence in the development of the pathology of different environmental factors such as nutrition **[132]**, and, in particular, mutations in other genes **[132]**. At the moment there

are no pharmacological care for this pathology. In PXE patients all organs of the body show extracellular matrix alterations, but eyes and skin are more severely involved independently of the type of mutation **[131]**. Usually the onset of the PXE occurs in late childhood or adolescence **[59]** and clinical manifestations progress with age **[131]**. Among the first manifestations of PXE we can find the appearance of yellow-ivory soft papules with a reticular pattern **[132]** and of plaques in the skin causing the lost of elasticity at level of antecubital fossae or sides of the neck **[52] [129]**; later these signs appear at the back of knees and at level of oral mucosa and anogenital skin **[132]**. In PXE patients we also find alterations of Fetuin-A, BMP-2 and vitamin K **[59]**, but, we don't find alterations in levels of calcium, phosphate or in the inflammation processes **[114]**. There is no satisfactory correlation between genotype and phenotype **[137]**, and diagnosis of PXE comes from the individuation of fragmented calcified elastic fibers thanks to a skin biopsy using von Kossa staining **[59]**. The different manifestations of PXE were standardized in 2007 and the system that groups them into various classes is called Phenodex (PXE phenotype index). The molecular mechanism that induces onset of PXE (when ABCC6 is not functional) is not clear **[138]**. The presence of low levels of ABCC6 protein in tissues of patients suffering from PXE (**Fig. 1.13**) suggests that PXE is a metabolic disorder **[139]**, resulting in the alteration of transport of substances from liver and from kidney to blood **[140]**.

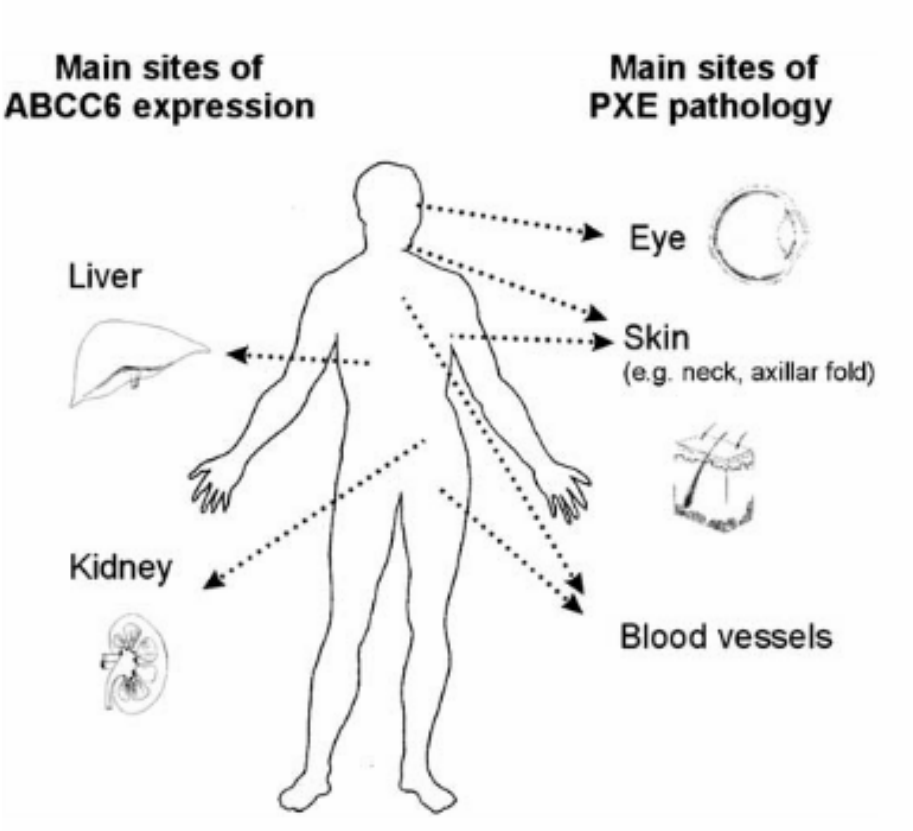

Fig. 1.13: Tissues in which ABCC6 protein is expressed and tissues affected by PXE disease **[52]**.

It is known that hepatic ATP is excreted with a mechanism related to the ABCC6 protein. Reducing the activity of ABCC6 decreases PP_i at the extracellular level **[120]**; it was, also, observed an alteration of metabolites related to ATP in PXE patients **[141]**. In PXE patients was observed a reduced concentration of vitamin K, cofactor of γ-carboxylation, a fundamental reaction activating some anti-mineralizing proteins such as OC and MGP **[113]**.

In stable *ABCC6*-silenced HepG2 cells, we find an increase of pro-mineralization factors and a decrease of anti-mineralization factors: TNAP is up-regulated at transcript, protein and activity levels; *NT5E*/CD73 are downregulated at transcript and protein levels; *Fetuin-A* and *OPN* result down-regulated at transcript level **[76]**. On the basis of these information for the treatment of PXE there are experimented the following treatments: oral administration of PP_i **[142]**, oral administration of bisphosphonates, a stable form of PP_i **[143]**, oral administration of phosphate binders **[144]**, modifiers of protein conformation (such as sodium 4-phenylbutyrate) that target the protein to the plasma membrane **[145]**.

1.8 Arterial calcification due to CD73 deficiency (ACDC) and generalized arterial calcification of infancy (GACI)

Other important diseases related to ectopic mineralization are arterial calcification due to CD73 deficiency (ACDC) and generalized arterial calcification of infancy (GACI); these diseases, together with PXE, are characterized by similar phenotypic traits, and by alterations of some factors involved in balancing pro-mineralization and anti-mineralization processes (**Fig. 1.14**).

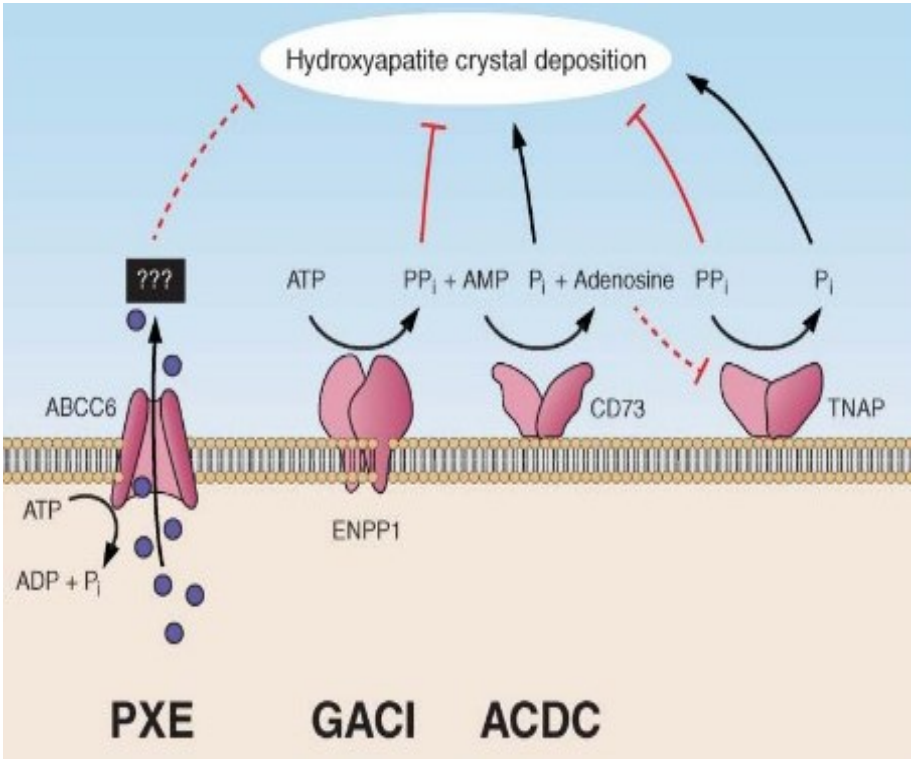

Fig. 1.14: Homeostasis of calcification processes depends on the functioning of some enzymes. Some diseases caused by altered functions of these proteins are: PXE, GACI and ACDC **[146]**.

ACDC (OMIM, 211800) is a disease caused by mutations in *NT5E* gene, and it is a rare autosomal recessive disease characterized by the calcification of the large arteries of upper and lower limbs and by the calcification of coronary circulation **[85] [121] [139]**. For these clinical manifestations ACDC is also known as CALJA (calcification of joints and arteries) (OMIM, 211800) **[112]**. In literature it is related to new mutations of *NT5E* gene **[147]**. The most frequent mutations observed

in patients affected by ACDC are S221X (where X is a stop codon), C358Y and a truncated protein caused by 1609dupA **[85]**. In patients affected by ACDC we find a decrease of *NT5E* gene and a decrease of protein and activity of CD73 protein **[85]**, with low levels of adenosine, but normal serum levels of calcium, phosphate and vitamin D. The reduction of extracellular adenosine, caused by alterations of CD73 activity, seems to increase the activity of TNAP protein, and, consequently, the hydrolysis of PP_i increases the ratio between P_i and PP_i favoring the calcification processes **[85-86] [148]**. The addition of adenosine reverses these effects both in presence of ACDC or in presence of PXE fibroblasts **[114]**. GACI (OMIM, 208000) is an autosomal recessive disease caused by mutations of *ENPP1* gene, that is mapped on chromosome 6 in position q22-q23 **[86] [149]**. In patients affected by GACI we find a severe calcification of the elastic lamina inside the large and medium-sized arteries producing an arterial stenosis and others cardiac diseases **[150-151]**, and a decrease of PP_i levels **[149]**. GACI is a rare condition (reported in about 180 individuals **[152-153]**) whose prognosis is extremely poor (85% of affected infants die within the first six months of life **[154]**). As reported in literature, mutations in *ENPP1* gene could be associated with a PXE phenotype **[155]**, but also mutations in *ABCC6* gene could be associated to GACI disease **[64] [155]**. The formation of PP_i as the result of the sequential action of ABCC6 and ENPP1 proteins could explain the correlation between PXE and GACI, while low levels of PP_i in PXE and GACI could explain their histopathological similarity.

1.9 Probenecid

Probenecid, 4-dipropylsulfamoylbenzoic acid, is a uricosuric drug used for the treatment of gout. In gout an excessive presence of uric acid, produced by the metabolism of purine nitrogenous bases, could promote the precipitation of uric acid in the form of crystals. Probenecid is able to increase the excretion of uric acid and block the reuptake at kidney level **[156]**. Probenecid, generally, is administered orally; its absorption is rapid and complete and it is metabolised in the liver and eliminated by kidneys. The inhibition of the renal tubular transporter thanks to probenecid is also clinically exploited to increase the effective concentrations of antibiotics, chemotherapeutics, and other medications **[157]**. Side effects can be nausea, vomiting, fatigue and skin rash. The block of cAMP or cGMP release from erythrocytes **[158-159]**, and, ATP release from glia cells **[160]** by probenecid show its involvement in the efflux of these substrates. For these reasons experiments have been carried out to investigate the correlation between probenecid and the mechanisms involved in the transport of ATP (such as pannexins, connexins and ABC transporters). The results of a study, in particular, show that probenecid is a powerful inhibitor of pannexin 1 channels, but it has no effects on connexin channels **[157]**. Probenecid is, also, a known ABC transporters inhibitor **[157] [161]**. In fact, a study show that probenecid is an effective chemosensitizer for MDR cells that overexpress MRPs, and, is a potential candidate for clinical use to reverse MDR phenotype **[162]**. The concentrations of

probenecid (0.1-0.5 mM) that reversed MRP-mediated MDR are readily achievable in vivo **[162]**. Moreover, ABCC6 transport is inhibited by organic anions such as probenecid **[75]**: 1 mM of probenecid, efficiently, inhibits MRP1 and MRP2, but it poorly inhibits ABCC6 (about 30%) **[75]**. Finally, it is also known that CD73 is related to MDR proteins, and, its increase in different kinds of tumors **[89]** such as glioblastoma multiform (GBM) **[163]** and breast cancer (where it is over-expressed) promotes a highly aggressive tumor phenotype **[105]**. In literature it is reported that using AOPCP, a CD73 inhibitor, it is possible to reverse the MDR phenotype in GBM cells through the decrease of expression and activity of MRP1 **[163]**; for these reasons, it could be possible to control CD73 expression using an inhibitor of ABC protein, such as probenecid.

Aims:

The aim of this scientific research is to study the role of ABCC6 protein in some fundamental cellular processes. It is known that ABCC6 protein is able to transport ATP outside the cells and that mutations in *ABCC6* gene cause the Pseudoxanthoma Elasticum (PXE) a disease characterized by a decrease of the amount of extracellular PP_i, by the ectopic mineralization processes in some regions of the body and by the alteration in releasing of extracellular nucleotides and purine nucleosides, with a possible involvement of the activation of purinergic system. ATP transported by ABCC6 is catalysed into PP_i and AMP by ENPP1 protein; AMP is catalysed into P_i and adenosine by CD73 protein. So we intended to investigate the role of ABCC6 in the purinergic system. In this scientific research we want to verify the effect of the ATP and of the adenosine, on the expression of ABCC6 and CD73 protein. In particular, the transport activity of ABCC6 in HepG2 cells was blocked by an inhibitor of ABC proteins and the gene and protein expression analysis was carried out on *NT5E*/CD73. Other effects related to the low activity of ABCC6, due to this inhibitor, have been studied with a particular attention to the role of CD73 in cancer progression. Furthermore, similar experiments were performed using doxorubicin and quercetin and other cellular types in order to highlight the correlation between ABCC6 and CD73. We performed some experiments in collaboration with the University of Bari and with the IRCCS-CROB of Rionero in Vulture.

Materials and Methods

All compounds used for the following scientific research were purchased from Sigma-Aldrich (unless otherwise indicated).

2.1 Mammalian cellular culture

Human embryonic kidney 293 cells (HEK293), human hepatocellular carcinoma cells (HepG2), human hepatocellular carcinoma well differentiated cells (HuH-7) and triple-negative human breast cancer poorly differentiated cells (MDA-MB-231) are the adherent mammalian cell lines used for the experiments of my research (**Fig. 2.1**). These cells were grown in Forma STERI-CYLE CO_2 incubator and were maintained in Dulbecco's Modified Eagle's Medium (DMEM) containing 4.5 g/L glucose, supplemented with 10% fetal bovine serum (FBS), 2 mM L-glutamine, penicillin (100 U/mL), and streptomycin (100 mg/mL) in polystyrene flasks at 37°C, in an atmosphere humidified with 5% of CO_2. The cell splitting was obtained using Trypsin-EDTA solution (1X) for 5 minutes at 37°C to detach cells from flasks; trypsin was inactivated with a double volume of complete medium. All cells (except HEK293) were washed with PBS 1X, phosphate buffered saline, (140 mM NaCl, 10 mM Na_2HPO_4, 2.7 mM KCl and 1.8 mM KH_2PO_4, pH 7.4) before trypsin treatment. All solutions were warmed at 37°C using Water bath SWBD Stuart before use. Cells were observed with microscope Nikon Eclipse TS100

and counted using Burker chamber. The number of cells was calculated with the following formula:

cells/mL = counted cells ∗ dilution factor ∗ 10^4 / number of counted squares

After counting, an appropriate group of cells was seeded in flasks (see next sections). The pellets of non-treated or treated cells were obtained transferring opportunely the cells into tubes and centrifuging them at 1200 rpm for 5 minutes at 4°C. After elimination of the medium, the pellets were immediately used or stored at -80°C.

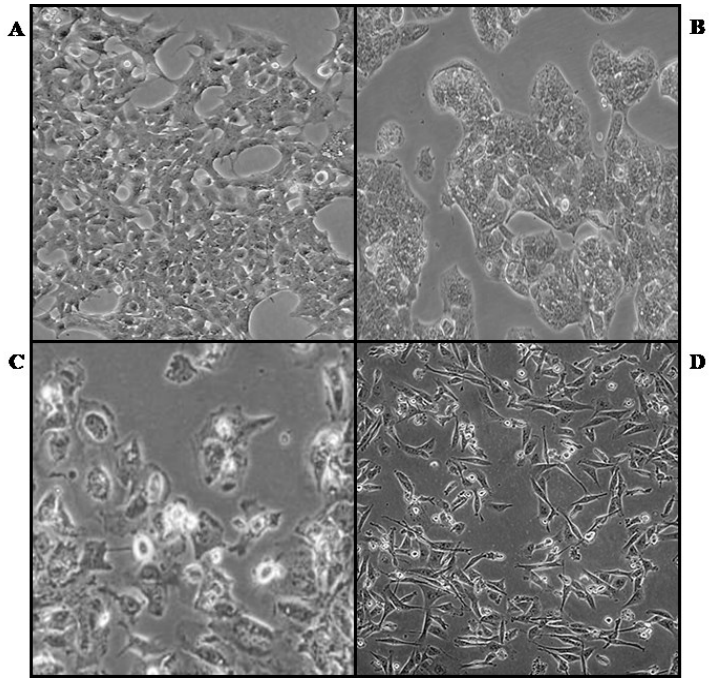

Fig. 2.1: Representative images of mammalian cellular culture: HEK293 cells (**A**), HepG2 cells (**B**), HuH-7 cells (**C**) and MDA-MB-231 cells (**D**).
These images are taken from ATCC (American Type Culture Collection).

2.2 Treatment with Probenecid

Probenecid is a well-known inhibitor of multidrug resistance-associated proteins, MRPs **[162]** (**Fig. 2.2**). It was dissolved in dimethyl sulfoxide (DMSO) at 30 mg/mL (100 mM) as stock solution and it was then diluted with DMEM to the desired concentrations. The final concentration of DMSO did not exceed 1% v/v in the MTT viability assay and in measurement of intracellular ROS assay; in the other experiments the final concentration of DMSO did not exceed 0.25% v/v. Control cells were treated at the same final percentage of DMSO. 6×10^5 HepG2, HuH-7 or HEK293 cells and 2.5×10^5 MDA-MB-231 cells were seeded in each well of 6-wells plates in 2 mL of DMEM. After 24 hours from their seeding, these cells were treated for 24 and 48 hours with 250 μM of probenecid.

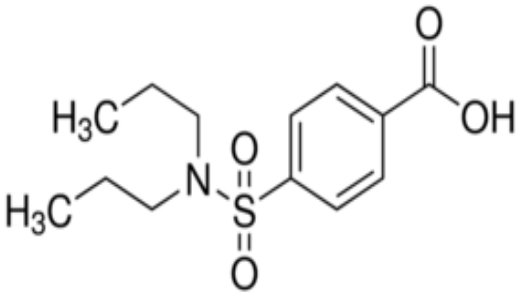

Fig. 2.2: Structure of Probenecid.

2.3 Treatment with adenosine

Adenosine is produced primarily from the metabolism of ATP and exerts pleiotropic functions throughout the body **[164]** (**Fig. 2.3**). It was dissolved in dimethyl sulfoxide (DMSO) at 80 mg/mL (300 mM) as stock solution and it was then diluted with DMEM to the desired concentrations; the percentage of DMSO deriving from adenosine is negligible if compared with the amount of DMSO used for probenecid. 6×10^5 HepG2, HuH-7 or HEK293 cells and 2.5×10^5 MDA-MB-231 cells were seeded in each well of 6-wells plates in 2 mL of DMEM. After 24 hours from their seeding, these cells were treated for 48 hours with 10 and 100 μM of adenosine. Other experiments using the cells, previously indicated, were performed in presence of both probenecid (250 μM) and adenosine (10 and 100 μM) for 48 hours.

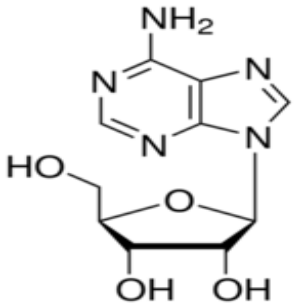

Fig. 2.3: Structure of adenosine.

2.4 Treatment with ATP

ATP, adenosine 5'-triphosphate, a component of energy storage and metabolism in vivo, is a substrate involved in cell signaling and in production of second messengers (such as cAMP) (**Fig. 2.4**). It was dissolved in PBS 1X at 27.5 mg/mL (50 mM) as stock solution, it was adjusted its pH value about neutrality, it was filtered and it was then diluted with DMEM to the desired concentrations. 6×10^5 HepG2, HuH-7 or HEK293 cells and 2.5×10^5 MDA-MB-231 cells were seeded in each well of 6-wells plates in 2 mL of DMEM. After 24 hours from their seeding, these cells were treated for 48 hours with 50 and 500 μM of ATP. Other experiments using the cells, previously indicated, were performed in presence of both probenecid (250 μM) and ATP (50 and 500 μM) for 48 hours.

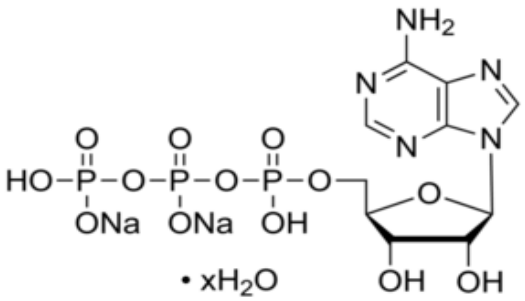

Fig. 2.4: Structure of ATP.

2.5 Treatment with Quercetin

Quercetin, a flavonoid, is another inhibitor of some multidrug resistance-associated proteins, MRPs **[165]** (**Fig. 2.5**). It was dissolved in dimethyl sulfoxide (DMSO) at 20 mg/mL (66 mM) as stock solution and it was then diluted with DMEM to the desired concentrations. In all experiments with quercetin, the final concentration of DMSO did not exceed 1% v/v. Control cells were treated at the same final percentage of DMSO. 6×10^5 HepG2 cells were seeded in each well of 6-wells plates in 2 mL of DMEM. After 24 hours from their seeding, these cells were treated for 24 hours with 165 μM of quercetin.

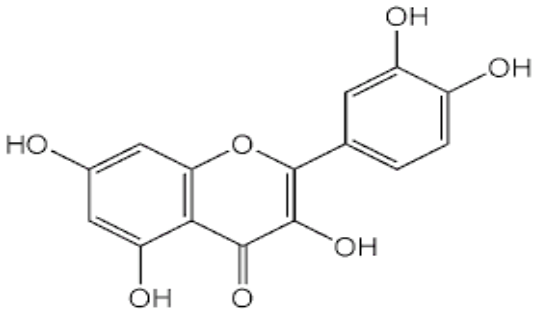

Fig. 2.5: Structure of Quercetin.

2.6 Treatment with Doxorubicin

Doxorubicin is an anthracycline and is a substrate of ABC proteins **[20]** (**Fig. 2.6**). It was dissolved in dimethyl sulfoxide (DMSO) at 10 mg/mL (17.24 mM) as stock solution and it was diluted with PBS 1X, and,

then, with DMEM to the desired concentrations. The final concentration of DMSO is negligible. Control cells were treated at the same final percentage of PBS 1X. The HepG2 cells were seeded in T25 flasks at about 50% of confluence in 5 mL of DMEM. After 24 hours from their seeding, these cells were treated with doxorubicin in the following way: for a week with 10 nM, for a week with 20 nM, for a week with 50 nM and then for a week with 100 nM.

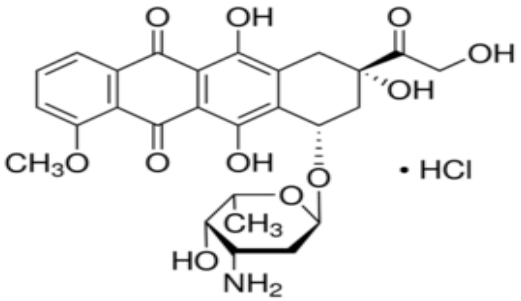

Fig. 2.6: Structure of Doxorubicin hydrochloride.

2.7 Stable transfection of *ABCC6* in HEK293 cells

Transfection is the process of introducing exogenous biological material (DNA, siRNA) into eukaryotic cells, in particular into mammalian cells (**Fig. 2.7**). This process can be transient if the genetic material does not integrate into the host genome, and, it can be stable if the genetic material is permanently integrated into the host genome. 2×10^5 HEK293 cells were seeded in each well of 12-wells plates

in 1 mL of DMEM. After 24 hours from their seeding (50-70% of confluence), the medium was changed and it was composed the transfection mix with 100 µL of incomplete medium and 3 µL of FuGene6 transfection reagent (Promega). This transfection mix was maintained for 5 minutes at 25°C and, then, mixed with 1 µg of empty Flag-pcDNA vector (pcDNA vector that codifies DYKDDDDK Flag tag, as control) or Flag-pcDNA containing sequence coding for *ABCC6* (*ABCC6*-Flag-pcDNA vector). After 15 minutes at 25°C, this transfection mix was added to cells drop by drop. The plates were rotated to distribute the added solution. Limiting dilution method was used to select individual clones. For 18 days the medium containing geneticin (800 µg/mL, Euroclone) was changed twice a week. As the clones grew, they were transferred in bigger culture flasks (the biggest once were T25 flasks); then, the cells were stored in cryovials or used for the experiments.

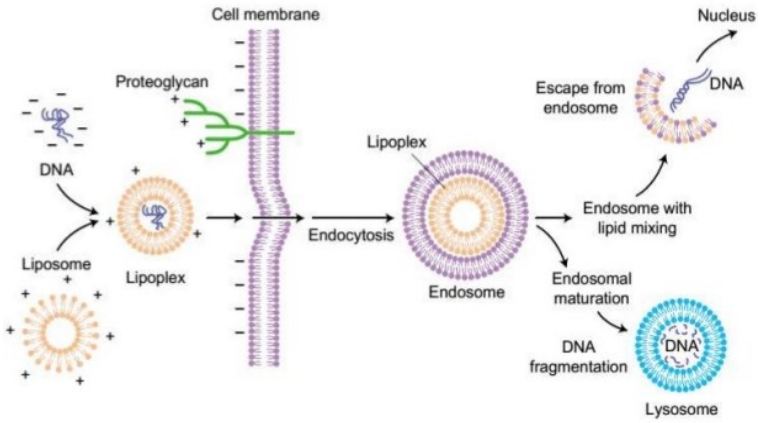

Fig. 2.7: Mechanism of transfection.

2.8 Doxorubicin efflux assay

It is known in literature that the ABCC6 transporter is also involved in transporting different drugs such as doxorubicin **[20]** (**Fig. 2.6**). For this reason the doxorubicin assay is important to understand the role of this transporter in the presence of probenecid, a specific inhibitor of MRPs. 3×10^5 HEK293 stably over-expressing *ABCC6* and control cells were seeded in each well of 12-wells plates, pre-treated with poly-D-lysine hydrobromide for 30 minutes, in 1 mL of DMEM. After 24 hours from their seeding, the medium was removed, and 300 µL of PBS 1X with 1 mM probenecid or with DMSO (as control) were added. The cells were incubated for 1 hour. The following steps were all performed in the dark to avoid the loss of fluorescence. Then in each well were added 5 µM of doxorubicin and the cells were incubated in the dark for 30 minutes at 37°C in 5% of CO_2. The cells were washed two times with cold PBS 1X and their external fluorescence was measured at different times using black 96-wells plates and GloMax Multi Detection System (Promega) with a blue filter (ex. 490 nm, em. 510-570 nm).

2.9 Viability assay

The 3-(4,5-dimethylthiazol-2-yl)-2,5-diphenyltetrazolim bromide (MTT) assay was used to assess the viability of cells treated with different compounds at different concentrations for different times of incubation. This is a colorimetric assay based on the conversion of 3-(4,5-dimethylthiazol-2-yl)-2,5-diphenyltetrazolim bromide salt, a yellow compound, into formazan, a violet compound, that absorbs at 570 nm (**Fig. 2.8**). The formazan produced by this reaction is directly proportional to the cell number and to the efficiency of mitochondrial enzymes of cells. 1×10^4 HepG2, HuH-7 or HEK293 cells and 8×10^3 MDA-MB-231 cells were seeded in each well of 96-wells plates in 100 μL of DMEM. After 24 hours from their seeding, the medium was removed and the cells were treated with different concentrations of probenecid (250, 500 and 1000 μM) for 24 and 48 hours. Another experiment in HepG2 cells was performed in the same conditions, above mentioned, but in presence of different concentrations of quercetin (165, 330, 660 μM) for 24 and 48 hours. The control cells were treated only with vehicle DMSO at the percentage of 1% v/v. After the treatment, the medium was removed and the cells were incubated with 100 μL of fresh medium containing 15% MTT for 4 hours at 37°C. The formazan crystals were finally dissolved for 1 hour at 37°C in 100 μL of a DMSO:isopropanol (1:1) solution with 1% of Triton X-100. MTT reduction was quantified by measuring

the light absorbance at 570 nm, with background subtraction at 630 nm, and by using a microplate reader Multiskan^{TM} GO Microplate Spectrophotometer (Thermo Scientific). Results were proportionally compared to the control cells. The cells were, also, observed thanks to a phase-contrast microscope and representative fields were photographed using a Nikon Coolpix P6000. Each test was repeated three times in triplicate.

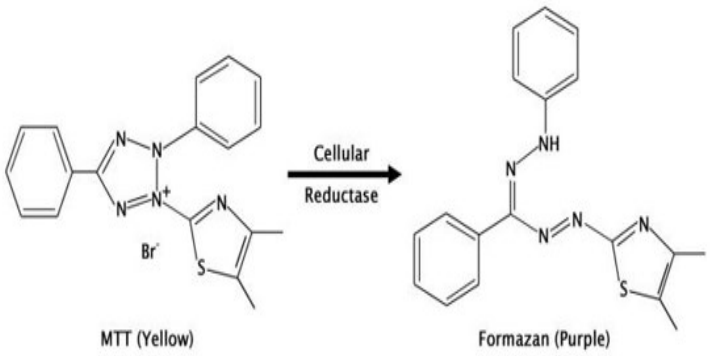

Fig. 2.8: Reaction of conversion of MTT salt (a yellow compound) in formazan (a violet compound).

2.10 Measurement of intracellular Reactive Oxygen Species (ROS)

The intracellular level of ROS was determined using a cell-permeable probe, 2',7'-dichlorofluorescein diacetate (DCFH-DA). This molecule, in the cell, is deacetylated by intracellular esterases and converted to

the dichlorodihydrofluorescein (DCFH) carboxylate anion, which is retained in the cell and oxidized rapidly into a highly fluorescent compound dichlorofluorescein (DCF) in the presence of ROS **[166]** (**Fig. 2.9**). 1×10^4 HepG2 cells were seeded in each well of dark 96-wells plates in 100 µL of DMEM. After 24 hours from their seeding, the medium was removed, and, the cells were treated with different concentrations of probenecid (250, 500 and 1000 µM) for 24 and 48 hours. The control cells were treated only with vehicle DMSO at the percentage of 1% v/v. As positive control of ROS presence, 500 µM of a tert-butyl hydroperoxide solution was used for 1 hour (1 hour before the end of treatment), only in control cells. Then, cells were treated with 10 µM of DCFH-DA for 30 minutes at 37°C. The fluorescence was measured by GloMax Multi Detection System (Promega) with a blue filter (ex. 490 nm, em. 510-570 nm). Results were proportionally compared to the control cells.

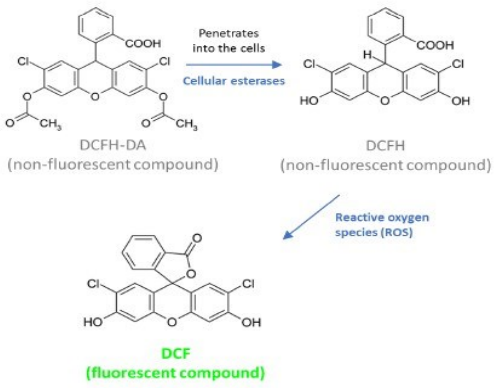

Fig. 2.9: Mechanism of DCFH-DA reaction.

2.11 Calcein assay

Calcein-AM is a non-fluorescent, hydrophobic compound that easily permeates (for diffusion) in living cells. The hydrolysis of calcein-AM by non-specific intracellular esterases **[167]** produces calcein, a hydrophilic, strongly green-fluorescent compound that is retained in the cytoplasm of the cells. This compound was insensitive to pH and to some cations (**Fig. 2.10**). It is transported out the cells by MRPs, except by P-gp and BCRP **[17]**. 3×10^5 HepG2 or HuH-7 cells and 1.3×10^5 MDA-MB-231 cells were seeded in each well of 12-wells plates in 1 mL of DMEM. After 24 hours from their seeding, the medium was removed, and the cells were treated with 400 µL of PBS 1X with 250 µM of probenecid or with 0.25% of DMSO (as control) for 1 hour. Another experiment in HepG2 cells was performed in the same conditions, above mentioned, but in presence of 165 µM of quercetin or with 0.25% of DMSO (as control). Following steps were all performed in the dark to avoid the loss of fluorescence. Then, both the treated and untreated cells were incubated with 1 µM of calcein-AM for 1 hour at 37°C in 5% of CO_2. After these treatments, the internal and the external fluorescence was measured using a black 96-wells plates and by GloMax Multi Detection System (Promega) with a blue filter (ex. 490 nm, em. 510-570 nm). The external fluorescence was measured taking 100 µL of medium from each well, while, the internal fluorescence was measured after lysing; the cells were lysed using 300

µL of TBS 1X, tris buffered saline, (150 mM NaCl and 10 mM Tris, pH 8.0) with 0.25% of SDS and transferred in tubes. After 15 minutes on ice, the tubes were centrifuged at 13000 rpm for 10 minutes at 4°C, and, the supernatants were used to measure the internal fluorescence (as previously described).

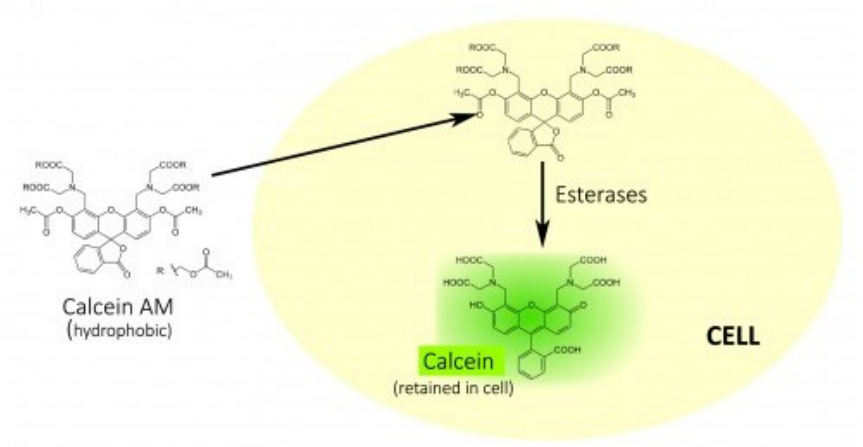

Fig. 2.10: Mechanism of Calcein-AM reaction.

2.12 RNA extraction from cellular lines

RNA was extracted from cellular pellets (6×10^5 cells) using Quick-RNA™ MiniPrep kit (Zymo Research) according to the manufacturer's instructions:

- 300 µL of RNA lysis buffer was added to each sample to resuspend and lyse cells;

- each sample was vortexed and centrifuged at 13000 rpm for 1 minute using the Microliter centrifuge Z 233 M-2 (Hermle Labor Technik GmbH);
- the supernatant was transferred in Spin-Away™ Filter (yellow) columns placed in collection tubes and centrifuged at 13000 rpm for 1 minute to eliminate the majority of genomic DNA (gDNA);
- an equal volume of 100% ethanol was added to the flowthrough and the mixed sample was transferred in Zymo-Spin™ IIICG (green) columns placed in collection tubes;
- each sample was centrifuged at 13000 rpm for 30 seconds and its flowthrough was eliminated:
- 400 µL of RNA wash buffer was added to wash column and it was centrifuged at 13000 rpm for 30 seconds;
- DNase I reaction mix: 64 µL of RNA wash buffer

  3 µL of DNase/RNase-free water

  5 µL of DNase I (1 U/µL)

  8 µL of 10X DNase I reaction buffer

was then added to each column, incubated for 15 minutes at 25°C and centrifuged at 13000 rpm for 30 seconds;

- each column was firstly washed with 400 µL of RNA prep buffer and centrifuged at 13000 rpm for 30 seconds, then with 700 µL of RNA wash buffer and centrifuged at 13000 rpm for 30 seconds and at the end with 400 µL of RNA wash buffer and centrifuged at 13000 rpm for 2 minutes;
- after, the ethanol evaporation, 25 µL of DNase/RNase-free water was added on each filter of column and, after 1 minute of incubation, RNA was eluted centrifuging it at 13000 rpm for 30 seconds.

Finally, 2 µL of extracted RNA were placed into µDrop Plate (Thermo Scientific) and used to measure its concentration with a Multiskan^{TM} GO Microplate Spectrophotometer (Thermo Scientific) and a SkanIt Software 3.2 for Multiskan GO (Thermo Scientific). The instrument was set to measure the absorbance at three wavelengths 230, 260 and 280 nm and then to calculate RNA concentration and 260nm/280nm and 260nm/230nm ratios. The last two values give us information about the purity of RNA sample; values of 2.0 and 2.0-2.2, respectively, indicate a good quality of RNA.

2.13 cDNA synthesis (RT-PCR)

After the extraction, RNA was transcribed to cDNA through reverse transcription reaction using random primers and High-Capacity cDNA Reverse Transcription Kit (Applied Biosystem). The mix of reaction is composed by:

RNA (1 µg)	10 µL
10X RT buffer	2 µL
dNTP mix (100 mM)	0.8 µL
10X RT random primers	2 µL
Nuclease free water	3.2 µL
RNase inhibitor (20 U/µL)	1 µL
Multiscribe reverse transcriptase (50 U/µL)	1 µL

Each sample was put in peqSTAR 96 Universal Thermo Cycler (EuroClone) and subjected to the following program:

25°C for 10 minutes

37°C for 2 hours

85°C for 5 minutes

Finally, 2 µL of cDNA were placed in µDrop Plate (Thermo Scientific) and used to measure its concentration using Multiskan^{TM} GO Microplate Spectrophotometer (Thermo Scientific) and a SkanIt Software 3.2 for Multiskan GO (Thermo Scientific). The instrument was set to measure the absorbance at three wavelengths 230, 260 and 280 nm and then to calculate cDNA concentration, 260nm/280nm and 260nm/230nm ratios. The last two values give us information about the purity of RNA sample; values of 1.8 and 2.0-2.2, respectively, indicate a good quality of cDNA.

2.14 Primers design for Real-Time PCR

The primers to amplify specific regions of mRNAs and to make transcriptomics studies were designed starting from nucleotide sequences deposited in the National Center for Biotechnology Information (NCBI) data base. For the primers design were used the following criteria:

- Melting temperature (Tm) between 55°C and 60°C;
- Tm difference between forward (for) and reverse (rev) primers not higher than 2°C (if possible);
- Specific primers for the selected transcripts (Basic Local Alignment Search Tool (BLAST));

- Selected couples of primers that don't form hairpins, self-dimers and hetero-dimers (Olygo Analyzer Tool);
- Specific designed primers that are able to span to exon-exon junctions, eliminating undesirable genomic DNA amplification.

All primers were purchased from Eurofins MWG Operon (Edersberg, DE) except primer sequences for *NT5E-1* and *NT5E-2* transcripts **[79]**.

2.15 Real-Time PCR

Real-Time PCR is a method for analysing and quantifying in real-time the amount of DNA amplification. In this reaction there is a fluorescent dye binding DNA. In this experiment was used as fluorescent dye SYBR green; this dye is an asymmetric cyanine with poor fluorescence, that increases after binding to double-stranded DNA (in a non-specific way). The specificity of this reaction is determined only by the primers used. In order to amplify cDNA via Real-Time PCR, we used iTaq™ SYBR® Green Supermix (Bio-Rad) including, in addition to SYBR green I, also AmpliTaq Gold DNA polymerase, dNTPs, an appropriate buffer and a passive reference ROX, to normalize the fluorescence signals due to differences in concentration and volume of each sample.

The mix of reaction is composed by:

Power SYBR Green PCR master mix	10 µL
Nuclease free water	7.8 µL
Primer forward (10 µM)	0.6 µL
Primer reverse (10 µM)	0.6 µL
cDNA (300 ng/µL)	1 µL

Each sample was put in MicroAmp® Fast Optical 96-well Reaction Plate with Barcode (0.1 mL) (Applied Biosystems) closed with MicroAmp™ Optical Adhesive Film (Applied Biosystems); then, the plates were inserted in 7500 Fast Real-Time PCR System instrument (Applied Biosystems) and 7500 Software v2.3 (Applied Biosystems) was used according to the following program:

95°C for 10 minutes

95°C for 15 seconds

60°C for 1 minute

The steps 2 and 3 were repeated for 40 cycles. The output of the instrument is an amplification plot (**Fig. 2.11**), showing the increase of fluorescence as function of the threshold cycle (Ct). In this cycle the fluorescence signal reaches the threshold level defined by a line that is set automatically by the instrument and is at least 3 times higher than

the baseline values of standard deviation. As shown in **Fig. 2.11**, the first part of this curve is indicated as baseline and corresponds to signals determined by the aspecific fluorescence; the second one is the exponential phase in which fluorescence is proportional to initial target amount; the third one is the linear phase in which there is no increase in fluorescence proportional to initial target amount.

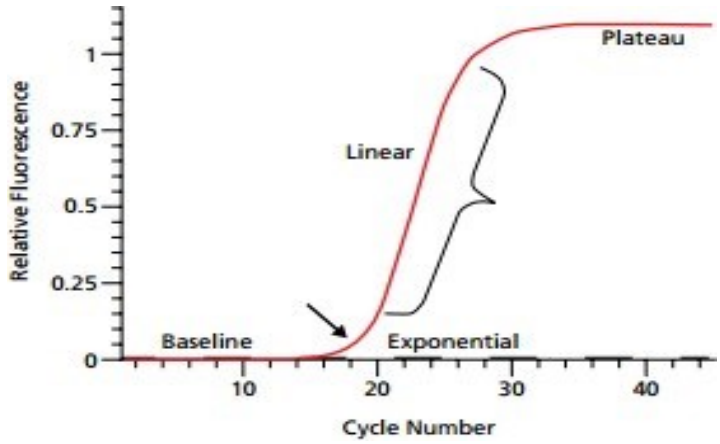

Fig. 2.11: Amplification plot and amplification phases (from qPCR Technical Guide, Sigma).

Ct is the numeric output of the instrument and is inversely correlated to the amount of template present in the mix of reaction; it is determined during the exponential phase, when the amplification is not inhibited by reaction-limiting conditions. The amplification was followed by a dissociation reaction with the following program:

95°C for 15 seconds

60°C for 1 minute

95°C for 30 seconds

60°C for 15 seconds

This method allows us to check if the amplification is specific through the identification of Tm of amplicons whose temperature depends on their nucleotide composition. Each amplicon is considered as a specific melting peak in the first derivate plot of fluorescence as function of temperature. The artefacts or non-specific amplifications determine, in this plot, the presence of other peaks with different Tm **[168]**. Finally, another way to evaluate the specificity of amplifications is the presence of a single band in the agarose gel electrophoresis analysis. In order to analyze the Real-Time PCR data we used the ΔΔCt method (if the amplification efficiencies of target genes and housekeeping gene are approximately equal) **[169]**. This method allows us to calculate ΔCt as the difference between Ct of target gene and Ct of housekeeping gene (such as β-actin) in each sample. The value of ΔCt is inversely proportional to the amount of relative gene. Then, ΔΔCt is calculated as difference between ΔCt of a target gene in each sample (such as treated-cells) and ΔCt of the same gene in the calibrator sample (such as untreated-cells). Finally, $2^{\wedge(-\Delta\Delta Ct)}$, also named Fold Change, is the number indicating how many times a gene is expressed in a sample considering that 1 is the expression of the gene in the calibrator sample. In particular $2^{\wedge(-\Delta\Delta Ct)}$ can be:

- egual to 1 if we have the same gene expression in the sample and in the calibrator;

- minor to 1 if we have a decrease of gene expression in the sample;
- major to 1 if we have an increase of gene expression in the sample.

Each test was repeated three times in triplicate. For the present scientific research, we used the following couples of primers to analyze the corresponding transcripts:

β-ACTIN:

for: 5'- CCTGGCACCCAGCACAAT -3'

rev: 5'- GCCGATCCACACGGAGTACT -3'

ABCB1:

for: 5'- CCTTCAGGGTTTCACATTTGG -3'

rev: 5'- ACTCACATCCTGTCTGAGCA -3'

ABCC1:

for: 5'- GCTGATGGAGGCTGACAAGG -3'

rev: 5'- GATGCTGAGGAAGGAGATGAAGAG -3'

ABCC2:

For: 5'- CCCTTGTCCTGGAAGATGTT -3'

rev: 5'- AGAGCCTTCATCAACCAGG -3'

ABCC3:

for: 5'- CCACACCACAACCACCTTCAC -3'

rev: 5'- CTCGGCGTCCAGCACATTG -3'

ABCC4:

for: 5'- GCACACCAGGATTTACATTCAGAG -3'

rev: 5'- CCAGACGGACGGCAAACC -3'

ABCC5:

for: 5'- CCACCATCCACGCCTACAATAAAG -3'

rev: 5'- ACAGCCAGCCACCGCATC -3'

ABCC6:

for: 5'- AAGGAACCACCATCAGGAGGAG -3'

rev: 5'- ACCAGCGACACAGAGAAGAGG -3'

ABCG2:

for: 5'- ATCACTGATCCTTCCATCTTG -3'

rev: 5'- GCTTAGACATCCTTTTCAGG -3'

ENPP1:

for: 5'-CCGTGGACAGAAATGACAGTTTC -3'

rev: 5'-ATGGACAGGACTAAGAGGAATTCTAAA -3'

NT5E:

for: 5'- GGGCGGAAGGTTCCTGTAG -3'

rev: 5'- GAGGAGCCATCCAGATAGACA -3'

p16:

for: 5'- GTGGACCTGGCTGAGGAG -3'

rev: 5'- CAATCGGGGATGTCTGAGGG -3'

p21:

for: 5'- CTGTCTTGTACCCTTGTGCCT -3'

rev: 5'- CGTTTGGAGTGGTAGAAATCTGTC -3'

p53:

for: 5'- TGAATGAGGCCTTGGAACTC -3'

rev: 5'- ACTTCAGGTGGCTGGAGTG -3'

TNAP:
for: 5'- TACAAGCACTCCCACTTCATCTG -3'
rev: 5'- GCTCGAAGAGACCCAATAGGTAGT -3'

2.16 Western blotting

Western blotting analysis allows us to identify one antigen or similar antigens by a specific antibody. The cellular pellets were lysed in Laemmli sample buffer (60 mM Tris-HCl pH 6.8, 10% glycerol, 1% β-mercaptoethanol and 0.002% of bromophenol blue) supplemented with a cocktail of proteases and phosphatases inhibitors. Subsequently, the cellular lysis is accomplished by three thermal shocks in order to denature the proteins within the cellular membranes. Finally, the samples were incubated at 95°C for 5 minutes in the Digital Dry Bath (Labnet) and centrifuged at 4000 rpm for 2 minutes. The proteins were resolved on 8%-4% or 15%-4% SDS-PAGE (sodium dodecyl sulfate - polyacrylamide gel electrophoresis) gels. This electrophoresis technique is helpful to analyse protein samples in a three-dimensional matrix, consisting of a polyacrylamide gel immersed in running buffer 1X (25 mM Tris, 192 mM Glycine and 0.1% SDS, pH 8.3). In order to form these gels we used a mixture of acrylamide and bis-acrylamide. When acrylamide polymerizes with other monomers and with bis-acrylamide we can observe a formation of crosslinks that create a gelatinous matrix with pores of size inversely

proportional to the amount of polyacrylamide. This polymerization reaction starts when N,N,N',N'-tetramethylethane-1,2-diamine (TEMED) catalyses the decomposition of persulfate ammonium (APS) in SO_4^{-}**.** free radical that triggers this reaction. SDS unfolds and charges negatively the proteins allowing their migration, in the gelatinous matrix, according to their molecular weight in presence of an electric field. The proteins with different sizes show different levels of steric encumbrance and migrate with different speeds. Gels were obtained through the polymerization between two slides separated by two spacers. The polyacrylamide gels used were made of two contiguous gels: a running gel with a higher amount of polyacrylamide and a staking gel in which a comb formed some wells able to load the samples.

The mix for running gel (15%) consisted of:

Water	2.3 mL
30% Acrylamide mix	5.0 mL
1.5 M Tris (pH 8.8)	2.5 mL
10% SDS	0.1 mL
10% APS	0.1 mL
TEMED	0.004 mL

The mix for running gel (8%) consisted of:

Water	4.6 mL
30% Acrylamide mix	2.7 mL
1.5 M Tris (pH 8.8)	2.5 mL
10% SDS	0.1 mL
10% APS	0.1 mL
TEMED	0.006 mL

The mix for staking gel (4%) consisted of:

Water	2.15 mL
30% Acrylamide mix	0.4 mL
1.0 M Tris (pH 6.8)	0.375 mL
10% SDS	0.03 mL
10% APS	0.03 mL
TEMED	0.003 mL

The samples were loaded in these polyacrylamide gels and electrophoresis was made in running buffer 1X at 120 V for 15 minutes

and at 140 V until the end of the experiment using PowerPac HC Power Supply (Bio-Rad). The next step of western blotting was the electroblotting on nitrocellulose or PVDF membranes (Amersham Protran, GE Healthcare Life Sciences). In this procedure the proteins pass from the gel to the membrane, where they are immobilized at 380 mA for 90 minutes at 4°C with an appropriate buffer, the transfer buffer 1X (25 mM Tris, 192 mM glycine and 20% methanol, pH 8.3). The membranes were stained with Ponceau S solution in order to verify this transfer, washed with PBS 1X in order to eliminate the staining and incubated with a blocking solution, 0.25% or 1% non-fat milk in PBS-T (PBS 1X with 0.05% of Tween-20), at 25°C for 1 hour on a shaking support. Later, the membranes were incubated overnight at 4°C, on a shaking support, with specific primary antibodies: 1:400 anti-β-ACTIN (C4) diluted in PBS-T with 5% non-fat milk (Abcam); 1:100 anti-ALKALINE PHOSPHATASE (H-300, is recommended for TNAP detection) diluted in PBS-T with 5% non-fat milk, 1:100 anti-MRP6 (H-70) and 1:100 anti-CD73 (IE9) diluted in PBS-T with 0.25% non-fat milk (Santa Cruz Biotechnology). The following day, the membranes were washed three times for 10 minutes with PBS-T and incubate with an appropriate horseradish peroxidase-conjugated secondary antibody at room temperature for 1 hour on a shaking support. Then, the membranes were washed again three times for 10 minutes with PBS-T and the protein signals were detected by Chemiluminescent Peroxidase Substrate-1 or Super Signal West Femto Maximun Sensivity Substrate (Thermo Scientific), using ChemidocTM

XRS detection system (BioRad) equipped with Image Lab Software for the image acquisition (BioRad). A densitometric analysis was performed by using ImageJ software (National Institute of Health, Bethesda, MD). The data of a specific protein of each sample were normalized with the respective β-actin signal; the protein expression level in the control sample is considered equal to 100%. Each result was expressed as percentage of the value of the control sample. Each test was repeated three times.

2.17 Migration assay

The ability of the probenecid to modulate the cell migration rate was evaluated by *in vitro* wound-healing migration assay. For the migration assay, 1 x 10^6 HepG2 cells were seeded in each 35-mm cell culture dish (Cellview cell culture dish, 35/10mm glass bottom, Greiner Bio-one) and cultured in DMEM containing 10% FBS to promote a nearly confluent cell monolayer. Then, a linear wound was generated in the cellular monolayer with a sterile 10 µl plastic pipette tip. Any cellular debris was removed by washing with PBS 1X and replaced with 2 mL of DMEM with 1% FBS containing 250 µM of probenecid; DMEM with 1% FBS containing 0.25% of DMSO was used as control. The cells were treated for 24 and 48 hours with probenecid or DMSO in DMEM with 1% FBS and the time-lapse images were obtained using a BioStation IM incubator,

version 2 (Nikon) (**Fig. 2.12**). The images acquired were further analysed by using computing software (ImageJ 1.46) and the results of migration rate were reported as µm/h.

Fig. 2.12: BioStation IM incubator, version 2 (Nikon).

2.18 Cellular cycle analysis

In order to analyse the effects of probenecid on the modulation of the HepG2 migration rate was performed an assay to study the cellular cycle, as described by Laurenzana et al. **[170]**. After 24 and 48 hours of probenecid treatment (see 2.2), HepG2 cells were detached and centrifuged at 1200 rpm for 5 minutes at 4°C. Subsequently the pellet was resuspended in 800 µL of PBS 1X, again centrifuged at 1200 rpm for 5 minutes at 4°C, then, were removed 700 µL of PBS 1X, and the cells resuspended in 100 µL of the remainder PBS 1X. Then, the cells were fixed in cold ethanol 70% (drop by drop) for 1 hour,

then, labeled with propidium iodide (ex./em.: 535/617 nm, Invitrogen^{TM}) and RNase staining solution for 30 minutes. The samples were acquired by Navios flow cytometer (Beckman Coulter), while, the data were analysed by ModFit LT Software (Verity Software House). Furthermore, in order to confirm the data obtained on the cellular cycle we performed experiments of Real-Time PCR (see 2.15) analysing different transcripts (*p16*, *p21* and *p53*).

2.19 Imaging assay using confocal microscopy

An immunofluorescence assay with phalloidin was performed in order to analyse the molecular effects of probenecid on the modulation of the HepG2 migration rate. The phalloidin is a bicyclic peptide present in the plant *Amanita Phalloides*, and, it is able to link specifically actin filaments; it is conjugated with a fluorescent dye visible with a fluorescence microscope. 1.5×10^5 HepG2 cells and 1.1×10^5 MDA-MB-231 cells were seeded on slides in each well of 12-wells plates in 1 mL of DMEM. After 24 hours from their seeding, these cells were treated for 24 and 48 hours with 250 µM of probenecid or with 0.25% of DMSO. After the treatment, the medium was removed, and, after one wash with PBS 1X, the cells were fixed in 400 µL of 4% paraformaldehyde for 10 minutes at room temperature. After three washes with PBS 1X, the cells were permeabilized with

Triton X-100 0.5% in PBS 1X for 5 minutes and, after three new washes in PBS 1X, blocked in saturation buffer (1% BSA in PBS 1X) for 15 minutes at room temperature. Then, the cells were incubated with Phalloidin Alexa Fluor 488 (ex./em.: 495/518 nm, Invitrogen™) diluted 1:1000 in saturation buffer for 1 hour at room temperature, in the dark. After three washes in PBS 1X, the nuclei were stained with 1.5 µM of propidium iodide (ex./em.: 535/617 nm, Invitrogen™) in PBS 1X for 10 minutes. Finally, after three washes in PBS 1X, the slides were assembled using 90% glycerol in PBS 1X. The images were obtained with a confocal fluorescence microscope (Leica TSC-SP2 HCX PL APO, ×63/1.32-0.60 oil objective) and acquired using the Leica Confocal Software W. In these images the actin filaments and the filopodia have a green colour and the nuclei have a red colour.

2.20 Statistical analysis

The data of each experiment were presented as means ± SD. Student's *t*-test was performed pairwise to compare control and treated samples. Each experiment was performed three times. Differences were considered significant whenever *p*-value < 0.05, in particular, the following legend was used for the significance of the data: $p < 0.05$ (*), $p < 0.01$ (**), $p < 0.001$ (***). Statistical analysis was performed using statistical GraphPad software.

Results and Discussion

Recent studies show that in *ABCC6*-silenced HepG2 cells there are changes in the cellular phenotype as a consequence of gene expression dysregulation and alteration in cellular cycle genes **[76] [77]**. These data suggest that ABCC6 protein could have other physiological roles in the cells besides the well-known role of promoting the PP_i accumulation outside the cells. In the present scientific research, we carried out a series of experiments in order to characterize the involvement of ABCC6 in some cellular processes through the use of probenecid, an inhibitor of ABC proteins **[75]**.

3.1 Inhibition of ABCC6 activity by Probenecid in HEK293 cells

In order to quantify the effective inhibition of probenecid on the transport activity of the ABCC6 protein, a doxorubicin efflux assay was conducted (this compound is a known substrate also transported by ABCC6 transporter **[20]**). This assay was conducted in HEK293 cells, a cellular line of human embryonic kidney 293 easily transfected, stably transfected with *ABCC6*-Flag-pcDNA and with Flag-pcDNA (as control cells), in presence and in absence of 1 mM of probenecid. As we can see in **Fig. 3.1**, the efflux of doxorubicin, in absence of probenecid, is significantly higher in *ABCC6*-Flag-pcDNA cells compared with Flag-pcDNA cells, suggesting an involvement

of ABCC6 transporter in the release of doxorubicin. In presence of probenecid, there is no significant difference in the doxorubicin efflux but there is a higher inhibition in doxorubicin efflux in *ABCC6*-Flag-pcDNA cells compared with Flag-pcDNA cells. Therefore, probenecid inhibits the transport activity carried out by ABCC6 protein **[171]**.

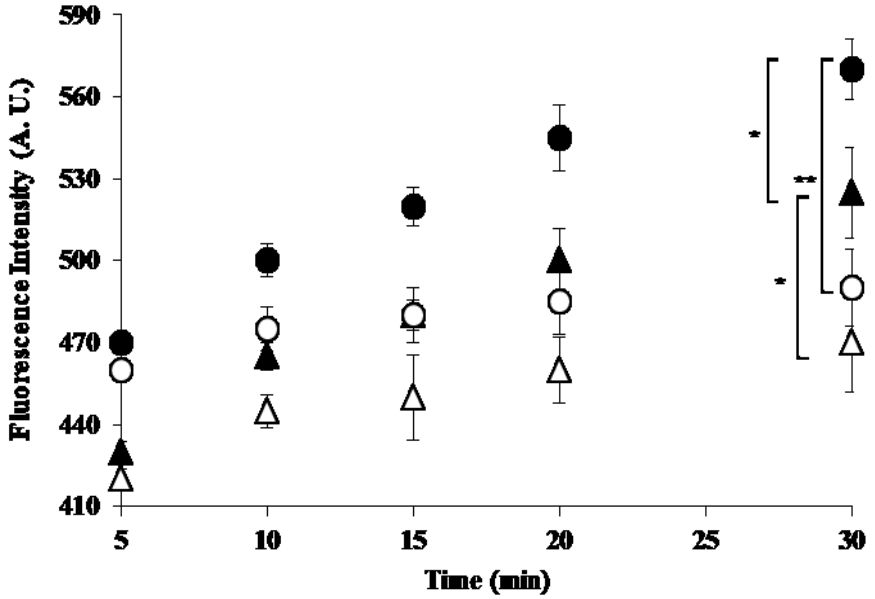

Fig. 3.1: Inhibition of efflux of doxorubicin by Probenecid in HEK293 cells. Doxorubicin efflux assay in HEK293 cells stably transfected with *ABCC6*-Flag-pcDNA in absence (●) or in presence (○) of 1 mM probenecid and in HEK293 cells stably transfected with Flag-pcDNA in absence (▲) or in presence (Δ) of 1 mM probenecid. Data are expressed as means ± SD of three independent experiments. * $p < 0.05$, ** $p < 0.01$, Student's t-test.

3.2 Effects of Probenecid in HepG2 cells

Other experiments were performed in HepG2 cells (cells in which *ABCC6* is abundantly expressed **[41]**, see **Fig. 3.31**), in order to understand the effects of a possible modulation of ABCC6 activity in some cellular processes.

3.2.1 Evaluation of cytotoxicity and morphology

A cytotoxicity assay was initially performed in HepG2 cells, a human hepatocellular carcinoma cellular line, in order to evaluate the effects time- and dose-dependent of probenecid. Probenecid did not show cellular toxicity up to 250 μM within 48 hours (about 90% of viability); after 48 hours of treatment at 500 μM the viability is about 70% and at 1000 μM the viability is about 50% (**Fig. 3.2**) **[171]**.

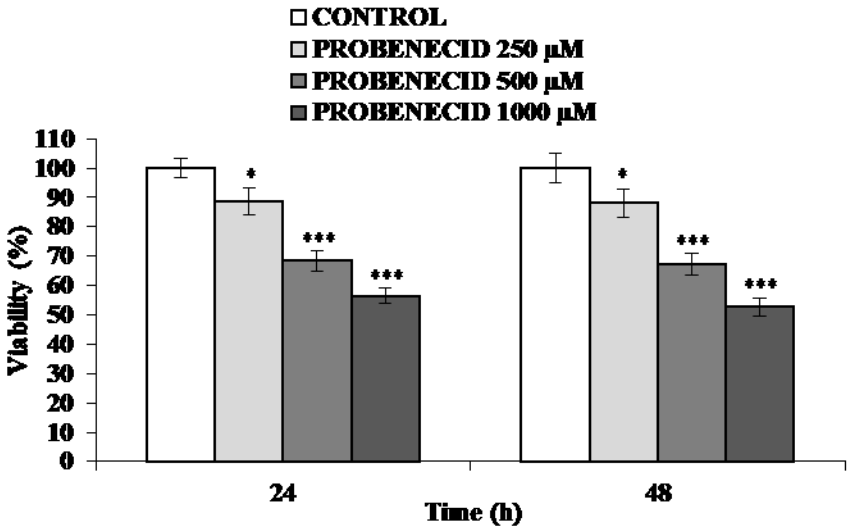

Fig. 3.2: Effects of Probenecid on viability of HepG2 cells. Cells were treated with probenecid at the concentration of 250, 500 and 1000 µM for 24 and 48 hours. Data are expressed as a percentage of the control group and presented as means ± SD of three independent experiments. * $p < 0.05$, *** $p < 0.001$, Student's t-test.

Subsequently, the cells were examined with a phase-contrast microscope in order to observe morphological changes induced by probenecid. The cells, after the treatment with probenecid, did not show noticeable alterations in shape, size and number of vacuoles (**Fig. 3.3**) **[171]**.

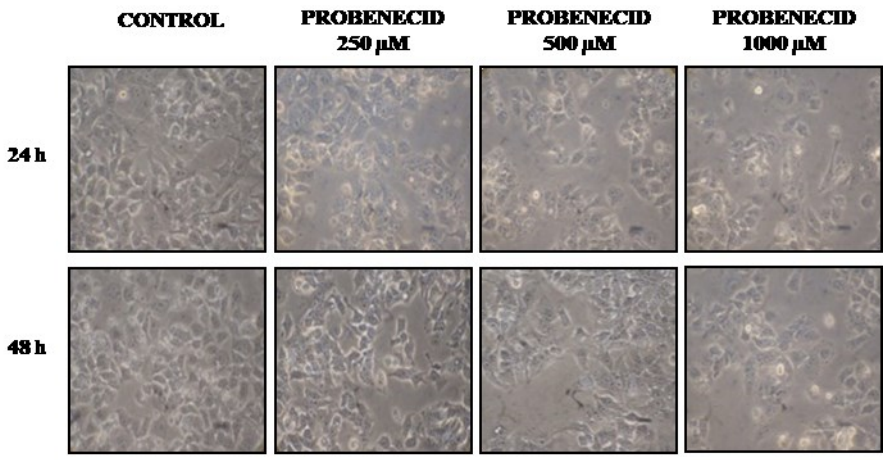

Fig. 3.3: Effects of Probenecid on morphology of HepG2 cells. Cells were treated with probenecid at the concentration of 250, 500 and 1000 µM for 24 and 48 hours. Representative images, after probenecid treatment, of control and treated HepG2 cells were acquired with a phase-contrast microscope. DMSO-treated cells were used as control.

3.2.2 Evaluation of intracellular ROS

An assay was performed in order to evaluate the effects of probenecid on intracellular ROS in HepG2 cells. As we can see in **Fig. 3.4**, probenecid, up to 250 µM within 48 hours, did not show significant variations of intracellular ROS. 500 and 1000 µM of probenecid showed a decrease of about 30% within 24 hours of intracellular ROS; the same concentrations within 48 hours did not show significant variations of intracellular ROS.

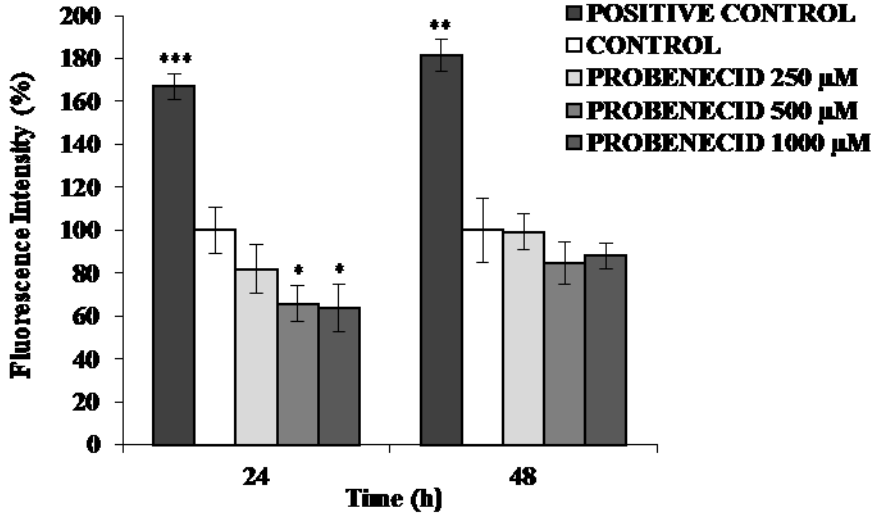

Fig. 3.4: Effects of Probenecid on intracellular level of ROS of HepG2 cells. Cells were treated with probenecid at the concentration of 250, 500 and 1000 µM for 24 and 48 hours. As positive control of ROS presence, 500 µM of tert-butyl hydroperoxide solution was used for 1 hour. Then, cells were treated with 10 µM of DCFH-DA for 30 minutes. Data are expressed as a percentage of the control group and presented as means ± SD of three independent experiments. * $p < 0.05$, ** $p < 0.01$, *** $p < 0.001$, Student's t-test.

3.2.3 Evaluation of inhibition of calcein transport

After analysing these preliminary results we decided to test 250 µM of probenecid (for a short period of time) in HepG2 cells in order to check if it could inhibit the transport of calcein by MRPs **[17]**. As we can see in **Fig. 3.5**, in HepG2 cells treated with probenecid there is a decrease of about 35% of external calcein and an increase of about 40% of internal calcein. These data suggest that all MRPs,

including ABCC6 (abundantly expressed in HepG2 cells **[41]**), are inhibited by the presence of probenecid. In fact, in presence of probenecid, the calcein, once metabolized inside the cells, can't be expelled outside them.

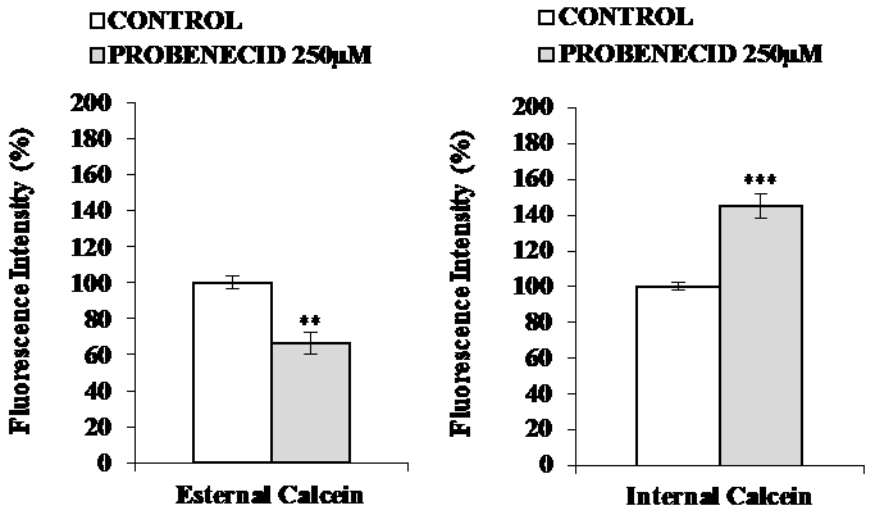

Fig. 3.5: Inhibition of calcein transport by Probenecid in HepG2 cells. Cells were treated for 1 hour with 250 µM of probenecid and then for 1 hour with 1 µM of calcein-AM. Data of external and internal calcein are expressed as a percentage of the control group and presented as means ± SD of three independent experiments. ** $p < 0.01$, *** $p < 0.001$, Student's t-test.

3.2.4 Evaluation of cellular density

A new experiment shows that *ABCC6* and *NT5E* genes are regulated by cellular confluence. As we can see in **Fig. 3.6**, at about 40% of confluence (6×10^5 HepG2 cells, in a well of 6-wells plates)

there is a greater expression of *ABCC6* gene compared with *NT5E* gene, while, at about 80% of confluence (after 48 hours from a possible pharmacological treatment) there is a greater expression of *NT5E* gene compared with *ABCC6* gene. These data highlight a possible correlation between the two genes; in particular ABCC6 could carry some substrates that could promote the expression of CD73, after their accumulation. Therefore the use of an ABC inhibitor, as probenecid, decreasing the transport activity of the ABCC6 could regulate the expression of CD73. This regulation could also regulate different phenomena related to these proteins such as mineralization and cancer processes.

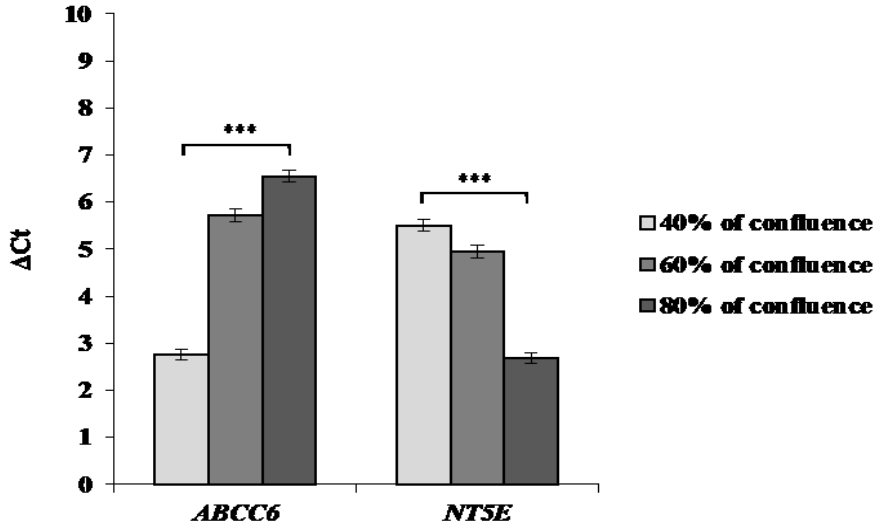

Fig. 3.6: The effects of cellular confluence, in HepG2 cells, on *ABCC6* and *NT5E* genes. ΔCt of *ABCC6* and *NT5E* mRNA levels in HepG2 cells at different cellular confluence. β-actin was used as housekeeping gene. Data are represented as the means ± SD of three independent experiments. *** $p < 0.001$, Student's t-test.

From the analysis of all these preliminary data we decided to use in HepG2 cells probenecid at the concentration of 250 μM for 24 and 48 hours, in order to understand the effects of partial modulation of ABCC6 transporter activity.

3.2.5 Effects of treatment with Probenecid for 24 hours

At first, HepG2 cells were treated with 250 μM of probenecid for 24 hours. As we can see in **Fig. 3.7** there is no significant variations in *ABCC6* and *NT5E* expression gene levels via Real-Time PCR, although previously we observed an influence of probenecid on the activity of the ABCC6 protein.

2^(-ΔΔCt)	
ABCC6	**0.93 ± 0.16**
NT5E	**1.02 ± 0.07**

Fig. 3.7: The effects of Probenecid, in HepG2 cells, on *ABCC6* and *NT5E* genes after 24 hours of treatment. Fold change of *ABCC6* and *NT5E* mRNA levels in HepG2 cells treated with 250 μM of probenecid for 24 hours compared to the control cells (treated with DMSO). β-actin was used as housekeeping gene. Data are represented as the means ± SD of three independent experiments.

3.2.6 Effects of treatment with Probenecid for 48 hours

Subsequently, HepG2 cells were treated with 250 μM of probenecid for 48 hours. As we can see in **Fig. 3.8** there is a significant decrease in the expression levels of genes *ABCC6* and *NT5E* via Real-Time PCR.

2^(-ΔΔCt)	
ABCC6	**0.57 ± 0.13**
NT5E	**0.55 ± 0.10**

Fig. 3.8: The effects of Probenecid, in HepG2 cells, on *ABCC6* and *NT5E* genes after 48 hours of treatment. Fold change of *ABCC6* and *NT5E* mRNA levels in HepG2 cells treated with 250 μM of probenecid for 48 hours compared to the control cells (treated with DMSO). β-actin was used as housekeeping gene. Data are represented as the means ± SD of three independent experiments.

Then, a protein analysis was performed, by western blotting; it confirmed a significant decrease of about 30% of ABCC6 and CD73 proteins (**Fig.3.9**) **[171]**.

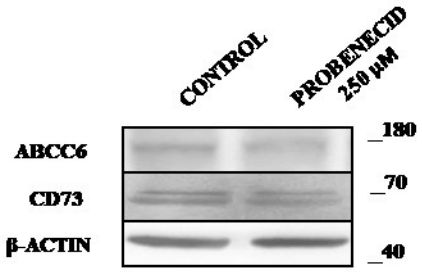

Fig. 3.9: The effects of Probenecid, in HepG2 cells, on ABCC6 and CD73 proteins after 48 hours of treatment. Representative western blotting images of ABCC6 and CD73 immunoreactive bands. β-actin was used as a loading control. These data were repeated in three independent experiments.

These data showed a correlation in the levels of the two genes and proteins after 48 hours of probenecid treatment. In particular, these data support our hypothesis of a functional correlation of the two proteins: in presence of a low expression of ABCC6, the levels of expression of CD73 decrease. Furthermore, the decreased expression of ABCC6 protein, caused by probenecid, could promote a smaller outflow of ATP, and consequently, the expression of CD73 protein could decrease because of a reduced presence of AMP (substrate of CD73), a product of ATP catabolism. In this context we also analysed the *ENPP1* gene expression and TNAP gene and protein expression, both involved in the degradation pathway of extracellular ATP. As we can see in **Fig. 3.10** *ENPP1* and *TNAP* gene expression is unchanged after a treatment for 48 hours with 250 µM of probenecid.

2^(-ΔΔCt)	
ENPP1	1.06 ± 0.21
TNAP	0.94 ± 0.14

Fig. 3.10: The effects of Probenecid, in HepG2 cells, on *ENPP1* and *TNAP* genes after 48 hours of treatment. Fold change of *ENPP1* and *TNAP* mRNA levels in HepG2 cells treated with 250 μM of probenecid for 48 hours compared to the control cells (treated with DMSO). β-actin was used as housekeeping gene. Data are represented as the means ± SD of three independent experiments.

After the treatment with probenecid, TNAP protein remains unchanged (**Fig. 3.11**).

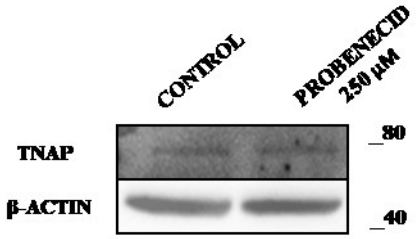

Fig. 3.11: The effects of Probenecid, in HepG2 cells, on TNAP protein after 48 hours of treatment. Representative western blotting image of TNAP immunoreactive band. β-actin was used as a loading control. This datum was repeated in three independent experiments.

The non-variation of *ENPP1* gene suggests that this gene does not suffer both of the partial inhibition of ABCC6 protein and the partial decrease of ATP efflux in the extracellular space. The expression of TNAP, in literature, is inversely related to the expression of CD73; in fact, the adenosine produced by CD73 is able to inhibit

the expression of TNAP. In this specific case, we can explain that the non-variation of TNAP is strictly related to the CD73 protein decrease. This decrease of about 30% would not allow a significant reduction of extracellular adenosine and consequently an increase in TNAP expression. The treatment with probenecid is able to control different processes at cellular level: the partial regulation of ABCC6 protein could limit the phenomenon of ectopic mineralization due to a smaller amount of ATP carried out in the extracellular space. The partial regulation of CD73 protein could also decrease the phenomenon of cancer progression. The non-activation of TNAP could limit both the formation of P_i and the mineralization processes.

Finally, we verified via Real-Time PCR if the treatment with probenecid was able to control some ABCs transporter gene (**Fig. 3.12**).

2^(-ΔΔCt)	
ABCB1	1.08 ± 0.10
ABCC1	1.06 ± 0.06
ABCC2	1.09 ± 0.08
ABCC3	1.10 ± 0.09
ABCC4	1.08 ± 0.07
ABCC5	1.07 ± 0.08
ABCG2	0.98 ± 0.06

Fig. 3.12: The effects of Probenecid, in HepG2 cells, on some *ABC* genes after 48 hours of treatment. Fold change of some *ABC* mRNA levels in HepG2 cells treated with 250 μM of probenecid for 48 hours compared to the control cells (treated with DMSO). β-actin was used as housekeeping gene. Data are represented as the means ± SD of three independent experiments.

No changes, after probenecid treatment, were observed in the transcript levels of the other ABC genes analysed **[171]**. In particular, probenecid is only able to decrease the ABCC6 gene and protein expression.

3.2.7 Effects of adenosine and ATP on the modulation of ABCC6 and CD73 expression

After verifying, in HepG2 cells, both a modulatory effect of probenecid on the activity and protein expression of ABCC6 and a modulation of CD73 protein expression, we performed other experiments in order to characterize the correlation between these two proteins. It is known that ABCC6 protein is indirectly involved in the production of extracellular adenosine (thanks to ENPP1 and CD73 proteins); therefore it could have a role in the activation of the purinergic system, that is able to control important cellular functions in the liver (**Fig. 3.13) [171]**.

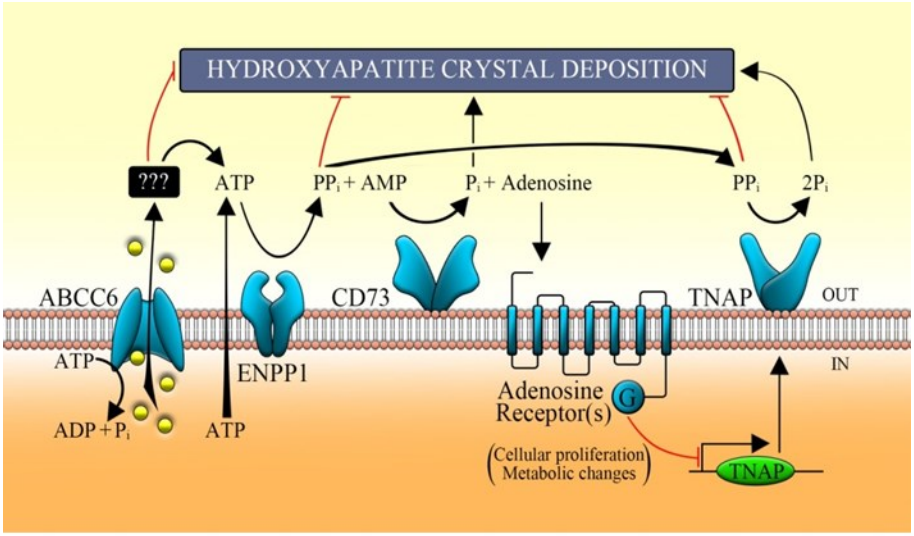

Fig. 3.13: Function of the main proteins involved in the purinergic pathway. ABCC6 transporter allows the partial release of ATP which is metabolized by some ecto-nucleotidases (such as ENPP1) in AMP, by CD73 in adenosine and by TNAP in P_i. ABCC6, ATP-binding cassette, sub-family C, member 6; ENPP1, ecto-nucleotide pyrophosphatase/phosphodiesterase type I; CD73, cluster of differentiation 73; TNAP, tissue nonspecific alkaline phosphatase; P_i, inorganic phosphate; PP_i, inorganic pyrophosphate [171].

In these experiments, we verified a possible modulation of ABCC6 and CD73 by some purinergic mediators such as adenosine and ATP, in presence and in absence of probenecid. This set of experiments was performed in order to check if ABCC6 protein is involved in the purinergic pathway. In the **Fig. 3.14**, the effects of adenosine and probenecid were observed on CD73 expression in HepG2 cells after 48 hours of treatment. CD73 protein levels were reduced of about 30% after treatment of cells only in presence of probenecid. Moreover, CD73 protein levels are increased by about 30% and 40% after

treatment respectively with 10 and 100 μM of adenosine. Finally, CD73 protein levels are decreased by about 10% if probenecid is added to treatment with adenosine **[171]**.

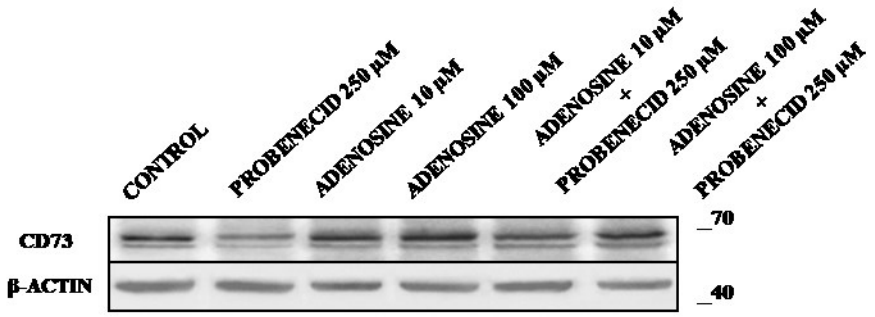

Fig. 3.14: The effects of adenosine, in HepG2 cells, on CD73 protein, in the presence and in absence of Probenecid, after 48 hours of treatment. Representative western blotting image of CD73 immunoreactive band. β-actin was used as a loading control. This datum was repeated in three independent experiments.

Then, as ATP is a possible substrate transported by ABCC6 protein, HepG2 cells were incubated for 48 hours with different concentrations of ATP, in presence and in absence of probenecid (**Fig. 3.15**). Also in this case, CD73 protein levels are decreased only in presence of probenecid; after a treatment with 50 and 500 μM of ATP, CD73 protein levels are increased respectively of about 20 and 60%. Finally, CD73 protein levels are decreased of about 10% if probenecid is added to treatment with ATP **[171]**.

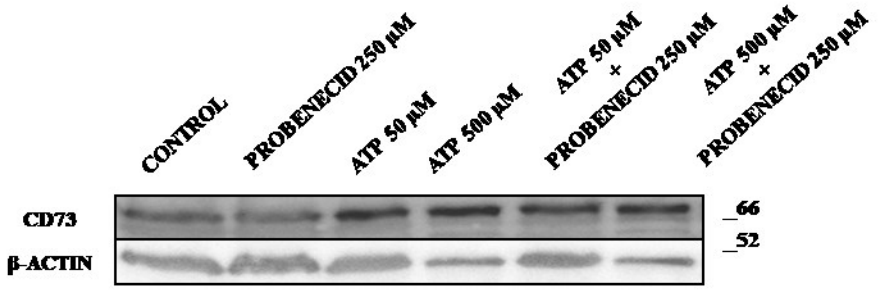

Fig. 3.15: The effects of ATP, in HepG2 cells, on CD73 protein, in the presence and in absence of Probenecid, after 48 hours of treatment. Representative western blotting image of CD73 immunoreactive band. β-actin was used as a loading control. This datum was repeated in three independent experiments.

The **Fig. 3.16** shows the effects of adenosine, in HepG2 cells, on ABCC6 protein expression after 48 hours of treatment. Also in this case, ABCC6 protein levels are decreased of about 30% only in presence of probenecid. After a treatment with 10 and 100 µM of adenosine, ABCC6 protein levels are increased respectively of about 30 and 50%, while, ABCC6 protein levels are slightly decreased if probenecid is added to the treatment with adenosine **[171]**.

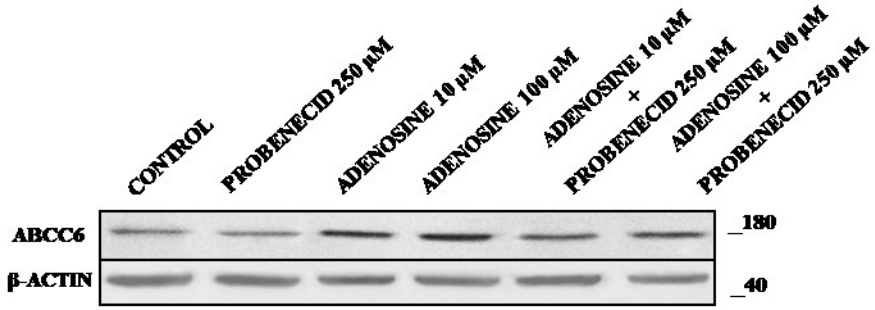

Fig. 3.16: The effects of adenosine, in HepG2 cells, on ABCC6 protein, in the presence and in absence of Probenecid, after 48 hours of treatment. Representative western blotting image of ABCC6 immunoreactive band. β-actin was used as a loading control. This datum was repeated in three independent experiments.

These data show that probenecid, an ABC transporters inhibitor, decreases CD73 protein levels, while, the adenosine increases CD73 expression in HepG2 cells. The same result was obtained by adding ATP, an ABCC6 substrate, to HepG2 cells; ATP is able to restore the levels of adenosine. These results suggest that ABCC6, promoting the efflux of ATP outside the cells, provides to the extracellular compartment both PP_i, necessary to prevent the calcification processes, and purine nucleotides and adenosine, key mediators of many physiological processes **[124] [125]**. The decrease of ABCC6 and CD73 protein levels thanks to probenecid and their increase thanks to ATP and adenosine, could suggest both a role of ABCC6 in the regulation and in the activation of the purinergic system and in the overlapping of clinical symptoms of ACDC and PXE diseases.

Finally, we could not exclude the possible involvement of ABCC6 protein, through the purinergic system, in other liver diseases.

3.2.8 Effects of CD73 modulation by Probenecid

It is known in literature that CD73 protein is an important key regulator in some cancer processes, in particular in growth and cancer metastasis **[103] [104]**. CD73 protein thanks to its ability to promote the migration and invasion of cancer cells, could be an excellent candidate for anticancer therapy. As we have already noted in previous experiments, it is possible to decrease *NT5E* gene and CD73 protein expression using probenecid. In order to verify the possible phenotypic changes produced by CD73 decrease and by the partial decrease of purinergic system, HepG2 cells were treated with 250 μM of probenecid for 24 and 48 hours in a migration assay called wound-healing. It was important to check if, in addition to a decrease of *NT5E* gene and CD73 protein expression, there was also a consequent variation of the migration cellular processes. As we can see in **Fig. 3.17** we found both no variation in migration rate of HepG2 cells treated for 24 hours with probenecid and no changes in *NT5E* gene levels (see 3.2.1 session). As we can see in **Fig. 3.17** we found a significant decrease in migration rate of HepG2 cells after 48 hours of treatment with probenecid. In particular, there is a decrease of about 40% in migration rate of these

cells between 24 and 48 hours of treatment, in accordance with a decrease in *NT5E* gene expression and in CD73 protein levels after 48 hours of treatment with probenecid (see 3.2.2 session).

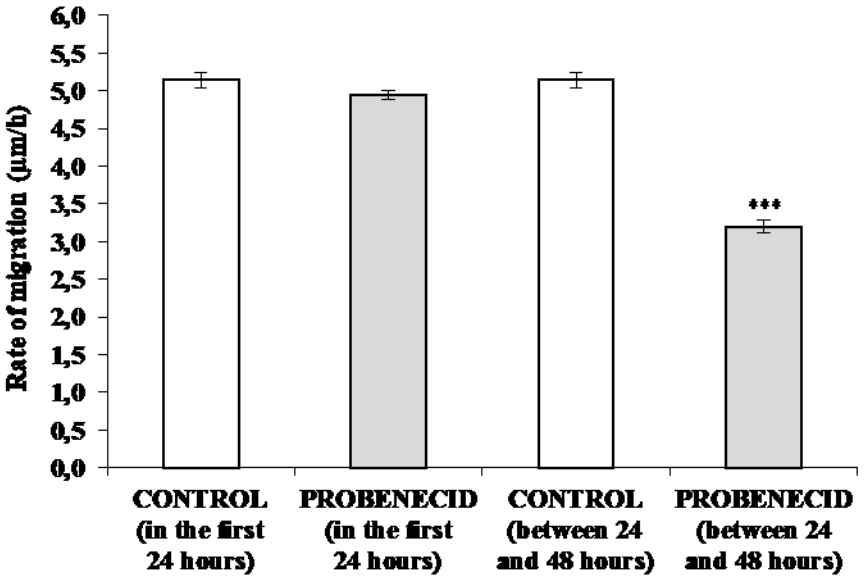

Fig. 3.17: The effects of Probenecid on HepG2 cells migration rate after 24 and 48 hours of treatment. In a monolayer of HepG2 cells was generated a linear wound and the cells were treated with 250 µM of probenecid for 24 and 48 hours. The migration rate of cells was monitored during the treatment. Data of migration rate are expressed as a percentage of the control group (both in the first 24 hours and between 24 and 48 hours of treatment) and represented as the means ± SD of three independent experiments. *** $p < 0.001$, Student's t-test.

Therefore, we can hypothesize a correlation between the CD73 protein expression level and the migration rate of HepG2 cells.

3.2.9 Evaluation of the mechanism promoting the decrease of HepG2 cells migration rate

Subsequently experiments were performed in order to understand a possible mechanism underlying the control of migration speed of HepG2 cells after a treatment with probenecid. A first experiment was performed on HepG2 cells treated with 250 μM of probenecid for 24 and 48 hours, in order to analyse their cellular cycle, using the flow cytometer. In the following figures, **Fig. 3.18** and **Fig. 3.19**, we can see the results of the cellular cycle analysis, respectively after 24 and 48 hours of the treatment with probenecid. As stressed in these figures there is no block of the cellular cycle in any specific phase and the population of untreated and treated cells in each phase is always the same. Consequently probenecid seems not to act on the slowing of the cellular cycle.

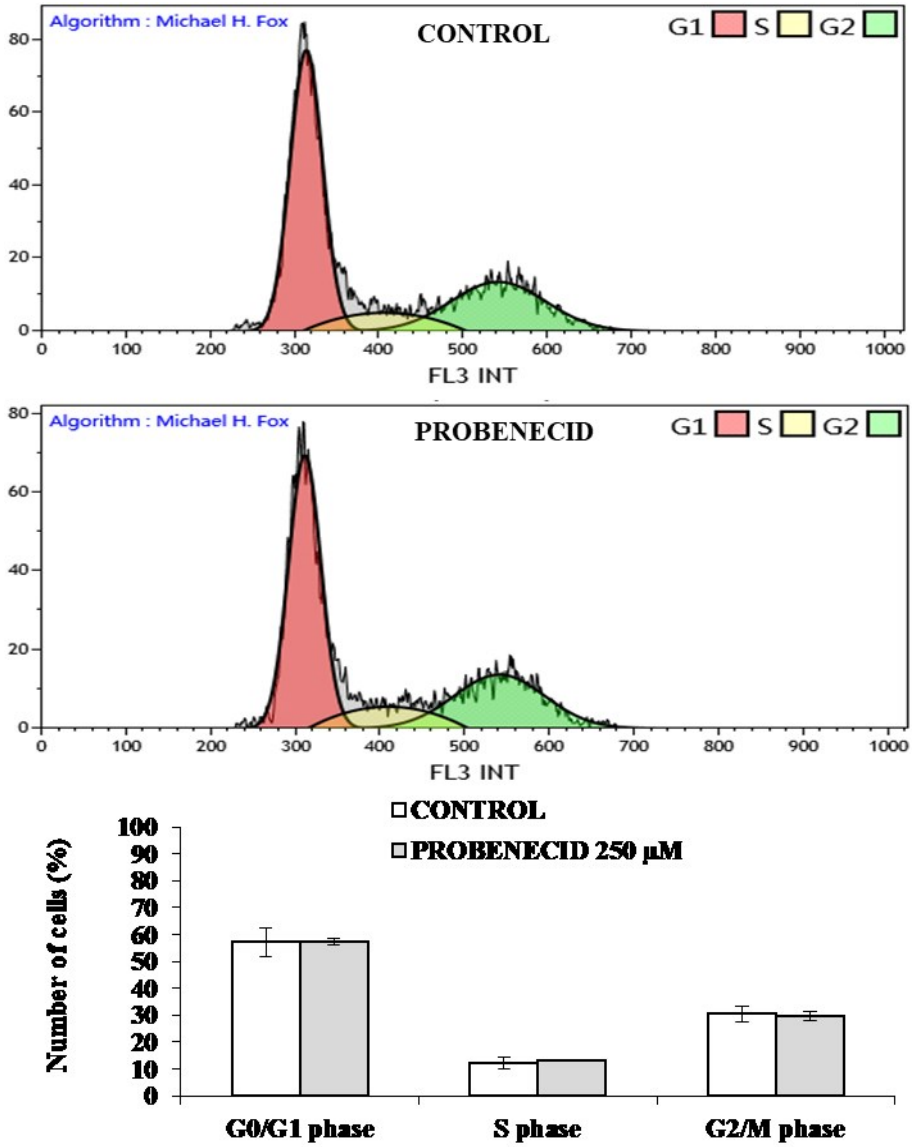

Fig. 3.18: Cellular cycle analysis, in HepG2 cells, after 24 hours of Probenecid treatment. Cellular cycle was analyzed by flow cytometer in HepG2 cells after 24 hours of treatment with 250 µM of probenecid. Histogram plots show a single representative experiment; data are expressed as a percentage of the control group and presented as the means ± SD of three independent experiments.

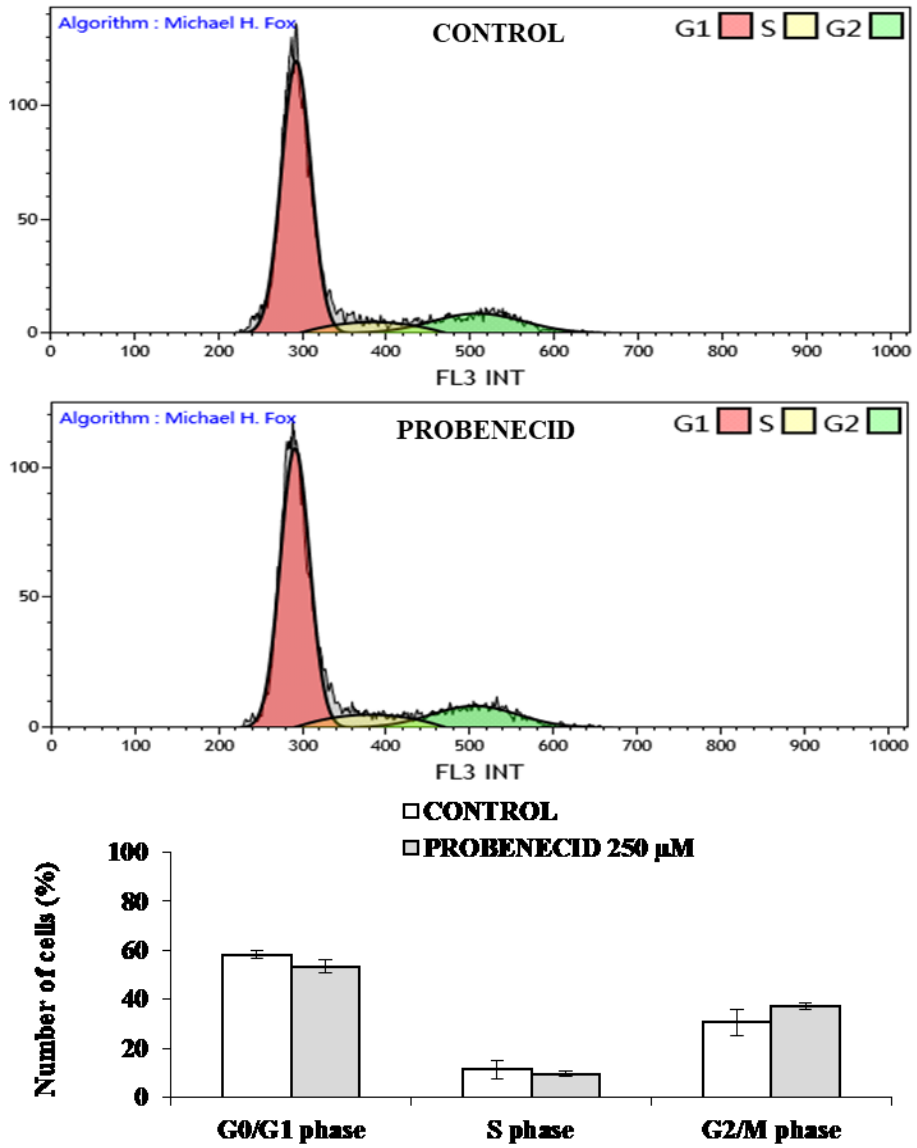

Fig. 3.19: Cellular cycle analysis, in HepG2 cells, after 48 hours of Probenecid treatment. Cellular cycle was analyzed by flow cytometer in HepG2 cells after 48 hours of treatment with 250 µM of probenecid. Histogram plots show a single representative experiment; data are expressed as a percentage of the control group and presented as the means ± SD of three independent experiments.

In order to confirm the cellular cycle data, we performed an analysis of *p16*, *p21* and *p53* expression gene levels, via Real-Time PCR, after 250 µM of the treatment with probenecid for 48 hours. p16, p21 and p53 proteins are able to inhibit the action of cyclin-dependent kinases (CDKs), and to block the cellular cycle. As we can see in **Fig. 3.20**, we found no significant variations of expression of these gene levels. These data confirm that probenecid does not act on the cellular cycle.

2^(-ΔΔCt)	
p16	0.93 ± 0.02
p21	1.11 ± 0.02
p53	0.90 ± 0.16

Fig. 3.20: The effects of Probenecid, in HepG2 cells, on *p16*, *p21* and *p53* genes after 48 hours of treatment. Fold change of *p16*, *p21* and *p53* mRNA levels in HepG2 cells treated with 250 µM of probenecid for 48 hours compared to the control cells (treated with DMSO). β-actin was used as housekeeping gene. Data are represented as the means ± SD of three independent experiments.

Then we performed an experiment in order to evaluate a possible modification of actin filaments, the main components of the cytoskeleton architecture and therefore of important cellular functions as the cellular movement. In order to study these modifications, an immunofluorescence assay was performed using the phalloidin, a bicyclic peptide, that specifically binds with actin filaments.

The cells were treated with 250 μM of probenecid for 24 and 48 hours. As we can see in **Fig. 3.21**, in the cells treated with DMSO (as control cells) and with 250 μM of probenecid for 24 hours there are no significant differences: these cells are not very compact and have many filopodia (green), that extend in all directions. Instead, in the cells treated with 250 μM of probenecid for 48 hours there are significant changes: the cells are very compact and the filopodia (green) are almost completely absent or, if present, they are very short. In addition, the actin filaments (green), which are depolymerized, are almost entirely concentrated in the periphery of the cells. Therefore we can deduce that probenecid, if used at the concentration of 250 μM for 48 hours, is able to decrease the cellular movement and to promote significant changes on the actin filaments and on the filopodia. Therefore the use of probenecid could be very important to decrease, in this type of cancer, the migration and metastasis processes.

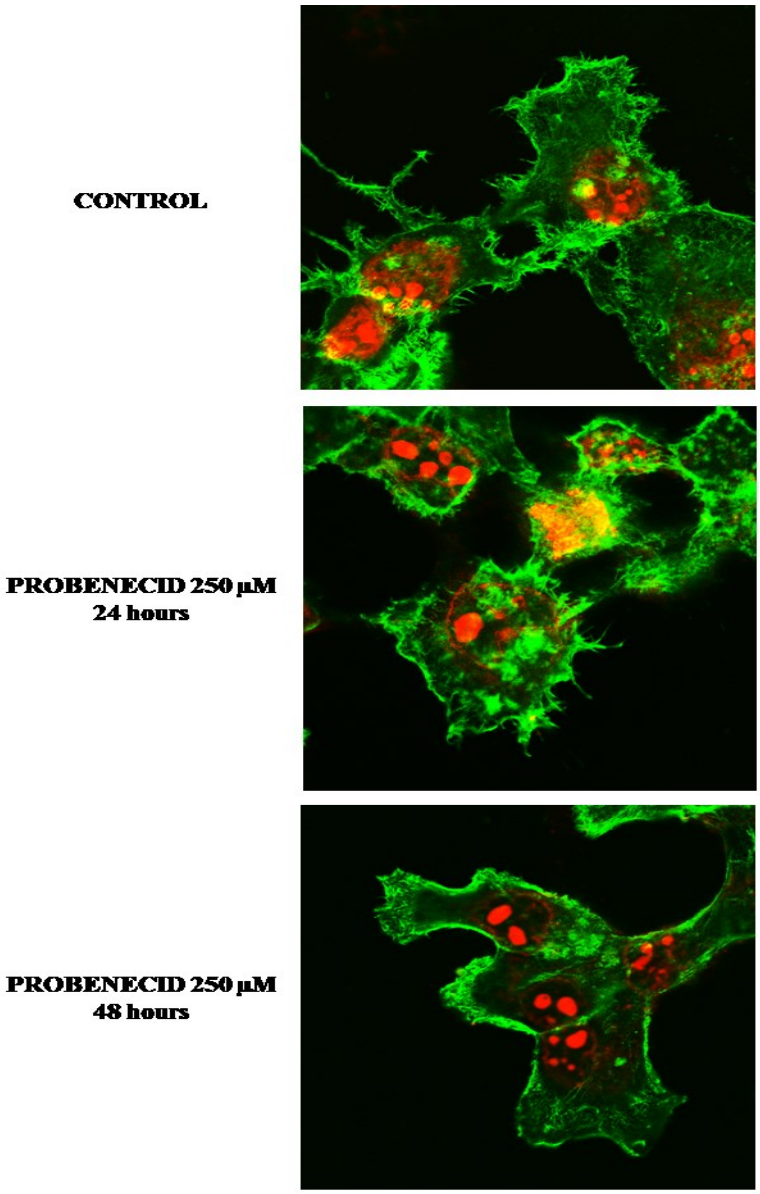

Fig. 3.21: The effects of Probenecid, in HepG2 cells, on actin filaments and filopodia after 24 and 48 hours of treatment. Cells were treated with 250 µM of probenecid for 24 and 48 hours. Representative images, after adding phalloidin, of control and probenecid-treated HepG2 cells were acquired with a confocal fluorescence microscope. DMSO-treated cells were used as control.

3.3 Effects of Quercetin and Doxorubicin in HepG2 cells

In order to highlight the correlation between the *ABCC6* and *NT5E* genes, we performed experiments on HepG2 cells with doxorubicin and quercetin, two compounds involved in the activity and in the regulation of MRP proteins **[20] [165]**.

3.3.1 Effects of Quercetin

We performed in HepG2 cells an experiment with quercetin, another inhibitor of some multidrug resistance-associated proteins, MRPs **[165]**. A cytotoxicity assay was initially performed on HepG2 cells in order to evaluate the effects time- and dose-dependent of quercetin. As we can see in **Fig. 3.22**, the quercetin does not show cellular toxicity up to 165 μM within 24 hours (about 95% of viability). After a treatment of 48 hours the cellular viability decreases of about 25% and the cells become smaller. At 330 and 660 μM of quercetin concentrations, the cells progressively reduce their viability and show significant morphological changes.

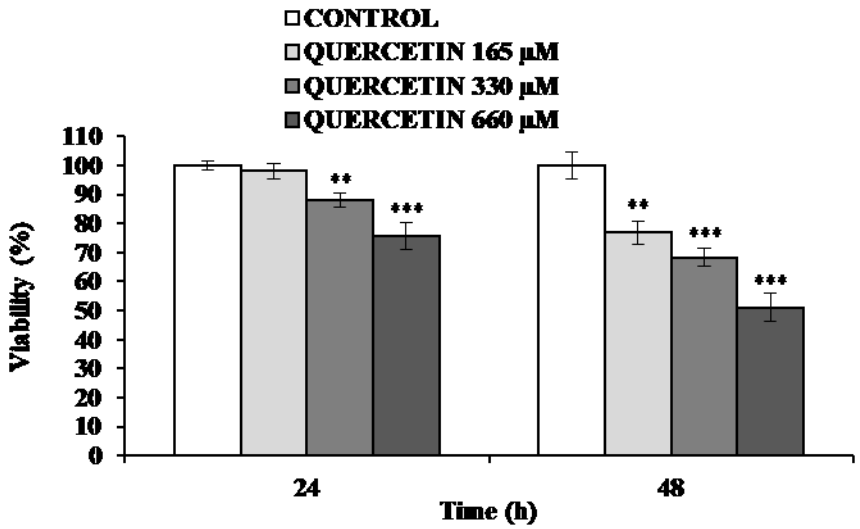

Fig. 3.22: Effects of Quercetin on viability of HepG2 cells. Cells were treated with quercetin at the concentration of 165, 330 and 660 µM for 24 and 48 hours. Data are expressed as a percentage of the control group and presented as means ± SD of three independent experiments. ** $p < 0.01$, *** $p < 0.001$, Student's t-test.

After analysing these preliminary results we decided to test 165 µM of calcein (for a short period of time) in HepG2 cells in order to check if this compound was able to inhibit the transport of calcein by MRPs **[17]**. As we can see in **Fig. 3.23**, in HepG2 cells treated with the quercetin we found a decrease of external calcein (of about 20%) and an increase of internal calcein (of about 30%). These data suggest that all MRPs, including ABCC6 (abundantly expressed in HepG2 cells), are inhibited by the presence of quercetin. In fact, in presence of quercetin, the calcein, once metabolized inside the cells, can't be expelled outside them. Analysing these data we can deduce that

quercetin is less able to inhibit the ABCs transport activity than probenecid in these cells.

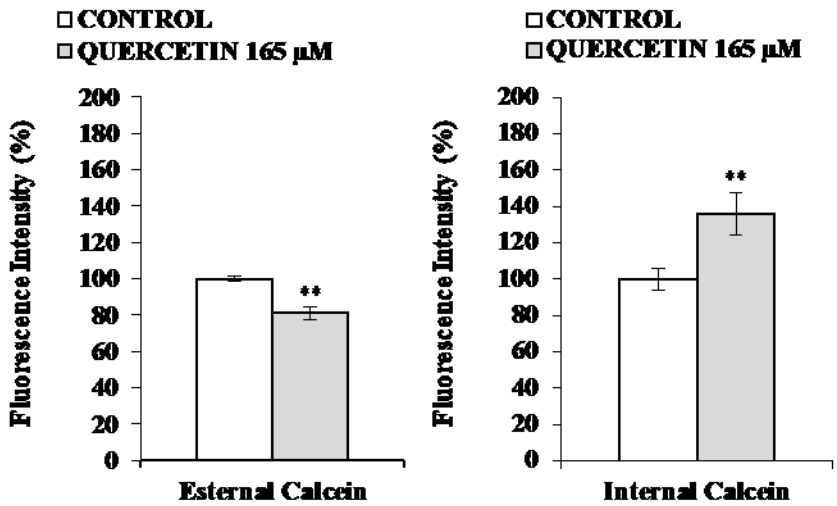

Fig. 3.23: Inhibition of calcein transport by Quercetin in HepG2 cells. Cells were treated for 1 hour with 165 µM of quercetin and then for 1 hour with 1 µM of calcein-AM. Data of external and internal calcein are expressed as a percentage of the control group and presented as means ± SD of three independent experiments. ** $p < 0.01$, Student's t-test.

After the analysis of all these preliminary data we decided to use in HepG2 cells the quercetin at the concentration of 165 µM for 24 hours, in order to understand the cellular variations in conditions of partial modulation of ABCC6 transporter activity. After the quercetin treatment, as we can see in **Fig. 3.24**, we found a slightly variation in *ABCC6* and *NT5E* expression gene levels via Real-Time PCR, although we previously observed an influence of quercetin on the activity of ABCC6 protein.

2^(-ΔΔCt)	
ABCC6	0.81 ± 0.07
NT5E	0.84 ± 0.08

Fig. 3.24: The effects of Quercetin, in HepG2 cells, on *ABCC6* and *NT5E* genes after 24 hours of treatment. Fold change of *ABCC6* and *NT5E* mRNA levels in HepG2 cells treated with 165 μM of quercetin for 24 hours compared to the control cells (treated with DMSO). β-actin was used as housekeeping gene. Data are represented as the means ± SD of three independent experiments.

The results obtained after 24 hours of the quercetin treatment, in HepG2 cells, are similar to those ones obtained previously using probenecid. Therefore, these data show similar cellular effects using different ABC proteins inhibitors in HepG2 cells and also confirm the correlation between the *ABCC6* and *NT5E* genes.

3.3.2 Effects of Doxorubicin

We performed in HepG2 cells an experiment with doxorubicin, a substrate of ABC proteins **[20]**. The cells were treated for several days with increasing concentrations of doxorubicin in order to allow an adaptation of the cells to this compound and at the same time to evaluate possible variations in the gene expression of some MRP transporters. As we can see in **Fig. 3.25**, this treatment is able to determine a cellular line resistant to doxorubicin and to increase

the *ABC* gene expression; specifically, there is a dose-dependent increase in *ABCB1* and *ABCC6* genes. Moreover, we found again a correlation between *ABCC6* and *NT5E* genes: they increase proportionally.

2^(-ΔΔCt)		
	50 nM	**100 nM**
ABCB1	**0.96 ± 0.06**	**1.26 ± 0.07**
ABCC6	**1.38 ± 0.07**	**1.69 ± 0.08**
NT5E	**1.52 ± 0.06**	**1.60 ± 0.09**

Fig. 3.25: The effects of different concentrations of Doxorubicin, in HepG2 cells, on *ABCB1*, *ABCC6* and *NT5E* genes. Fold change of *ABCB1*, *ABCC6* and *NT5E* mRNA levels in HepG2 cells treated with 50 and 100 nM of doxorubicin compared to the control cells (treated with PBS 1X). β-actin was used as housekeeping gene. Data are represented as the means ± SD of three independent experiments.

The doxorubicin and the inhibitors of MRPs protein, the probenecid and the quercetin in HepG2 cells are able to modulate respectively positively or negatively *ABCC6* and *NT5E* gene expression.

3.4 Effects of Probenecid in other cellular lines

Finally, we performed some experiments in order to verify whether probenecid was able to produce the same results in other cellular types, in particular we focused our attention on the control of CD73 expression. So, we tested probenecid, adenosine and ATP on HuH-7, MDA-MB-231 and HEK293 cellular lines.

3.4.1 Effects of Probenecid in HuH-7 cells

A cytotoxicity assay was initially performed in HuH-7 cells, a cellular line of human hepatocellular carcinoma more differentiated than HepG2 cells, in order to evaluate the effects time- and dose-dependent of probenecid. Probenecid did not show cellular toxicity up to 250 μM within 48 hours (about 85% of viability); after 48 hours of treatment with probenecid at 500 μM the viability is about 80% and at 1000 μM the viability is about 60% (**Fig. 3.26**). The cells after the treatment with probenecid did not show significant alterations in their morphology.

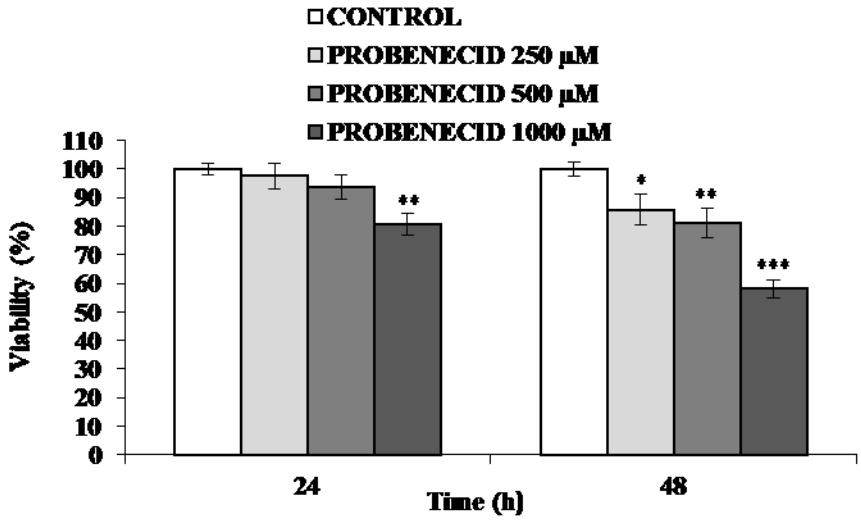

Fig. 3.26: Effects of Probenecid on viability of HuH-7 cells. Cells were treated with probenecid at the concentration of 250, 500 and 1000 µM for 24 and 48 hours. Data are expressed as a percentage of the control group and presented as means ± SD of three independent experiments. * $p < 0.05$, ** $p < 0.01$, *** $p < 0.001$, Student's t-test.

After analysing these preliminary results we decided to test 250 µM of probenecid (for a short period of time) in HuH-7 cells in order to check if this compound was able to inhibit the transport of calcein by MRPs **[17]**. As we can see in **Fig. 3.27**, in HuH-7 cells treated with probenecid there is a decrease of about 20% of external calcein and an increase of about 15% of internal calcein. These data suggest that all MRPs, including ABCC6, are slightly inhibited by the presence of probenecid. In fact, in presence of probenecid, the calcein, once metabolized inside the cells, can't be expelled outside them.

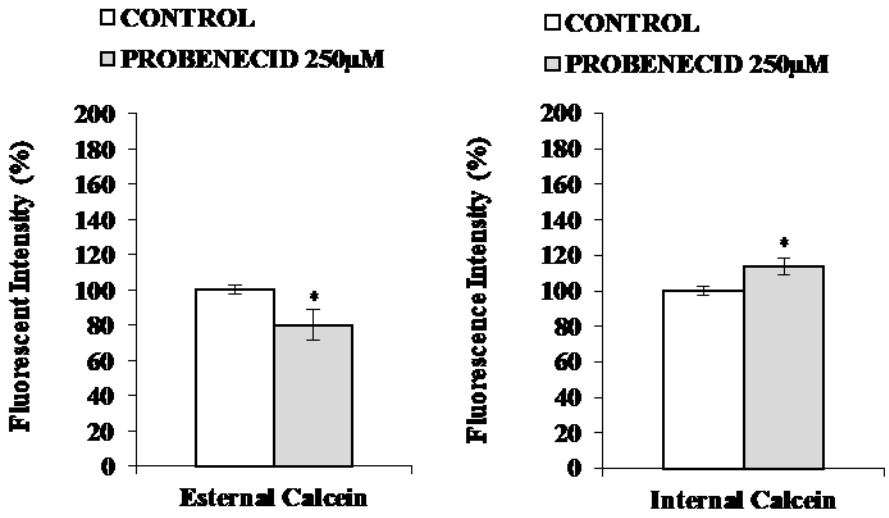

Fig. 3.27: Inhibition of calcein transport by Probenecid in HuH-7 cells. Cells were treated for 1 hour with 250 µM of probenecid and then for 1 hour with 1 µM of calcein-AM. Data of external and internal calcein are expressed as a percentage of the control group and presented as means ± SD of three independent experiments. * $p < 0.05$, Student's t-test.

Then, we decided to use probenecid in HuH-7 cells at the concentration of 250 µM for 48 hours, in order to understand if CD73 protein could change its expression levels. As we can see in **Fig. 3.28**, no significant variation in CD73 protein expression was found after the treatment with probenecid.

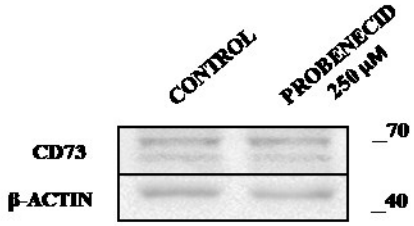

Fig. 3.28: The effects of Probenecid, in HuH-7 cells, on CD73 protein after 48 hours of treatment. Representative western blotting images of CD73 immunoreactive band. β-actin was used as loading control. This datum was repeated in three independent experiments.

We performed other experiments with different concentrations of adenosine and ATP, in order to evaluate the correlation between these compounds and CD73 expression. At first, the effects of adenosine were evaluated in HuH-7 cells after 48 hours of treatment, in presence and in absence of probenecid. In **Fig. 3.29**, CD73 protein levels remain unchanged after the treatment of these cells only in presence of probenecid. Moreover, CD73 protein levels are increased of about 10-20% after the treatment respectively with 10 and 100 µM of adenosine. Finally, CD73 protein levels always remain slightly over-expressed of about 10-20% if probenecid is added to treatment with adenosine.

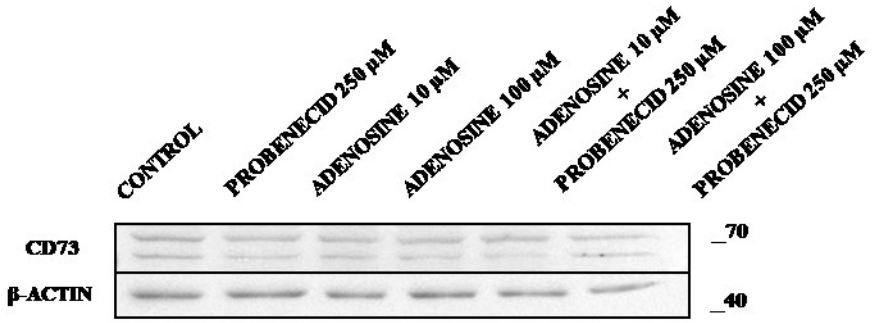

Fig. 3.29: The effects of adenosine, in HuH-7 cells, on CD73 protein, in the presence and in absence of Probenecid, after 48 hours of treatment. Representative western blotting image of CD73 immunoreactive band. β-actin was used as a loading control. This datum was repeated in three independent experiments.

The effects of ATP were evaluated in HuH-7 after 48 hours of treatment, in presence and in absence of probenecid. In **Fig. 3.30**, CD73 protein levels remain unchanged after the treatment of these cells only in presence of probenecid, while, CD73 protein levels are increased of about 10-20% after the treatment respectively with 50 and 500 µM of ATP. Finally, CD73 protein levels always remain slightly over-expressed of about 10-20% if probenecid is added to treatment with ATP.

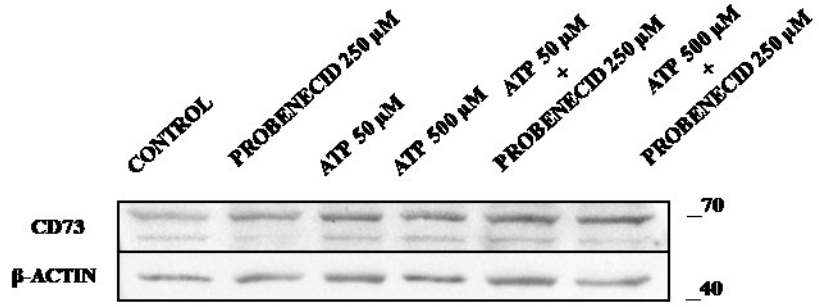

Fig. 3.30: The effects of ATP, in HuH-7 cells, on CD73 protein, in the presence and in absence of Probenecid, after 48 hours of treatment. Representative western blotting image of CD73 immunoreactive band. β-actin was used as a loading control. This datum was repeated in three independent experiments.

So, in HuH-7 cells we found a poor effect of probenecid, adenosine and ATP in CD73 modulation. As we can see in **Fig. 3.31**, the basal levels of *ABCC6* gene expression in these cells are lower than those ones in HepG2 cells; the amount of ATP and adenosine transported by ABCC6 could be too low to regulate CD73. The lowest *ABCC6* gene expression in these cells could explain the poor effect of probenecid. Probably in these cells the CD73 protein is less regulated by adenosine and ATP.

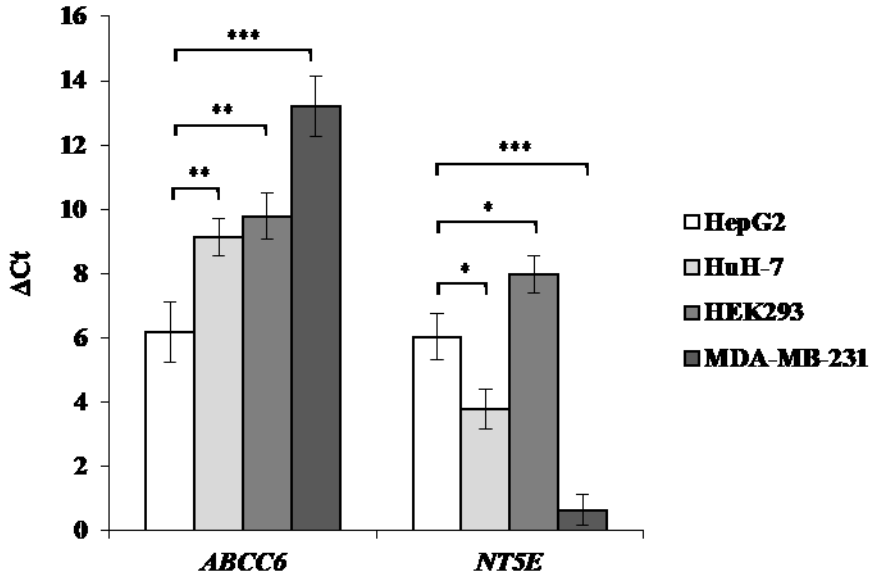

Fig. 3.31: *ABCC6* and *NT5E* genic expression in HepG2, HuH-7, HEK293 and MDA-MB-231 cellular lines. ΔCt of *ABCC6* and *NT5E* mRNA levels in HepG2, HuH-7, HEK293 and MDA-MB-231 cellular lines. β-actin was used as housekeeping gene. Data are represented as the means ± SD of three independent experiments. * $p < 0.05$, ** $p < 0.01$, *** $p < 0.001$, Student's t-test.

3.4.2 Effects of Probenecid in MDA-MB-231 cells

A cytotoxicity assay was initially performed on MDA-MB-231 cells, a cellular line of triple-negative human breast cancer poorly differentiated, in order to evaluate the effects time- and dose-dependent of probenecid. This cellular line is characterized by high levels of *NT5E* gene (see **Fig. 3.31**), and a partial control of CD73 protein by probenecid could promote a decrease of cancer processes. Probenecid did not show cellular toxicity up to 250 μM within 48 hours (about 90% of viability); after 48 hours of treatment with probenecid at 500 μM the viability is about 80% and at 1000 μM the viability is about 60% (**Fig. 3.32**). The cells after the treatment with probenecid did not show significant alterations in their morphology.

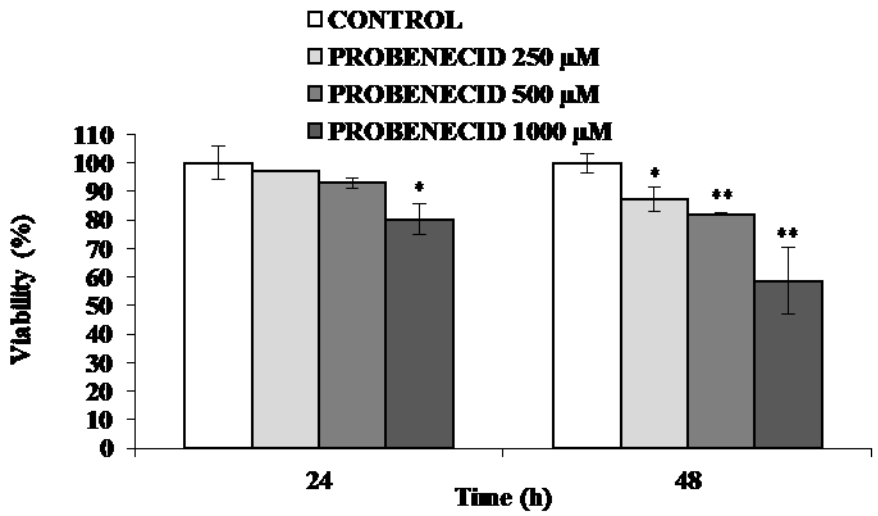

Fig. 3.32: Effects of Probenecid on viability of MDA-MB-231 cells. Cells were treated with probenecid at the concentration of 250, 500 and 1000 µM for 24 and 48 hours. Data are expressed as a percentage of the control group and presented as means ± SD of three independent experiments. * $p < 0.05$, ** $p < 0.01$, Student's t-test.

We decided to test 250 µM of probenecid (for a short period of time) in MDA-MB-231 cells in order to check if this compound was able to inhibit the transport of calcein by MRPs **[17]**. As we can see in **Fig. 3.33**, in MDA-MB-231 cells treated with probenecid we did not find any significant variation both in the amount of external and internal calcein. These data suggest that the MRPs are not inhibited by the presence of probenecid. In fact, in presence of probenecid, the calcein, once metabolized inside the cells, can be normally expelled outside them.

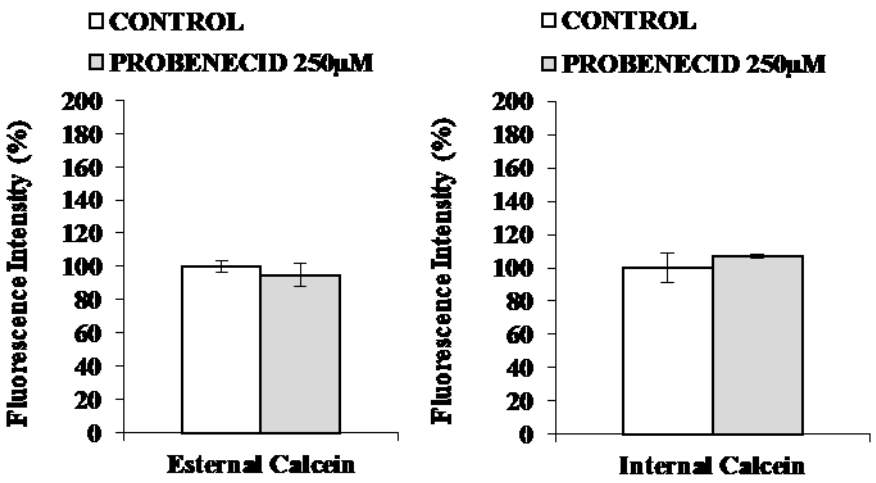

Fig. 3.33: Inhibition of calcein transport by Probenecid in MDA-MB-231 cells. Cells were treated for 1 hour with 250 µM of probenecid and then for 1 hour with 1 µM of calcein-AM. Data of external and internal calcein are expressed as a percentage of the control group and presented as means ± SD of three independent experiments.

In MDA-MB-231 cells we found no effect of probenecid in the modulation of MRPs activity. As previously seen in **Fig. 3.31**, the lowest *ABCC6* expression, in these cells compared to HepG2 and HuH-7 cells could explain this effect. Then, we decided to use in MDA-MB-231 cells the probenecid at the concentration of 250 µM for 48 hours, in order to understand if CD73 protein could change its expression levels and to further correlate the modulation of CD73 via ABCC6. As we can see in **Fig. 3.34**, we found no significant variation in CD73 protein expression after the treatment with probenecid.

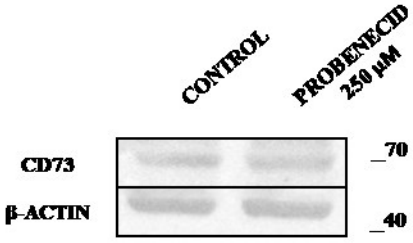

Fig. 3.34: The effects of Probenecid, in MDA-MB-231 cells, on CD73 protein after 48 hours of treatment. Representative western blotting image of CD73 immunoreactive band. β-actin was used as a loading control. This datum was repeated in three independent experiments.

We performed experiments with different concentrations of adenosine and ATP, in order to evaluate the correlation between these compounds and CD73 expression. At first, the effects of adenosine were evaluated in MDA-MB-231 cells after 48 hours of treatment, in presence and in absence of probenecid. In **Fig. 3.35**, CD73 protein levels remain unchanged after the treatment of these cells only in presence of probenecid. Moreover, CD73 protein levels are increased of about 15-20% after the treatment respectively with 10 and 100 µM of adenosine. Finally, CD73 protein levels always remain slightly over-expressed of about 15-20% if probenecid is added to the treatment with adenosine.

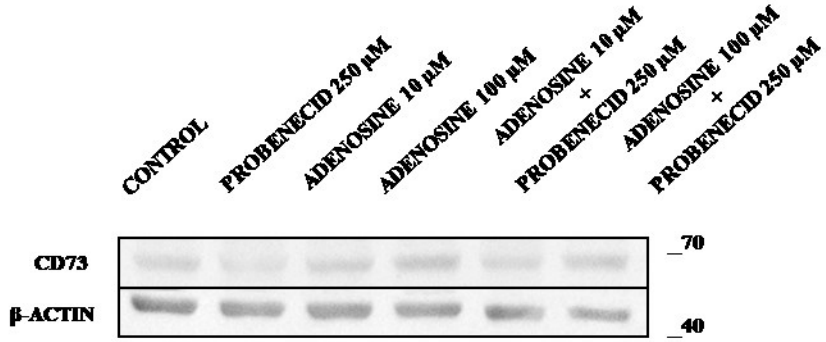

Fig. 3.35: The effects of adenosine, in MDA-MB-231 cells, on CD73 protein, in the presence and in absence of Probenecid, after 48 hours of treatment. Representative western blotting image of CD73 immunoreactive band. β-actin was used as a loading control. This datum was repeated in three independent experiments.

Then, the effects of ATP were evaluated in MDA-MB-231 cells after 48 hours of treatment, in presence and in absence of probenecid. In **Fig. 3.36**, CD73 protein levels remain unchanged after the treatment of these cells only in presence of probenecid, while, CD73 protein levels are increased of about 20-25% after the treatment respectively with 50 and 500 µM of ATP. Finally, CD73 protein levels always remain slightly over-expressed of about 20-25% if probenecid is added to the treatment with ATP.

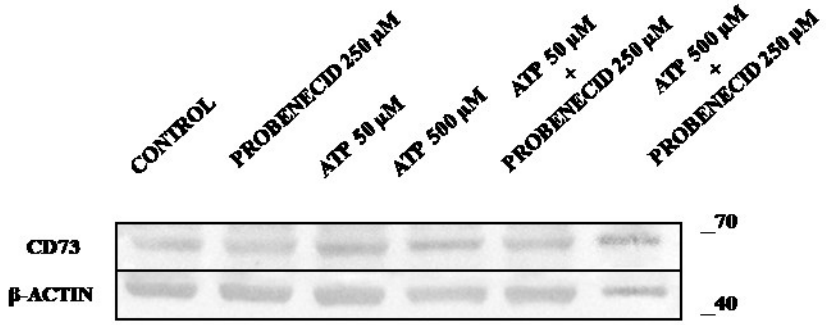

Fig. 3.36: The effects of ATP, in MDA-MB-231 cells, on CD73 protein, in the presence and in absence of Probenecid, after 48 hours of treatment. Representative western blotting image of CD73 immunoreactive band. β-actin was used as a loading control. This datum was repeated in three independent experiments.

So, in MDA-MB-231 cells we found no effect of probenecid and a poor effect of adenosine and ATP in CD73 modulation. As previously seen in **Fig. 3.31**, the lowest *ABCC6* expression, in these cells could explain no effect of probenecid. In this context, probably the CD73 protein is less regulated by adenosine and ATP because the basal levels of *ABCC6* expression in these cells are very lower than those ones in HepG2 and HuH-7 cells. So, the amount of ATP and adenosine transported by ABCC6 could be too low to regulate CD73. In order to validate the results obtained with probenecid, we performed an experiment on the possible modifications of actin filaments. An immunofluorescence assay was performed using the phalloidin, that is able to highlight possible molecular changes on the actin filaments induced by a treatment with 250 µM of probenecid for 48 hours. As we

can see in **Fig. 3.37**, these cells, more elongated and isolated than HepG2 cells, do not show any alterations after treatment with probenecid: the filopodia (green) are long and always present, while the actin filaments (green) are present on the whole cellular surface; therefore probenecid could not able to decrease the cellular migration in these cells. We can correlate these results with those ones obtained with CD73 modulation after the treatment with probenecid: the possible non-reduction of MDA-MB-231 migration rate could be caused by the non-reduction of CD73 and not significant morphological changes.

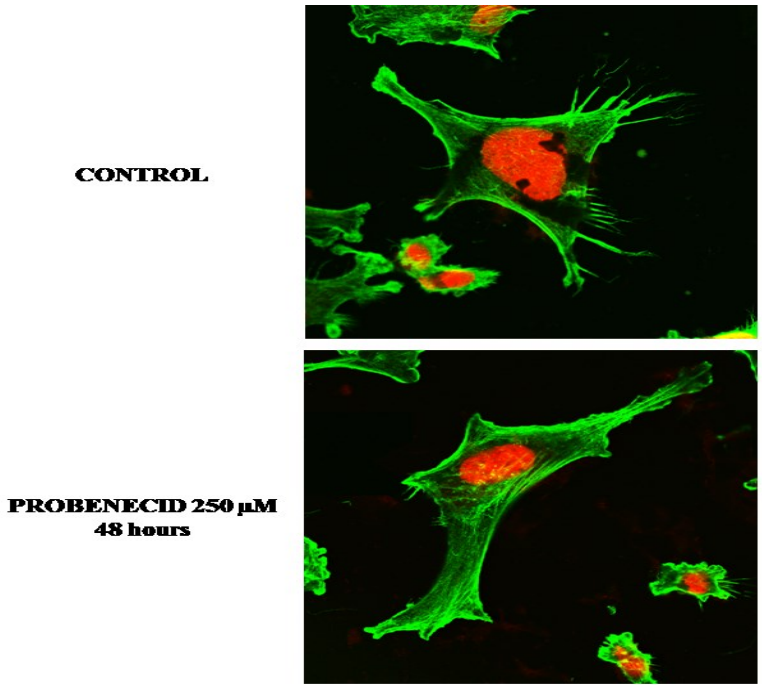

Fig. 3.37: The effects of Probenecid, in MDA-MB-231 cells, on actin filaments and filopodia after 48 hours of treatment. Cells were treated with 250 µM of probenecid for 48 hours. Representative images, after adding phalloidin, of control and probenecid-treated HepG2 cells were acquired with a confocal fluorescence microscope. DMSO-treated cells were used as control.

3.4.3 Effects of Probenecid in HEK293 cells

A cytotoxicity assay was initially performed in HEK293 cells, a cellular line of human embryonic kidney 293, in order to evaluate the effects time- and dose-dependent of probenecid. Probenecid did not show cellular toxicity up to 250 µM within 48 hours (about 90% of viability); after 48 hours of treatment with probenecid at 500 µM the viability is about 80% and at 1000 µM the viability is about 70% (**Fig. 3.38**). These cells are more resistant to probenecid than other kind of cells examined. These cells after the treatment with probenecid did not show significant alterations in their morphology.

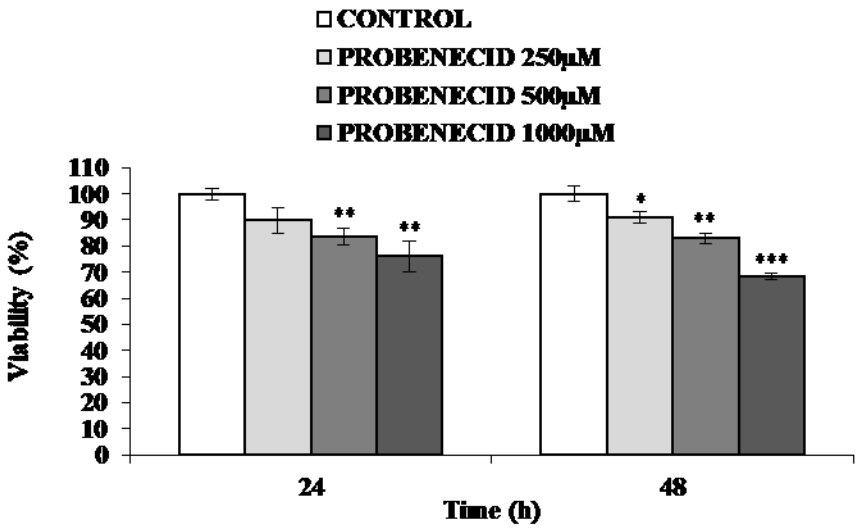

Fig. 3.38: Effects of Probenecid on viability of HEK293 cells. Cells were treated with probenecid at the concentration of 250, 500 and 1000 µM for 24 and 48 hours. Data are expressed as a percentage of the control group and presented as means ± SD of three independent experiments. * $p < 0.05$, ** $p < 0.01$, *** $p < 0.001$, Student's t-test.

As previously seen in **Fig. 3.1**, in HEK293 cells transfected with only Flag-pcDNA and treated with probenecid we found a small decrease of doxorubicin efflux. This datum suggests that the MRPs are slightly inhibited by the presence of probenecid. Then, we decided to use in these cells probenecid at the concentration of 250 μM for 48 hours, in order to understand if CD73 protein could change its expression levels. As we can see in **Fig. 3.39**, we found no significant variations in CD73 protein expression after the treatment with probenecid.

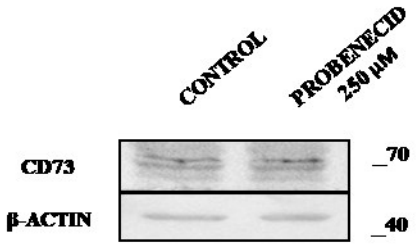

Fig. 3.39: The effects of Probenecid, in HEK293 cells, on CD73 protein after 48 hours of treatment. Representative western blotting image of CD73 immunoreactive band. β-actin was used as a loading control. This datum was repeated in three independent experiments.

We performed other experiments with different concentrations of adenosine and ATP, in order to evaluate a possible correlation between these compounds and CD73 expression. At first, the effects of adenosine were evaluated in HEK293 cells after 48 hours of treatment, in presence and in absence of probenecid. In **Fig. 3.40**, CD73 protein levels remain unchanged after the treatment of these cells only in presence of probenecid. Moreover, CD73 protein levels are increased

of about 15% after treatment respectively with 10 and 100 μM of adenosine. Finally, CD73 protein levels remain unchanged if probenecid is added to the treatment with adenosine.

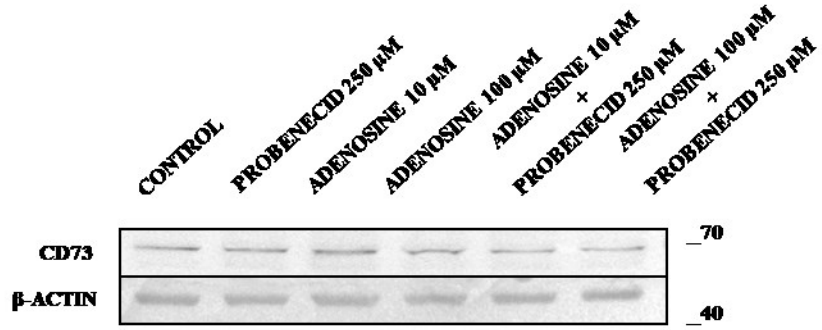

Fig. 3.40: The effects of adenosine, in HEK293 cells, on CD73 protein, in the presence and in absence of Probenecid, after 48 hours of treatment. Representative western blotting image of CD73 immunoreactive band. β-actin was used as a loading control. This datum was repeated in three independent experiments.

Then, the effects of ATP were evaluated in HEK293 after 48 hours of treatment, in presence and in absence of probenecid. In **Fig. 3.41**, CD73 protein levels remain unchanged after the treatment of these cells only in presence of probenecid, while CD73 protein levels are increased of about 20% after treatment respectively with 50 and 500 μM of ATP. Finally, CD73 protein levels always remain slightly over-expressed of about 10-20% if probenecid is added to treatment with ATP.

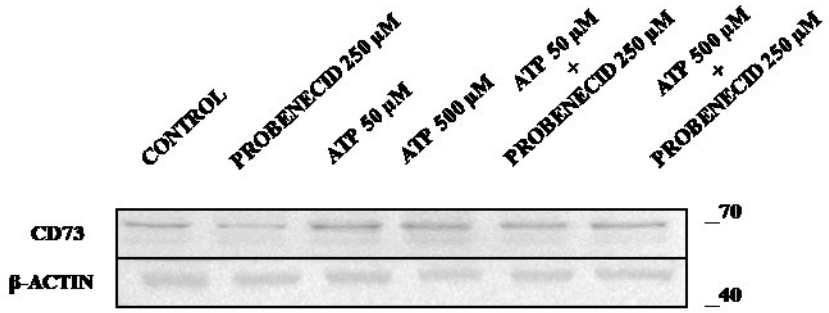

Fig. 3.41: The effects of ATP, in HEK293 cells, on CD73 protein, in the presence and in absence of Probenecid, after 48 hours of treatment. Representative western blotting image of CD73 immunoreactive band. β-actin was used as a loading control. This datum was repeated in three independent experiments.

In this cellular line we obtained the same results of HuH-7 cellular line treated with probenecid, adenosine and ATP. In HEK293 cells we found a poor effect of probenecid, adenosine and ATP in CD73 modulation. As previously seen in **Fig. 3.31**, the lowest *ABCC6* expression could explain the poor effect of probenecid. In these cells, probably, the CD73 protein expression is slightly regulated by adenosine and ATP because the basal levels of *ABCC6* expression in these cells are lower than those ones in HepG2 cells. So, the amount of ATP and adenosine transported by ABCC6 could be too low to regulate CD73.

Conclusions and future perspectives

ABCC6 protein, belonging to sub-family C of ABC transporters, is codified by *ABCC6* gene and it is mainly expressed in the liver and the kidney, in particular at level of basolateral membrane **[41]**. It is also probably involved in determining low levels of resistance to some drugs. *ABCC6* mutations cause a rare recessive disease called Pseudoxanthoma Elasticum, characterized by ectopic calcification of connective fibers **[112]**; the mutations of *ABCC6* in PXE stress the role of this protein in the ectopic mineralization processes. The aim of this scientific research is to characterize the role of ABCC6 protein in particular in the activation of purinergic system and in the cancer processes. The research is based on two evidences. The first one concerns how the stable transfection with *ABCC6* gene in HEK293 cells is able to promote a major efflux of ATP in extracellular space **[119] [120]**; ATP consequently produces PP_i and other molecules, such as AMP, adenosine and P_i, involved in the balance both of mineralization and of purinergic processes. The second one concerns how, using AOPCP, a CD73 inhibitor, it is possible to partially reduce MDR phenotype in GBM cells by the expression and the activity of MRP1 modulation **[163]**. It could be possible to control CD73 protein expression using an inhibitor of MRPs protein, such as probenecid. In this scientific research, we performed a set of experiments in order to evaluate the function of ABCC6 in the processes previously mentioned and in particular to verify the correlation between ABCC6 and CD73 proteins. CD73 is a protein involved in cancer processes and in the pathway metabolizing the

extracellular ATP also carried out by ABCC6. We performed a preliminary experiment in order to verify if the transport activity of ABCC6 was significant decreased with probenecid in HEK293 cells stably transfected with *ABCC6*-Flag-pcDNA; specifically ABCC6 activity was partially inhibited by probenecid **[171]**. Then, we performed an experiment with probenecid in HepG2 cells, a cellular line of human hepatocellular carcinoma in which ABCC6 is very expressed. The results showed both a significant decrease of about 30% of MRPs activity and of about 30% of ABCC6 protein after a treatment with 250 μM of probenecid for 48 hours **[171]**. Therefore, it is possible to control the expression and activity of ABCC6 protein by probenecid. CD73 protein expression decreases of about 30% **[171]** while TNAP protein remains unchanged. The role of probenecid in HepG2 cells is important because: it is able to regulate ABCC6 expression and also other MRPs activity, probably decreasing the possible effects of multidrug resistance; it is able to regulate CD73 expression probably decreasing the cancer processes and the amount of extracellular P_i; it is not able to determine changes in TNAP expression and subsequently not to promote an accumulation of P_i. Then, we performed experiments in presence of adenosine and ATP and observed an increase of about 20-60% of ABCC6 and CD73 proteins after a treatment with 10 and 100 μM of adenosine and a new treatment with 50 and 500 μM of ATP for 48 hours **[171]**. These data suggest an important role of ABCC6 protein in regulating and in particular in the activation of purinergic system, one of the major players in supplying

this system of adenosine and ATP. ATP, a possible physiological substrate of ABCC6, is able to increase CD73 protein: this datum could explain the correlation between ABCC6 and CD73 proteins. This correlation is also confirmed by treating HepG2 cells with quercetin and doxorubicin, two compounds able to slightly decrease and significantly increase these proteins. In order to verify if there was a correlation between the decrease of CD73 and its ability to promote cellular migration in cancer cells, we performed a wound-healing assay. This migration assay showed a significant decrease of about 40% of cellular migration, maybe, due to a down-regulation of CD73. This decrease of HepG2 migration rate does not depend on the probenecid's ability to block the cellular cycle (no significant change in *p16*, *p21* and *p53* gene expression was observed). Another experiment shows that the decrease of HepG2 migration rate is correlated with significant changes of the arrangement of depolymerized actin filaments and of filopodia. Finally, in order to confirm the correlation between ABCC6 and CD73 were performed other experiments using probenecid, adenosine and ATP in HuH-7, HEK293 and MDA-MB-231 cells; these cellular lines express less ABCC6 than that one expressed in HepG2 cells. The results obtained in these cells show that there are poor effects of probenecid to inhibit the MRPs, including ABCC6 protein, and to decrease CD73 expression. This data could be correlated with a less expression of ABCC6 in these cells than that one expressed in HepG2 cells. The poor effects of probenecid in modulation of ABCC6 transporter activity and in controlling of CD73

expression in MDA-MB-231 cells were also confirmed by observing no significant morphological changes in actin filaments and in filopodia. Therefore probenecid may not be able to decrease the cellular migration in these cells. Furthermore in HuH-7, HEK293 and MDA-MB-231cells the adenosine and ATP slightly increase CD73 levels. From the analysis of all these data emerges a significant role of ABCC6 protein in the regulation of processes above mentioned, and in particular in controlling of CD73 expression and functionality. In conclusion, the ABCC6 transporter is involved in the activation of the purinergic system, as it supplies of ATP the extracellular space, where are located the purinergic receptors; this datum was confirmed both with the addition of probenecid alone and with the addition of adenosine and ATP and confirmed in various cellular lines expressing ABCC6 differently. This result raises new perspectives on the possibility of inhibiting the purinergic system with all the positive and negative consequences deriving from it and its importance on the immune system. Further experiments are needed however to clarify the role of the ABCC6 protein in the purinergic system.

Bibliography:

[1] K.W. Scotto, Transcriptional regulation of ABC drug transporters, Oncogene. 22 (2003) 7496–7511.

[2] F.L. Theodoulou, Plant ABC transporters, Biochim. Biophys. Acta - Biomembr. 1465 (2000) 79–103.

[3] D.L. Mason, S. Michaelis, Requirement of the N-terminal extension for vacuolar trafficking and transport activity of yeast Ycf1p, an ATP-binding cassette transporter, Mol. Biol. Cell. 13 (2002) 4443–4455.

[4] T. Kretzschmar, B. Burla, Y. Lee, E. Martinoia, R. Nagy, Functions of ABC transporters in plants, Essays Biochem. 50 (2011) 145–160.

[5] D.C. Rees, E. Johnson, O. Lewinson, ABC transporters : The power to change, Nat Rev Mol Cell Biol. 10 (2009) 218–227.

[6] J. ter Beek, A. Guskov, D.J. Slotboom, Structural diversity of ABC transporters, J. Gen. Physiol. 143 (2014) 419–435.

[7] C. Thomas, R. Tampé, Multifaceted structures and mechanisms of ABC transport systems in health and disease, Curr. Opin. Struct. Biol. 51 (2018) 116–128.

[8] M. Dean, A. Rzhetsky, R. Allikmets, The Human ATP-Binding Cassette (ABC) transporter superfamily, Genome Res. 11 (2001) 1156–1166.

[9] K. Hollenstein, R.J. Dawson, K.P. Locher, Structure and mechanism of ABC transporter proteins, Curr. Opin. Struct. Biol. 17 (2007) 412–418.

[10] S.F. Zhou, Role of multidrug resistance associated proteins in drug development., Drug Discov. Ther. 2 (2008) 305–32.

[11] M.M. Gottesman, Mechanisms of cancer drug resistance., Annu. Rev. Med. 53 (2002) 615–627.

[12] S. Shukla, S. Ohnuma, S. V. Ambudkar, Improving cancer chemotherapy with modulators of ABC drug transporters, Curr. Drug Targets. 12 (2011) 621–630.

[13] S. Trowitzsch, R. Tampé, ABC Transporters in Dynamic Macromolecular Assemblies, J. Mol. Biol. (2018).

[14] A. Adamska, M. Falasca, ATP-binding cassette transporters in progression and clinical outcome of pancreatic cancer: What is the way forward?, World J. Gastroenterol. 24 (2018) 3222–3238.

[15] R. Deeley, C. Westlake, S. Cole, Transmembrane transport of endo-and xenobiotics by mammalian ATP-binding cassette multidrug resistance proteins, Physiol. Rev. (2006) 849–899.

[16] L.F. Payen, M. Gao, C.J. Westlake, S.P.C. Cole, R.G. Deeley, Role of carboxylate residues adjacent to the conserved core Walker B motifs in the catalytic cycle of multidrug resistance protein 1 (ABCC1), J. Biol. Chem. 278 (2003) 38537–38547.

[17] F.J. Sharom, ABC multidrug transporters: Structure, function and role in chemoresistance, Pharmacogenomics. 9 (2008) 105–127.

[18] V. Vasiliou, K. Vasiliou, D.W. Nebert, Human ATP-binding cassette (ABC) transporter family, Hum. Genomics. 3 (2009) 281–290.

[19] A. Haimeur, G. Conseil, R.G. Deeley, S.P.C. Cole, The MRP-Related and BCRP/ABCG2 Multidrug Resistance Proteins: Biology, Substrate Specificity and Regulation, Curr. Drug Metab. 5 (2004) 21–53.

[20] L. Couture, J.A. Nash, J. Turgeon, The ATP-binding cassette transporters and their implication in drug disposition: a special look at the heart, Pharmacol Rev. 58 (2006) 244–258.

[21] Y. Fukuda, J.D. Schuetz, ABC transporters and their role in nucleoside and nucleotide drug resistance, Biochem. Pharmacol. 83 (2012) 1073–1083.

[22] M.F. Rosenberg, R. Callaghan, S. Modok, C.F. Higgins, R.C. Ford, Three-dimensional structure of P-glycoprotein: The transmembrane regions adopt an asymmetric configuration in the nucleotide-bound state, J. Biol. Chem. 280 (2005) 2857–2862.

[23] T.A. Chen ZS, Multidrug Resistance Proteins (MRPs/ABCCs) in Cancer Chemotherapy and Genetic Diseases, Febs J. 278 (2012) 3226–3245.

[24] N. Khunweeraphong, T. Stockner, K. Kuchler, The structure of the human ABC transporter ABCG2 reveals a novel mechanism for drug extrusion, Sci. Rep. 7 (2017) 1–15.

[25] K. Ueda, ABC Proteins Protect the Human Body and Maintain Optimal Health, Biosci. Biotechnol. Biochem. 75 (2011) 401–409.

[26] G. Mamo, A. Pandi, A Review on ATP Binding Cassette (ABC) Transporters, Int J Pharma Res Heal. Sci. 5 (2017) 1607–1615.

[27] J. Štefková, R. Poledne, J.A. Hubáček, ATP-binding cassette (ABC) transporters in human metabolism and diseases, Physiol. Res. 53 (2004) 235–243.

[28] M. Mimeault, S.K. Batra, Altered gene products involved in the malignant reprogramming of cancer stem/progenitor cells and multitargeted therapies, Mol. Aspects Med. 39 (2014) 3–32.

[29] L.M. Hodgesa, S.M. Markovac, L.W. Chinnc, J.M. Gowc, D.L. Kroetzc, T.E. Kleina, R.B. Altman, Very important pharmacogene summary: ABCB1 (MDR1, P-glycoprotein), Pharmacogenet Genomics. 21 (2011) 152–161.

[30] R.W. Robey, K.M. Pluchino, M.D. Hall, A.T. Fojo, S.E. Bates, M.M. Gottesman, Revisiting the role of ABC transporters in multidrug-resistant cancer, Nat. Rev. Cancer. 18 (2018) 452–464.

[31] E.M. Leslie, R.G. Deeley, S.P.C. Cole, Multidrug resistance proteins: Role of P-glycoprotein, MRP1, MRP2, and BCRP (ABCG2) in tissue defense, Toxicol. Appl. Pharmacol. 204 (2005) 216–237.

[32] S. Al-Dimassi, T. Abou-Antoun, M. El-Sibai, Cancer cell resistance mechanisms: A mini review, Clin. Transl. Oncol. 16 (2014) 511–516.

[33] Y. Toyoda, Y. Hagiya, T. Adachi, K. Hoshijima, M.T. Kuo, T. Ishikawa, MRP class of human ATP binding cassette (ABC) transporters: Historical background and new research directions, Xenobiotica. 38 (2008) 833–862.

[34] S. Choudhuri, C. Klaassen, Structure, function, expression, genomic organization, and single nucleotide polymorphisms of human ABCB1 (MDR1), ABCC (MRP), and ABCG2 (BCRP) efflux transporters, Int. J. Toxicol. 25 (2006) 231–259.

[35] M. Kool, M. Van Der Linden, M. De Haas, G. Mrp, C. Cells, Expression of Human MRP6 , a Homologue of the Multidrug Resistance Protein Gene MRP1 , in Tissues and Cancer Cells Expression of Human MRP6 , a Homologue of the Multidrug Resistance Protein, Cancer. (1999) 175–182.

[36] H. Yabuuchi, S. ichiro Takayanagi, K. Yoshinaga, N. Taniguchi, H. Aburatani, T. Ishikawa, ABCC13, an unusual truncated ABC transporter, is highly expressed in fetal human liver, Biochem. Biophys. Res. Commun. 299

(2002) 410–417.

[37] Y. Qian, W. Qiu, M. Gao, C.J. Westlake, S.P.C. Cole, R.G. Deeley, Characterization of Binding of Leukotriene C4 by Human Multidrug Resistance Protein 1: evidence of differential interactions with NH2- and COOH-proximal halves of the protein, J. Biol. Chem. 276 (2001) 38636–38644.

[38] C.J. Westlake, L. Payen, M. Gao, S.P.C. Cole, R.G. Deeley, Identification and characterization of functionally important elements in the multidrug resistance protein 1 COOH-terminal region, J. Biol. Chem. 279 (2004) 53571–53583.

[39] G.E. Tusnády, B. Sarkadi, I. Simon, A. Váradi, Membrane topology of human ABC proteins, FEBS Lett. 580 (2006) 1017–1022.

[40] K. Bera, P. Rani, G. Kishor, S. Agarwal, A. Kumar, D.V. Singh, Structural elucidation of transmembrane domain zero (TMD0) of EcdL: A multidrug resistance-associated protein (MRP) family of ATP-binding cassette transporter protein revealed by atomistic simulation, J. Biomol. Struct. Dyn. 1102 (2017) 1–13.

[41] R. Miglionico, A. Gerbino, A. Ostuni, M.F. Armentano, M. Monné, M. Carmosino, F. Bisaccia, New insights into the roles of the N-terminal region of the ABCC6 transporter, J. Bioenerg. Biomembr. 48 (2016) 259–267.

[42] S. Dallas, D.S. Miller, R. Bendayan, Multidrug resistance-associated proteins: expression and function in the central nervous system., Pharmacol. Rev. 58 (2006) 140–161.

[43] R. Evers, G.J. Zaman, L. van Deemter, H. Jansen, J. Calafat, L.C. Oomen, R.P. Oude Elferink, P. Borst, a H. Schinkel, Basolateral localization and export activity of the human multidrug resistance-associated protein in

polarized pig kidney cells., J. Clin. Invest. 97 (1996) 1211–8.

[44] C.J. Westlake, Y.M. Qian, M. Gao, M. Vasa, S.P.C. Cole, R.G. Deeley, Identification of the Structural and Functional Boundaries of the Multidrug Resistance Protein 1 Cytoplasmic Loop 3, Biochemistry. 42 (2003) 14099–14113.

[45] P. Bandler, C. Westlake, C. Grant, Identification of regions required for apical membrane localization of human multidrug resistance protein 2, Mol. Pharmacol. 74 (2008) 9–19.

[46] E. Bakos, R. Evers, G. Szakacs, G.E. Tusnady, E. Welker, K. Szabo, M. de Haas, L. van Deemter, P. Borst, a Varadi, B. Sarkadi, Functional multidrug resistance protein (MRP1) lacking the N- terminal transmembrane domain, J. Biol. Chem. 273 (1998) 32167–32175.

[47] S.B. Mateus Fernández, Z. Holló, A. Kern, É. Bakos, P.A. Fischer, P. Borst, R. Evers, Role of the N-terminal transmembrane region of the multidrug resistance protein MRP2 in routing to the apical membrane in MDCKII cells, J. Biol. Chem. 277 (2002) 31048–31055.

[48] A.P. Babenko, J. Bryan, SUR Domains that Associate with and Gate KATP Pores Define a Novel Gatekeeper, J. Biol. Chem. 278 (2003) 41577–41580.

[49] K. Fang, L. Csanády, K.W. Chan, The N-terminal transmembrane domain (TMD0) and a cytosolic linker (L0) of sulphonylurea receptor define the unique intrinsic gating of KATP channels, J. Physiol. 576 (2006) 379–389.

[50] F. Ringpfeil, M.G. Lebwohl, a M. Christiano, J. Uitto, Pseudoxanthoma elasticum: mutations in the MRP6 gene encoding a transmembrane ATP-binding cassette (ABC) transporter., Proc. Natl. Acad. Sci. U. S. A. 97 (2000) 6001–6.

[51] B. Parreira, J.C.R. Cardoso, R. Costa, A.R. Couto, J. Bruges-Armas, D.M. Power, Persistence of the ABCC6 genes and the emergence of the bony skeleton in vertebrates, Sci. Rep. 8 (2018) 1–13.

[52] A.A.B. Bergen, A.S. Plomp, X. Hu, P.T.V.M. De Jong, T.G.M.F. Gorgels, ABCC6 and pseudoxanthoma elasticum, Pflugers Arch. Eur. J. Physiol. 453 (2007) 685–691.

[53] C.E. Grant, G. Valdimarsson, D.R. Hipfner, K.C. Aimquist, S.P.C. Cole, R.G. Deeley, Overexpression of Multidrug Resistance-associated Protein (MRP) Increases Resistance to Natural Product Drugs Resistance to Natural Product Drugs I, Cancer Res. 54 (1994) 357–361.

[54] M.F. Armentano, A. Ostuni, V. Infantino, V. Iacobazzi, M.A. Castiglione Morelli, F. Bisaccia, Identification of a New Splice Variant of the Human ABCC6 Transporter, Res. Lett. Biochem. 2008 (2008) 1–4.

[55] O. Le Saux, K. Beck, C. Sachsinger, C. Silvestri, C. Treiber, H.H. Göring, E.W. Johnson, A. De Paepe, F.M. Pope, I. Pasquali-Ronchetti, L. Bercovitch, a S. Marais, D.L. Viljoen, S.F. Terry, C.D. Boyd, A spectrum of ABCC6 mutations is responsible for pseudoxanthoma elasticum, Am J Hum Genet. 69 (2001) 749–764.

[56] L. Pulkkinen, A. Nakano, F. Ringpfeil, J. Uitto, Identification of ABCC6 pseudogenes on human chromosome 16p: Implications for mutation detection in pseudoxanthoma elasticum, Hum. Genet. 109 (2001) 356–365.

[57] Z. Lian, J. Liu, J. Pan, N.L. Satiroglu Tufan, M. Zhu, P. Arbuthnot, M. Kew, M.M. Clayton, M.A. Feitelson, A cellular gene up-regulated by hepatitis B virus - Encoded X antigen promotes hepatocellular growth and survival, Hepatology. 34 (2001) 146–157.

[58] A.P. Piehler, M. Hellum, J.J. Wenzel, E. Kaminski, K.B.F. Haug, P. Kierulf, W.E. Kaminski, The human ABC transporter pseudogene family: Evidence for transcription and gene-pseudogene interference, BMC Genomics. 9 (2008) 1–13.

[59] A. Varadi, Z. Szabo, V. Pomozi, H. De Boussac, K. Fulop, A. T, ABCC6 as a target in pseudoxanthoma elasticum, Curr. Drug Targets. 12 (2011) 671–682.

[60] Q. Jiang, Y. Matsuzaki, K. Li, J. Uitto, Transcriptional regulation and characterization of the promoter region of the human ABCC6 gene, J. Invest. Dermatol. 126 (2006) 325–335.

[61] Q. Li, Q. Jiang, E. Pfendner, A. Varadi, U. J, Pseudoxanthoma elasticum: Clinical phenotypes, molecular genetics and putative pathomechanisms, Exp. Dermatol. 18 (2009) 1–11.

[62] S. Zhou, L. Wang, Y.M. Di, C.C. Xue, W. Duan, Substrates and Inhibitors of Human Multidrug Resistance Associated Proteins and the Implications in Drug Development, Curr Med Chem. 15 (2008) 1981–2039.

[63] T. Arányi, C. Bacquet, H. de Boussac, M. Ratajewski, V. Pomozi, K. Fülöp, C.N. Brampton, L. Pulaski, O. Le Saux, A. Váradi, Transcriptional regulation of the ABCC6 gene and the background of impaired function of missense disease-causing mutations, Front. Genet. 4 (2013) 1–7.

[64] O. Le Saux, L. Martin, Z. Aherrahrou, G. Leftheriotis, A. Váradi, C.N. Brampton, The molecular and physiological roles of ABCC6: More than meets the eye, Front. Genet. 3 (2012) 1–10.

[65] G.L. Scheffer, X. Hu, A.C.L.M. Pijnenborg, J. Wijnholds, A.A.B. Bergen, R.J. Scheper, MRP6 (ABCC6) detection in normal human tissues and tumors, Lab. Investig. 82 (2002) 515–518.

[66] J. Madon, B. Hagenbuch, L. Landmann, P.J. Meier, B. Stieger, Transport function and hepatocellular localization of mrp6 in rat liver., Mol. Pharmacol. 57 (2000) 634–41.

[67] F. Cuviello, Å. Tellgren-Roth, P. Lara, F. Ruud Selin, M. Monné, F. Bisaccia, I. Nilsson, A. Ostuni, Membrane insertion and topology of the amino-terminal domain TMD0 of multidrug-resistance associated protein 6 (MRP6), FEBS Lett. 589 (2015) 3921–3928.

[68] A.M. Salvia, F. Cuviello, S. Coluzzi, R. Nuccorini, I. Attolico, S.P. Pascale, F. Bisaccia, M. Pizzuti, A. Ostuni, Expression of some ATP-binding cassette transporters in acute myeloid leukemia, Hematol. Rep. 9 (2017) 137–141.

[69] A. Ostuni, R. Miglionico, F. Bisaccia, M.A. Castiglione Morelli, Biochemical characterization and NMR study of the region E748-A785 of the human protein MRP6/ABCC6., Protein Pept. Lett. 17 (2010) 861–866.

[70] A. Ostuni, R. Miglionico, M. Antonietta Castiglione Morelli, F. Bisaccia, Study of the Nucleotide-Binding Domain 1 of the Human Transporter Protein MRP6, Protein Pept. Lett. 17 (2010) 1553–1558.

[71] A. Ostuni, R. Miglionico, M. Monné, M.A. Castiglione Morelli, F. Bisaccia, The nucleotide-binding domain 2 of the human transporter protein MRP6, J. Bioenerg. Biomembr. 43 (2011) 465–471.

[72] M.G. Belinsky, Z.S. Chen, I. Shchaveleva, H. Zeng, G.D. Kruh, Characterization of the drug resistance and transport properties of multidrug resistance protein 6 (MRP6, ABCC6), Cancer Res. 62 (2002) 6172–6177.

[73] L.N. Eadie, P. Dang, J.M. Goyne, T.P. Hughes, D.L. White, ABCC6 plays a significant role in the transport of nilotinib and dasatinib, and contributes to TKI resistance in vitro, in both cell lines and primary patient mononuclear

cells, PLoS One. 13 (2018) 1–18.

[74] Q. Li, J. Kingman, K. van de Wetering, S. Tannouri, J.P. Sundberg, J. Uitto, Abcc6 Knockout Rat Model Highlights the Role of Liver in PPi Homeostasis in Pseudoxanthoma Elasticum, J. Invest. Dermatol. 137 (2017) 1025–1032.

[75] A. Iliás, Z. Urbán, T.L. Seidl, O. Le Saux, E. Sinkó, C.D. Boyd, B. Sarkadi, A. Váradi, Loss of ATP-dependent transport activity in pseudoxanthoma elasticum-associated mutants of human ABCC6 (MRP6), J. Biol. Chem. 277 (2002) 16860–16867.

[76] R. Miglionico, M.F. Armentano, M. Carmosino, A.M. Salvia, F. Cuviello, F. Bisaccia, A. Ostuni, Dysregulation of gene expression in ABCC6 knockdown HepG2 cells, Cell. Mol. Biol. Lett. 19 (2014) 517–526.

[77] R. Miglionico, A. Ostuni, M.F. Armentano, L. Milella, E. Crescenzi, M. Carmosino, F. Bisaccia, ABCC6 knockdown in HepG2 cells induces a senescent-like cell phenotype, Cell. Mol. Biol. Lett. 22 (2017) 1–10.

[78] S.A. Hunsucker, B.S. Mitchell, J. Spychala, The 5′-nucleotidases as regulators of nucleotide and drug metabolism, Pharmacol. Ther. 107 (2005) 1–30.

[79] N.T. Snider, P.J. Altshuler, S. Wan, T.H. Welling, J. Cavalcoli, M.B. Omary, Alternative splicing of human NT5E in cirrhosis and hepatocellular carcinoma produces a negative regulator of ecto-5'-nucleotidase (CD73), Mol. Biol. Cell. 25 (2014) 4024–4033.

[80] K. Synnestvedt, G.T. Furuta, K.M. Comerford, N. Louis, J. Karhausen, H.K. Eltzschig, K.R. Hansen, L.F. Thompson, S.P. Colgan, Ecto-5'-nucleotidase (CD73) regulation by Hypoxia-Inducible Factor-1 Mediates Permeability Changes in Intestinal Epithelia, J. Clin. Invest. 110 (2002) 993–1002.

[81] H.K. Eltzschig, J.C. Ibla, G.T. Furuta, M.O. Leonard, K.A. Jacobson, K.

Enjyoji, S.C. Robson, S.P. Colgan, Coordinated Adenine Nucleotide Phosphohydrolysis and Nucleoside Signaling in Posthypoxic Endothelium: role of ectonucleotidases and adenosine A2b receptors, J. Exp. Med. 198 (2003) 783–796.

[82] P.A. Beavis, J. Stagg, P.K. Darcy, M.J. Smyth, CD73: A potent suppressor of antitumor immune responses, Trends Immunol. 33 (2012) 231–237.

[83] F.S. Regateiro, D. Howie, K.F. Nolan, E.I. Agorogiannis, D.R. Greaves, S.P. Cobbold, H. Waldmann, Generation of anti-inflammatory adenosine byleukocytes is regulated by TGF-β, Eur. J. Immunol. 41 (2011) 2955–2965.

[84] S. Loi, S. Pommey, B. Haibe-Kains, P.A. Beavis, P.K. Darcy, M.J. Smyth, J. Stagg, CD73 promotes anthracycline resistance and poor prognosis in triple negative breast cancer, Proc. Natl. Acad. Sci. 110 (2013) 11091–11096.

[85] C. St. Hilaire, S.G. Ziegler, T.C. Markello, A. Brusco, C. Groden, F. Gill, H. Carlson-Donohoe, R.J. Lederman, M.Y. Chen, D. Yang, M.P. Siegenthaler, C. Arduino, C. Mancini, B. Freudenthal, H.C. Stanescu, A.A. Zdebik, R.K. Chaganti, R.L. Nussbaum, R. Kleta, W.A. Gahl, M. Boehm, NT5E mutations and arterial calcifications, N. Engl. J. Med. 364 (2011) 432–442.

[86] T.C. Markello, L.K. Pak, C. St. Hilaire, H. Dorward, S.G. Ziegler, M.Y. Chen, K. Chaganti, R.L. Nussbaum, M. Boehm, W.A. Gahl, Vascular pathology of medial arterial calcifications in NT5E deficiency: implications for the role of adenosine in pseudoxanthoma elasticum, Mol. Genet. Metab. 103 (2011) 44–50.

[87] D.P.H.M. Heuts, M.J. Weissenborn, R. V. Olkhov, A.M. Shaw, J. Gummadova, C. Levy, N.S. Scrutton, Crystal Structure of a Soluble Form of Human CD73 with Ecto-5'-Nucleotidase Activity, ChemBioChem. 13 (2012) 2384–2391.

[88] L.F. Thompson, H.K. Eltzschig, J.C. Ibla, C.J. Van De Wiele, R. Resta, J.C. Morote-Garcia, S.P. Colgan, Crucial Role for Ecto-5′-Nucleotidase (CD73) in Vascular Leakage during Hypoxia, J. Exp. Med. 200 (2004) 1395–1405.

[89] S.P. Colgan, H.K. Eltzschig, T. Eckle, L.F. Thompson, Physiological roles for ecto-5′-nucleotidase (CD73), Purinergic Signal. 2 (2006) 351–360.

[90] K. Knapp, M. Zebisch, J. Pippel, A. El-Tayeb, C.E. Müller, N. Sträter, Crystal structure of the human ecto-5′-nucleotidase (CD73): Insights into the regulation of purinergic signaling, Structure. 20 (2012) 2161–2173.

[91] N. Sträter, Ecto-5′-nucleotidase: Structure function relationships, Purinergic Signal. 2 (2006) 343–350.

[92] S. Ogata, Y. Hayashi, Y. Misumi, Y. Ikehara, Membrane-Anchoring Domain of Rat Liver 5′-Nucleotidase: Identification of the COOH-Terminal Serine-523 Covalently Attached with a Glycolipid, Biochemistry. 29 (1990) 7923–7927.

[93] V. Roberts, B. Lu, S. Rajakumar, P.J. Cowan, K.M. Dwyer, The CD39-adenosinergic axis in the pathogenesis of renal ischemia-reperfusion injury, Purinergic Signal. 9 (2013) 135–143.

[94] B. Allard, P.A. Beavis, P.K. Darcy, J. Stagg, Immunosuppressive activities of adenosine in cancer, Curr. Opin. Pharmacol. 29 (2016) 7–16.

[95] M. V Sitkovsky, S. Hatfield, R. Abbott, B. Belikoff, D. Lukashev, A. Ohta, Hostile, hypoxia-A2-adenosinergic tumor biology as the next barrier to overcome for tumor immunologists, Cancer Immunol. Res. 2 (2014) 598–605.

[96] L. Antonioli, G.G. Yegutkin, P. Pacher, C. Blandizzi, G. Haskó, Anti-CD73 in Cancer Immunotherapy: Awakening New Opportunities, Trends in Cancer. 2 (2016) 95–109.

[97] T. Raskovalova, X. Huang, M. Sitkovsky, L.C. Zacharia, E.K. Jackson, E. Gorelik, Gs Protein-Coupled Adenosine Receptor Signaling and Lytic Function of Activated NK Cells, J. Immunol. 175 (2005) 4383–4391.

[98] V. Kumar, Adenosine as an endogenous immunoregulator in cancer pathogenesis: Where to go?, Purinergic Signal. 9 (2013) 145–165.

[99] Z.W. Gao, K. Dong, H.Z. Zhang, The roles of CD73 in cancer, Biomed Res. Int. 2014 (2014).

[100] S. V Novitskiy, S. Ryzhov, R. Zaynagetdinov, A.E. Goldstein, Y. Huang, O.Y. Tikhomirov, M.R. Blackburn, I. Biaggioni, D.P. Carbone, I. Feoktistov, M.M. Dikov, Adenosine receptors in regulation of dendritic cell differentiation and function, Blood. 112 (2008) 1822–1831.

[101] L. Antonioli, C. Blandizzi, P. Pacher, G. Haskó, Immunity, inflammation and cancer: A leading role for adenosine, Nat. Rev. Cancer. 13 (2013) 842–857.

[102] P. Ujházy, E.S. Berleth, J.M. Pietkiewicz, H. Kitano, J.R. Skaar, M.J. Ehrke, E. Mihich, Evidence for the involvement of ecto-5'-nucleotidase (CD73) in drug resistance, Int. J. Cancer. 68 (1996) 493–500.

[103] X. Zhi, Y. Wang, X. Zhou, J. Yu, R. Jian, S. Tang, L. Yin, P. Zhou, RNAi-mediated CD73 suppression induces apoptosis and cell-cycle arrest in human breast cancer cells, Cancer Sci. 101 (2010) 2561–2569.

[104] X. Zhi, S. Chen, P. Zhou, Z. Shao, L. Wang, Z. Ou, L. Yin, RNA interference of ecto-5′-nucleotidase (CD73) inhibits human breast cancer cell growth and invasion, Clin. Exp. Metastasis. 24 (2007) 439–448.

[105] L. Wang, X. Zhou, T. Zhou, D. Ma, S. Chen, X. Zhi, L. Yin, Z. Shao, Z. Ou, P. Zhou, Ecto-5′-nucleotidase promotes invasion, migration and adhesion of human breast cancer cells, J. Cancer Res. Clin. Oncol. 134 (2008) 365–372.

[106] P. Zhou, X. Zhi, T. Zhou, S. Chen, X. Li, L. Wang, L. Yin, Z. Shao, Z. Ou, Overexpression of ecto-5′-nucleotidase (CD73) promotes T-47D human breast cancer cells invasion and adhesion to extracellular matrix, Cancer Biol. Ther. 6 (2007) 426–431.

[107] L. Wang, S. Tang, Y. Wang, S. Xu, J. Yu, X. Zhi, Z. Ou, J. Yang, P. Zhou, Z. Shao, Ecto-5′-nucleotidase (CD73) promotes tumor angiogenesis, Clin. Exp. Metastasis. 30 (2013) 671–680.

[108] W.G. Junger, Immune cell regulation by autocrine purinergic signaling, Nat Rev Immunol. 11 (2011) 201–212.

[109] C.E. Muller, K.A. Jacobson, Recent Developments in Adenosine Receptor Ligands and Their Potential as Novel Drugs, Biochim. Biophys. Acta - Biomembr. 1808 (2011) 1290–1308.

[110] B. Allard, M.S. Longhi, S.C. Robson, J. Stagg, The ectonucleotidases CD39 and CD73: Novel checkpoint inhibitor targets, Immunol. Rev. 276 (2017) 121–144.

[111] B.B. Fredholm, A.P. IJzerman, K.A. Jacobson, J. Linden, C.E. Muller, International Union of Basic and Clinical Pharmacology. LXXXI. Nomenclature and classification of adenosine receptors - An Update, Pharmacol. Rev. 63 (2011) 1–34.

[112] Q. Li, Q. Jiang, J. Uitto, Ectopic mineralization disorders of the extracellular matrix of connective tissue: molecular genetics and pathomechanisms of aberrant calcification, Matrix Bio. 0 (2014) 23–28.

[113] O.M. Vanakker, L. Martin, L.J. Schurgers, D. Quaglino, L. Costrop, C. Vermeer, I. Pasquali-Ronchetti, P.J. Coucke, A. De Paepe, Low serum vitamin K in PXE results in defective carboxylation of mineralization

inhibitors similar to the GGCX mutations in the PXE-like syndrome, Lab. Investig. 90 (2010) 895–905.

[114] I. Ronchetti, F. Boraldi, G. Annovi, P. Cianciulli, D. Quaglino, Fibroblast involvement in soft connective tissue calcification, Front. Genet. 4 (2013) 1–16.

[115] J. Zhao, J. Kingman, J.P. Sundberg, J. Uitto, Q. Li, Plasma PPi Deficiency Is the Major, but Not the Exclusive, Cause of Ectopic Mineralization in an Abcc6–/–Mouse Model of PXE, J. Invest. Dermatol. 137 (2017) 2336–2343.

[116] R.A. Terkeltaub, Inorganic pyrophosphate generation and disposition in pathophysiology, Am. J. Physiol. - Cell Physiol. 281 (2001) C1–C11.

[117] Q. Li, J. Kingman, J.P. Sundberg, M.A. Levine, J. Uitto, Etidronate prevents, but does not reverse, ectopic mineralization in a mouse model of pseudoxanthoma elasticum (Abcc6-/-)., Oncotarget. 9 (2018) 30721–30730.

[118] A.W. Lohman, M. Billaud, B.E. Isakson, Mechanisms of ATP release and signalling in the blood vessel wall, Cardiovasc. Res. 95 (2012) 269–280.

[119] R.S. Jansen, A. Küçükosmanoglu, M. de Haas, S. Sapthu, J.A. Otero, I.E.M. Hegman, A.A.B. Bergen, T.G.M.F. Gorgels, P. Borst, K. van de Wetering, ABCC6 prevents ectopic mineralization seen in pseudoxanthoma elasticum by inducing cellular nucleotide release., Proc. Natl. Acad. Sci. U. S. A. 110 (2013) 20206–11.

[120] R.S. Jansen, S. Duijst, S. Mahakena, D. Sommer, F. Szeri, A. Váradi, A. Plomp, A.A. Bergen, R.P.J. Oude Elferink, P. Borst, K. Van De Wetering, ABCC6-mediated ATP secretion by the liver is the main source of the mineralization inhibitor inorganic pyrophosphate in the systemic circulation - Brief report, Arterioscler. Thromb. Vasc. Biol. 34 (2014) 1985–1989.

[121] E.Y. De Vilder, O.M. Vanakker, From variome to phenome: Pathogenesis, diagnosis and management of ectopic mineralization disorders, World J. Clin. Cases. 3 (2015) 556.

[122] G. Favre, A. Laurain, T. Aranyi, F. Szeri, K. Fulop, O. Le Saux, C. Duranton, G. Kauffenstein, L. Martin, G. Lefthériotis, The ABCC6 Transporter: A New Player in Biomineralization, Int. J. Mol. Sci. 18 (2017) 1941.

[123] A. Mahmut, M.C. Boulanger, R. Bouchareb, F. Hadji, P. Mathieu, Adenosine derived from ecto-nucleotidases in calcific aortic valve disease promotes mineralization through A2a adenosine receptor, Cardiovasc. Res. 106 (2015) 109–120.

[124] G. Burnstock, Purinergic signalling: Its unpopular beginning, its acceptance and its exciting future, BioEssays. 34 (2012) 218–225.

[125] G. Burnstock, Purinergic signalling: Therapeutic developments, Front. Pharmacol. 8 (2017) 1–55.

[126] S.G. Ziegler, F. C.R., E.G. MacFarlane, R.C. Riddle, R.E. Tomlinson, E.Y. Chew, L. Martin, C.-T. Ma, E. Sergienko, A.B. Pinkerton, J.L. Millan, W.A. Gahl, H.C. Dietz, Ectopic calcification in pseudoxanthoma elasticum responds to inhibition of tissue-nonspecific alkaline phosphatase, Sci. Transl. Med. 9 (2017) 29–39.

[127] H. Meng, I. Vera, N. Che, X. Wang, S.S. Wang, L. Ingram-Drake, E.E. Schadt, T.A. Drake, A.J. Lusis, Identification of Abcc6 as the major causal gene for dystrophic cardiac calcification in mice through integrative genomics, Proc. Natl. Acad. Sci. 104 (2007) 4530–4535.

[128] A.A.B. Bergen, A.S. Plomp, E.J. Schuurman, S. Terry, M. Breuning, H. Dauwerse, J. Swart, M. Kool, S. Van Soest, F. Baas, J.B. Ten Brink,

P.T.V.M. De Jong, Mutations in ABCC6 cause pseudoxanthoma elasticum, Nat. Genet. 25 (2000) 228–231.

[129] J.F. Klement, Y. Matsuzaki, Q.-J. Jiang, J. Terlizzi, H.Y. Choi, N. Fujimoto, K. Li, L. Pulkkinen, D.E. Birk, J.P. Sundberg, J. Uitto, Targeted Ablation of the Abcc6 Gene Results in Ectopic Mineralization of Connective Tissues, Mol. Cell. Biol. 25 (2005) 8299–8310.

[130] P. Kuzaj, J. Kuhn, M. Dabisch-Ruthe, I. Faust, C. Götting, C. Knabbe, D. Hendig, ABCC6- A new player in cellular cholesterol and lipoprotein metabolism?, Lipids Health Dis. 13 (2014) 1–17.

[131] D. Gheduzzi, R. Guidetti, C. Anzivino, P. Tarugi, E. Di Leo, D. Quaglino, I.P. Ronchetti, ABCC6 mutations in Italian families affected by pseudoxanthoma elasticum (PXE)., Hum. Mutat. 24 (2004) 438–439.

[132] R.P. Finger, P.C. Issa, M.S. Ladewig, C. Götting, C. Szliska, H.P.N. Scholl, F.G. Holz, Pseudoxanthoma Elasticum: Genetics, Clinical Manifestations and Therapeutic Approaches, Surv. Ophthalmol. 54 (2009) 272–285.

[133] I. Georgalas, I. Tservakis, D. Papaconstaninou, M. Kardara, C. Koutsandrea, I. Ladas, Pseudoxanthoma elasticum, ocular manifestations, complications and treatment, Clin. Exp. Optom. 94 (2011) 169–180.

[134] A.S. Plomp, J. Toonstra, A.A.B. Bergen, M.R. Van Dijk, P.T.V.M. De Jong, Proposal for updating the pseudoxanthoma elasticum classification system and a review of the clinical findings, Am. J. Med. Genet. Part A. 152A (2010) 1049–1058.

[135] K. Moitra, S. Garcia, M. Jaldin, C. Etoundi, D. Cooper, A. Roland, P. Dixon, S. Reyes, S. Turan, S. Terry, M. Dean, ABCC6 and pseudoxanthoma elasticum: The face of a rare disease from genetics to advocacy, Int. J. Mol.

Sci. 18 (2017) 1–13.

[136] D.P. Germain, Pseudoxanthoma elasticum, Orphanet J. Rare Dis. 12 (2017) 85.

[137] E.G. Pfendner, O.M. Vanakker, S.F. Terry, S. Vourthis, P.E. McAndrew, M.R. McClain, S. Fratta, A.S. Marais, S. Hariri, P.J. Coucke, M. Ramsay, D. Viljoen, P.F. Terry, A. De Paepe, J. Uitto, L.G. Bercovitch, Mutation detection in the ABCC6 gene and genotype-phenotype analysis in a large international case series affected by pseudoxanthoma elasticum, J. Med. Genet. 44 (2007) 621–628.

[138] S. Miksch, A. Lumsden, U.P. Guenther, D. Foernzler, S. Christen-Zäch, C. Daugherty, R.S. Ramesar, M. Lebwohl, D. Hohl, K.H. Neldner, K. Lindpaintner, R.I. Richards, B. Struk, Molecular genetics of Pseudoxanthoma elasticum: Type and frequency of mutations in ABCC6, Hum. Mutat. 26 (2005) 235–248.

[139] J. Uitto, L. Bercovitch, S.F. Terry, P. Terry, Pseudoxanthoma Elasticum: Progress in Diagnostics and Research Towards Treatment Summary of the 2010 PXE International Research Meeting, Am. J. Med. Genet. Part A. 155 (2011) 1517–1526.

[140] O.M. Vanakker, B.P. Leroy, P. Coucke, L.G. Bercovitch, J. Uitto, D. Viljoen, S.F. Terry, P. Van Acker, D. Matthys, B. Loeys, A. De Paepe, Novel clinico-molecular insights in pseudoxanthoma elasticum provide an efficient molecular screening method and a comprehensive diagnostic flowchart., Hum. Mutat. 29 (2008) 205.

[141] G. Kauffenstein, G.G. Yegutkin, S. Khiati, V. Pomozi, O. Le Saux, G. Leftheriotis, G. Lenaers, D. Henrion, L. Martin, Alteration of Extracellular Nucleotide Metabolism in Pseudoxanthoma Elasticum, J. Invest. Dermatol.

138 (2018) 1862–1870.

[142] D. Dedinszki, F. Szeri, E. Kozák, V. Pomozi, N. Tőkési, T.R. Mezei, K. Merczel, E. Letavernier, E. Tang, O. Le Saux, T. Arányi, K. van de Wetering, A. Váradi, Oral administration of pyrophosphate inhibits connective tissue calcification, EMBO Mol. Med. 9 (2017) e201707532.

[143] S.N. Moore, S. Bobo Tanner, J.G. Schoenecker, Bisphosphonates: From softening water to treating PXE, Cell Cycle. 14 (2015) 1354–1355.

[144] D.W. Sherer, G. Singer, J. Uribarri, R.G. Phelps, A.N. Sapadin, K.B. Freund, L. Yanuzzi, W. Fuchs, M. Lebwohl, Oral phosphate binders in the treatment of pseudoxanthoma elasticum, J. Am. Acad. Dermatol. 53 (2005) 610–615.

[145] V. Prulière-Escabasse, C. Planès, E. Escudier, P. Fanen, A. Coste, C. Clerici, Modulation of epithelial sodium channel trafficking and function by sodium 4-phenylbutyrate in human nasal epithelial cells, J. Biol. Chem. 282 (2007) 34048–34057.

[146] Q. Li, T.P. Price, J.P. Sundberg, J. Uitto, Juxta-articular joint-capsule mineralization in CD73 deficient mice: Similarities to patients with NT5E mutations, Cell Cycle. 13 (2014) 2609–2615.

[147] Z. Zhang, J.W. He, W.Z. Fu, C.Q. Zhang, Z.L. Zhang, Calcification of joints and arteries: Second report with novel NT5E mutations and expansion of the phenotype, J. Hum. Genet. 60 (2015) 561–564.

[148] H. Jin, C.S. Hilaire, Y. Huang, D. Yang, N.I. Dmitrieva, A. Negro, R. Schwartzbeck, Y. Liu, Z. Yu, A. Walts, M. Davaine, D. Lee, D. Donahue, K.S. Hsu, J. Chen, T. Cheng, W. Gahl, G. Chen, M. Boehm, Increased activity of TNAP compensates for reduced adenosine production and promotes ectopic calcification in the genetic disease ACDC, Sci. Signal. 9

(2017).

[149] Q. Li, J.L. Brodsky, L.K. Conlin, B. Pawel, A.C. Glatz, R.I. Gafni, L. Schurgers, J. Uitto, H. Hakonarson, M.A. Deardorff, M.A. Levine, Mutations in the ABCC6 Gene as a Cause of Generalized Arterial Calcification of Infancy: Genotypic Overlap with Pseudoxanthoma Elasticum, J. Invest. Dermatol. 134 (2014) 658–665.

[150] F. Rutsch, S. Vaingankar, K. Johnson, I. Goldfine, B. Maddux, P. Schauerte, H. Kalhoff, K. Sano, W.A. Boisvert, A. Superti-Furga, R. Terkeltaub, PC-1 nucleoside triphosphate pyrophosphohydrolase deficiency in idiopathic infantile arterial calcification, Am. J. Pathol. 158 (2001) 543–554.

[151] F. Rutsch, N. Ruf, S. Vaingankar, M.R. Toliat, A. Suk, W. Höhne, G. Schauer, M. Lehmann, T. Roscioli, D. Schnabel, J.T. Epplen, A. Knisely, A. Superti-Furga, J. McGill, M. Filippone, A.R. Sinaiko, H. Vallance, B. Hinrichs, W. Smith, M. Ferre, R. Terkeltaub, P. Nürnberg, Mutations in ENPP1 are associated with “idiopathic” infantile arterial calcification, Nat. Genet. 34 (2003) 379–381.

[152] F. Rutsch, P. Böyer, Y. Nitschke, N. Ruf, B. Lorenz- Depierieux, T. Wittkampf, G. Weissen-Plenz, R.-J. Fischer, Z. Mughal, J.W. Gregory, J.H. Davies, C. Loirat, T.M. Strom, D. Schnabel, P. Nürnberg, R. Terkeltaub, G.S. Group, Hypophosphatemia, Hyperphosphaturia, and Bisphosphonate Treatment Are Associated With Survival Beyond Infancy in Generalized Arterial Calcification of Infancy, Circ. Cardiovasc. Genet. 1 (2008) 133–140.

[153] N. Dlamini, M. Splitt, A. Durkan, A. Siddiqui, S. Padayachee, S. Hobbins, F. Rutsch, E. Wraige, Generalized arterial calcification of infancy: Phenotypic spectrum among three siblings including one case without obvious arterial calcifications, Am. J. Med. Genet. Part A. 149 (2009) 456–460.

[154] D. Federici, S. Torii, M. Ciuffreda, L. Galletti, L. Lorini, E. Bonanomi, A. Gianatti, M. Iascone, J. Park, L. Guo, M.E. Romero, F.D. Kolodgie, G. Guagliumi, R. Virmani, Coronary pathology of inherited generalized arterial calcification of infancy: a case report, Cardiovasc. Pathol. 36 (2018) 15–19.

[155] Y. Nitschke, G. Baujat, U. Botschen, T. Wittkampf, M. Du Moulin, J. Stella, M. Le Merrer, G. Guest, K. Lambot, M.F. Tazarourte-Pinturier, N. Chassaing, O. Roche, I. Feenstra, K. Loechner, C. Deshpande, S.J. Garber, R. Chikarmane, B. Steinmann, T. Shahinyan, L. Martorell, J. Davies, W.E. Smith, S.G. Kahler, M. McCulloch, E. Wraige, L. Loidi, W. Höhne, L. Martin, S. Hadj-Rabia, R. Terkeltaub, F. Rutsch, Generalized arterial calcification of infancy and pseudoxanthoma elasticum can be caused by mutations in either ENPP1 or ABCC6, Am. J. Hum. Genet. 90 (2012) 25–39.

[156] J. V. Møller, The Tubular Site of Urate Transport in the Rabbit Kidney, and the Effect of Probenecid on Urate Secretion, Acta Pharmacol. Toxicol. (Copenh). 23 (1965) 329–336.

[157] W. Silverman, S. Locovei, G. Dahl, Probenecid, a gout remedy, inhibits pannexin 1 channels, Am. J. Physiol. - Cell Physiol. 295 (2008) C761–C767.

[158] P.R. Davoren, E.W. Sutherland, The effect of L-epinephrine and other agents on the synthesis and release of adenosine 3',5'- phosphate by whole pigeon erythrocytes., J. Biol. Chem. 238 (1963) 3009–15.

[159] K. Flo, M. Hansen, A. Ørbo, K.E. Kjørstad, J.M. Maltau, G. Sager, Effect of probenecid, verapamil and progesterone on the concentration-dependent and temperature-sensitive human erythrocyte uptake and export of guanosine 3'5' cyclic monophosphate (cGMP), Scand. J. Clin. Lab. Invest. 55 (1995) 715–721.

[160] P. Ballerini, I.P. Di, R. Ciccarelli, E. Nargi, I. D'Alimonte, U. Traversa, M.P.

Rathbone, F. Caciagli, Glial cells express multiple ATP binding cassette proteins which are involved in ATP release, Neuroreport. 13 (2002) 1789–1792.

[161] W. Ma, H. Hui, P. Pelegrin, A. Surprenant, Pharmacological Characterization of Pannexin-1 Currents Expressed in Mammalian Cells, J. Pharmacol. Exp. Ther. 328 (2009) 409–418.

[162] S. Gollapudi, C.H. Kim, B.-N. Tran, S. Sangha, S. Gupta, Probenecid reverses multidrug resistance in multidrug resistance-associated protein-overexpressing HL60/AR and HL69/AR cells but not in P-glycoprotein-overexpressing HL60/Tax and P388/ADR cells, Cancer Chemother. Pharmacol. 40 (1997) 150–158.

[163] C. Quezada, W. Garrido, C. Oyarzun, K. Fernandez, R. Segura, R. Melo, P. Casanello, L. Sobrevia, R. San Martin, 5'-Ectonucleotidase Mediates Multiple-Drug Resistance in Glioblastoma Multiforme Cells, J. Cell. Physiol. 228 (2013) 602–608.

[164] S. Sheth, R. Brito, D. Mukherjea, L.P. Rybak, V. Ramkumar, Adenosine receptors: Expression, function and regulation, Int. J. Mol. Sci. 15 (2014) 2024–2052.

[165] J.J. Van Zanden, H.M. Wortelboer, S. Bijlsma, A. Punt, M. Usta, P.J. van Bladeren, I.M.C.M. Rietjens, N.H.P. Cnubben, Quantitative structure activity relationship studies on the flavonoid mediated inhibition of multidrug resistance proteins 1 and 2, Biochem. Pharmacol. 69 (2004) 699–708.

[166] M.F. Armentano, F. Bisaccia, R. Miglionico, D. Russo, N. Nolfi, M. Carmosino, P.B. Andrade, P. Valentão, M.S. Diop, L. Milella, Antioxidant and proapoptotic activities of sclerocarya birrea [(A. Rich.) Hochst.] methanolic root extract on the hepatocellular carcinoma cell line HepG2,

Biomed Res. Int. 2015 (2015).

[167] L. Homolya, Z. Holló, U.A. Germanns, I. Pastan, M.M. Gottesman, B. Sarkadi, Fluorescent cellular indicators are extruded by the Multidrug Resistance Protein, J. Biol. Chem. 268 (1993) 21493–21496.

[168] C. Lee, S. Lee, S.G. Shin, S. Hwang, Real-time PCR determination of rRNA gene copy number: Absolute and relative quantification assays with Escherichia coli, Appl. Microbiol. Biotechnol. 78 (2008) 371–376.

[169] K.J. Livak, T.D. Schmittgen, Analysis of relative gene expression data using real-time quantitative PCR and the 2-ΔΔCT method, Methods. 25 (2001) 402–408.

[170] I. Laurenzana, A. Caivano, F. La Rocca, S. Trino, L. De Luca, F. D'Alessio, S. Schenone, G. Falco, M. Botta, L. Del Vecchio, P. Musto, A pyrazolo[3,4-d]pyrimidine compound reduces cell viability and induces apoptosis in different hematological malignancies, Front. Pharmacol. 7 (2016) 1–9.

[171] F. Martinelli, F. Cuviello, M.C. Pace, M.F. Armentano, R. Miglionico, A. Ostuni, F. Bisaccia, Extracellular ATP Regulates CD73 and ABCC6 Expression in HepG2 Cells, Front. Mol. Biosci. 5 (2018) 1–8.

Published Papers

1. **Fabio Martinelli**, Flavia Cuviello, Maria C. Pace, Maria F. Armentano, Rocchina Miglionico, Angela Ostuni and Faustino Bisaccia, **"Extracellular ATP regulates CD73 and ABCC6 expression in HepG2 cells"**, Frontiers in Molecular Biosciences, vol. 5, no. 75, pp.1-8, 2018.

2. Faustino Bisaccia et al., **"Control of CD73 expression in cellular cultures"** (in preparation).

Other communications:

➢ Oral presentations:

1. **Fabio Martinelli**, Rocchina Miglionico, Maria C. Pace, Maria F. Armentano, Angela Ostuni, and Faustino Bisaccia (2017) **"ABCC6 transporter inactivation modulates genic expression in HepG2 cells"**. Second scientific day of the membrane group of SIB (Italian Society of Biochemistry and Molecular Biology); Catania (Italy), 12 June 2017.

2. **Fabio Martinelli**, Maria C. Pace, Angela Ostuni and Faustino Bisaccia (2018) **"The ABCC6 expression is regulated by adenosine and ATP externally added to the HepG2 cells"**. International annual meeting of GIBB (Italian group of Biomembranes and Bioenergetics); Modena (Italy), 21-23 June 2018.

➢ Posters:

1. **Fabio Martinelli**, Maria C. Pace, Angela Ostuni, Maria F. Armentano, Rocchina Miglionico and Faustino Bisaccia (2017) **"Is the Pseudoxanthoma Elasticum (PXE) a purinergic disease?"**. 59th Congress of the Italian Society of Biochemistry and Molecular Biology (SIB); Caserta (Italy), 20-22 September 2017.

2. Agata Petillo, **Fabio Martinelli**, Maria A. Castiglione Morelli, Alfonso Bavoso, Angela Ostuni and Faustino Bisaccia (2018) **"Effect of some cellular metabolic intermediates on the mitochondrial carrier expression"**. 43rd FEBS Congress (Federation of European Biochemical Societies); Prague (Czech Republic), 7-12 July 2018.

➢ Abstract in conference proceedings:

1. Angela Ostuni, Agata Petillo, Flavia Cuviello, **Fabio Martinelli** and Faustino Bisaccia (2016) **"Modulation of mitochondrial pyruvate carrier expression in HEK293 and HepG2 cells"**. ABCD meeting (Association of cell and differentiation biology) - Cell Stress: Survival and Apoptosis; Bari (Italy), 9-10 September 2016.

➢ Auditor:

1. First International annual meeting of GIBB (Italian Group of Biomembranes and Bioenergetics); Catania (Italy), 14-16 June 2017.

Ackowledgements:

I thank my tutor, Professor Faustino Bisaccia. He welcomed me into his laboratory, for the third time, and gave me the opportunity to work in his research group. He was a guide and he gave me valuable advices, teachings and friendly support.

I thank my Co-tutor, Professor Magnus Monné, for his advices.

I thank Dr.ssa Angela Ostuni. She has always encouraged me especially in the most difficult moments, giving me a constant human, scientific and moral support.

I would also like to thank all people I worked with and that I met in the last three years of laboratory: professors, Ph.D. students, students and friends with whom I shared successes and disappointments.

I thank my family, my father Domenico, my mother Filomena, my brother Daniele for all their support and exhortations.

A special thanks to my little princesses, my nieces Alessia e Sofia whose smiles gave me the strength to believe in my scientific research.

I thank my grandfather Donato who has always been so proud of me.

This experience helped me to grow both professionally and personally. There were many difficult moments of discouragement but I was always able to find the strength to continue my research.

Fabio